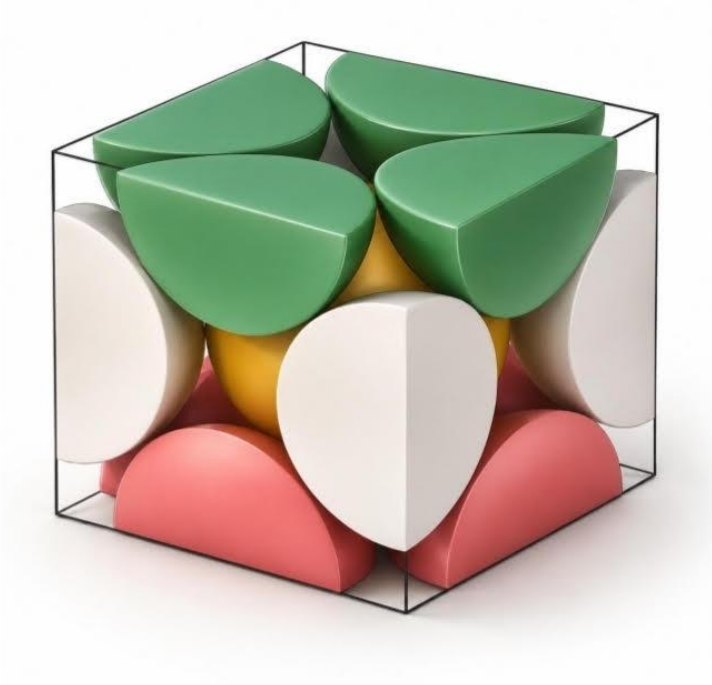
Ramionics

Geometric Calculation of the Fine-Structure Constant, Theory of Everything

Author: Ramin Khosravi
Last version: https://Ramionics.com/

Email: Ramionics@gMail.com



Electron Family Genetic Sequence represents their growth pattern:

$$\mathring{N} = 4^{0} \,.\, 4 \,.\, 4 \,.\, 6 \,.\, 6 \,.\, 4 \,.\, 4 \,.\, 2 \,.\, 2 = 36864$$

Number of Ramions (energy quanta) on each of the 12 wings of the Baryon:

$$N = \text{Ceil}10\left((\pi^{2}/10)\mathring{N} \right) = 36390$$

The quantization factors of SpaceTime and PotentialEnergy:

$$\alpha^{-1} = 160\sqrt[3]{(\pi/5)} \,.\, (1 - 1/N)$$

$$\alpha^{-1} = 137.03599920783327093$$

Game over! Welcome to the geometric depths of the physics of the Universe:
Ramionics Based on Spacetime Geometry and Kissing Numbers!

The Ramionics Framework

Ramin Khosravi

https://Ramionics.com/
RaminKhosravi.London@gMail.com

English translation
Source manuscript dated 2 November 2026

The original equations and reported results are retained. Read this translation together with the accompanying technical review, which records identified errors and unresolved issues. Paragraph identifiers P001 onwards are provided for review.

Contents

1 Introduction and nomenclature 4
2 Theorem 0 Definition of physics 4
3 Theorem 1 5
4 Theorem 2 6
5 Theorem 3 6
6 Theorem 4 7
7 Theorem 5 Energy is the only real quantity in the Universe 7
8 Theorem 6 8
9 Definition of matter 8
10 Definitions of electricity and magnetism 9
11 The 12-wing model 9
12 Fundamental particle structure 9
13 Particle notation 10
14 Scale factors 11
15 Empirical reference values 12
16 FCC spacetime quantisation factors 13
17 Fermion generations 15
18 Ramion energy equation 25
19 Exploratory factors 27
20 Speed of light and internal speed of the energy constituents 27
21 Mass and charge distributions over the twelve wings 28
22 Planck constant 28
23 Quantisation of the wing potential 29
24 Electric charge projection 30
25 Coulomb constant projection 30
26 Calculation of the fine-structure constant α 30
27 Gravitational constant 31
28 The 12+9 potential model in the zero-alpha approximation 34
29 The 12+9 potential model including α 35
30 Electron gyromagnetic factor g_e 35
31 Zero-alpha approximation for g_e 36
32 Exact calculation of g including α 37

33 Calculation of the quark, proton and neutron masses 39
34 Cosmology 69
35 Formula for the kissing number in different dimensions 94
36 Theorem 37 Relativistic dynamics and the chain of reasoning 94
37 Gravitational time dilation and light deflection from the energy metric distribution of spatial ramions 96
38 Experimental values for the muon and tau 99
39 Historical reference data 99

1 Introduction and nomenclature

P001 Ramionics, a physical theory of everything, describes the Universe as a face-centred cubic (FCC) lattice of spherical atoms of energy, termed ramions, whose energy is manifested as spacetime. Ramions have variable and even fractional spacetime dimensionalities. In our Universe, however, they have, on average, three spatial dimensions and one temporal dimension; calculations are performed using these dimensions through elementary multiplication and division.

P002 Ⓡamion: Ⓡotational Ⓐnd Linear Ⓐbsolute Ⓔnergy, Ⓐntimatter Ⓐnd Ⓜatter ⓉⓄⓃ

P003 E_s is the minimum and reference energy of ramions. The subscript s denotes the reference ramions:

P004 Ⓢettled, Ⓢpherical, Ⓢymmetric, Ⓢtandard Ramions in distant Ⓢteady-Ⓢtate Ⓢpace

P005 The energy E_r of other ramions is expressed relative to E_s as $N.E_s$. It is shown that N is the common metric of energy, space and time.

2 Theorem 0 Definition of physics

P006 In Ramionics, physics is defined as the study of: (1) the reality of the Universe; (2) the reality of its constituents; (3) the truth of the relationships between those constituents; and (4) the truth of the parameters of the Universe, including the parameters of its constituents and of the relationships between them.

P007 This definition incorporates four postulates, or axioms. (1) The Universe is real; alternatively, even if it is not real—for example, if it is a simulation, a dream or a product of someone's imagination—we are justified in treating it as real. (2) The Universe consists of real constituents, or we are justified in assuming that it does. (3) Its constituents truly interact, exchanging force and torque or, more generally, energy and information, or we are justified in assuming that they do. (4) The Universe is truly computable at each instant and observable, in the sense that its processes are computable, or we are justified in making these assumptions.

P008 Anyone who accepts this definition of physics, or a definition encompassing at least these domains, thereby accepts that these four principles are contained in the definition itself. Otherwise, they must be regarded as the axioms of Ramionics, together with Theorems 1–6 if necessary.

P009 Using only these simple, minimal principles 1–4, the corresponding philosophical and geometrical Theorems 1–4, and then Theorems 5 and 6, Ramionics derives the geometrical structure of spacetime. From this structure, the framework proceeds through elementary calculations to the fine-structure constant and even to quantum gravity.

P010 Ramionics may be represented as a triangle whose three sides are physics, philosophy and experience. Mathematics lies at the intersection of physics and philosophy. Logic and fields such as set theory connect mathematics to philosophy, whereas algebra and geometry connect it to physics. A third component, pure mathematics, underpins the other two, while its roles in physics and philosophy become apparent progressively. For example, in Ramionics the electron mass arises from prime numbers and Mersenne numbers, such as $2^5-1 = 31$, for which both 5 and 31 are prime. Within this framework, this explains why the electron mass is constant throughout the Universe and brings Mersenne numbers from pure mathematics into a fundamental aspect of physics.

P011 Experience connects physics to philosophy: its intersection with physics is reality, and its intersection with philosophy is truth.

P012 Consider a circle comprising philosophy, mathematics—from logic to algebra and geometry—physics, reality, experience and truth. Ramionics is each of these 6 foundations, grounded in the other five. It is, for example, physics grounded in reality, experience, truth, philosophy and mathematics; simultaneously, it is mathematics grounded in philosophy and physics. The same approach is used to calculate kissing numbers in different dimensions. These numbers are required to calculate spacetime structures in universes with spatial and temporal dimensionalities other than 3 and 1.

P013 Definitions of ‘real’ and ‘true’. Real entities are self-subsistent and independent. True entities depend for their existence on real entities; examples include properties such as the colour or length of a pencil, which depend on the pencil's existence and cease to be true, without any time delay, if the pencil does not exist. Reality concerns existence or non-existence: whether something is or is not real. Truth concerns the correctness or incorrectness, quantity or quality, or possession or absence of a property of a real entity. However, not every correct proposition refers to something true: correct propositions or entities that depend on something non-real are classified here as virtual rather than true.

P014 Definition of a system. A system is a partition or subset of the constituents of the Universe, usually with strong interactions, that has one or more inputs X, representing effects received from other constituents, and one or more outputs Y, representing effects exerted on them. It usually also has parameters defining its state S. The complement of this subset, comprising the other constituents of the Universe, is itself a system, termed the feedback of the first system. The first system’s outputs are inputs to its complement, whose outputs in turn provide inputs to the first system. For computational simplicity, this feedback is generally restricted to constituents that interact more strongly with the system.

P015 Definition of system computability. At a given instant, an output y can be calculated if the necessary parameters in S and X are known. Knowing more of the required parameters, and knowing them more accurately, improves the accuracy of y. Computability therefore means that the parameters of a system obey determinate quantitative relationships at every instant.

P016 Definition of system observability. Given S at time t_0 and X throughout the interval from t_0 to t_1, it must be possible to calculate S and Y over that interval; that is, the evolution of the parameters is computable. More precisely, the statement that X and S before t_0 are unnecessary means that everything the system has experienced up to t_0 can be retained only in its state: there is no additional, unexplained memory. The statement that X and S after t_1 are unnecessary means that the system is causal and has no knowledge of the future.

P017 The Universe is therefore itself a closed system: the vectors X, Y and S, or all its parameters, reduce to S, which includes all interacting constituents. Computability of the Universe means that unknown parameters can be calculated from the necessary known parameters. Its observability means that, if all its parameters are known, it must be possible to estimate or predict their states over a preceding and subsequent time interval, with an accuracy determined by that of the available knowledge.

3 Theorem 1

P018 If the Universe is real, it has at least one real quantity. As a preliminary observation, phenomena such as positive feedback, resonance, the butterfly effect and emergence require a change or fluctuation, at

either macroscopic or quantum scales, in a real quantity in order to exert a true effect on the Universe. No real entity emerges from a collection of non-real entities, however complex that collection may be.

P019 For reality is imposed in the domain of logic; it does not propagate through spacetime as a property and is neither relative nor dependent on an observer. Reality is therefore discrete, rather than continuous, variable or subject to fluctuations. The emergence of real entities from non-real entities is consequently not merely improbable, with exactly zero probability, but impossible: it is excluded not only from probability and estimation, but from the domain of possibility itself.

P020 The independence of real quantities also implies that they are absolute rather than relative. This does not concern the choice of measurement units: changing the units or scaling of a quantity plainly changes its numerical value.

4 Theorem 2

P021 If the Universe consists of real constituents, it contains at least one real quantity that is discrete or encapsulated.

P022 These capsules, or ramions, must repel one another. If they were non-interacting or mutually attractive, they would eventually merge, whereas a continuum does not admit distinct constituents in this sense. Their internal constituents must therefore also repel one another. Ramions must consequently exert pressure on one another or, even beyond this, undergo continuous expansion.

P023 If the internal constituents of ramions form a continuum, comprising differential elements of the real quantity, there is no constituent-based universe within them. If their constituents are discrete particles, however, each ramion in our Universe may itself be another universe, while our Universe may be a ramion in another universe: a hierarchy of nested universes. For the present calculations, these alternatives are equivalent, because even in the discrete case the number of particles within each ramion is sufficiently large that summation and integration are effectively indistinguishable.

5 Theorem 3

P024 If the constituents of the Universe interact with their surroundings at every location, they can exchange energy or information. Since Theorem 2 establishes that ramions exert pressure on one another or even expand, ramions must be present throughout the Universe.

P025 To set aside temporarily the complications of spatial curvature and expansion, the condition is formulated as follows: between any two particles anywhere in the Universe, there must be a chain of particles whose adjacent members can exchange energy, light and information. Geometrically, between any two points of the Universe there must be a sequence of points such that a line can be drawn between each adjacent pair.

P026 This replaces the stronger statement that any two particles anywhere in the Universe must be able to exchange energy, light and information directly, or, geometrically, that a single line can be drawn between any two points.

P027 Ramions are present everywhere: space is filled with them or, more precisely, they are filled with space. Nevertheless, gaps remain between ramions, as between pieces of fruit in a bag. These gaps are termed NonSpace. Space and NonSpace together form a superset, termed SuperSpace, with an infinite or very large number of dimensions, an exactly zero or very low energy density, and an infinite or very high

speed of light. Numerous universes may exist within SuperSpace, either widely separated or occupying different dimensions; these are parallel universes.

6 Theorem 4

P028 If the Universe is computable, physical equations must hold. Each equation contains an equality, whose justification derives from another physical equation. Ultimately, at least one balance equation between real quantities, or presentations of real quantities, must hold and provide the connection between physics and mathematics.

P029 Here, "presentation" denotes, for example, the perimeter P and area S of a circle. The balance relation between these two presentations is: $4\pi S = P^2$

P030 If the Universe is observable, something real must remain constant in time. If equations relate derivatives and hence integrals, the integration constant must be determined elsewhere. Thus, at least one real quantity, a sum of real quantities, or presentations of real quantities must be conserved.

7 Theorem 5 Energy is the only real quantity in the Universe

P031 Every physical quantity is either explicitly related to space—for example, through a length, area or volume element, or through its vector character—explicitly related to time, for example through a derivative, an integral or a factor Δt or dt, or implicitly related to spacetime, as in temperature, which arises from molecular motion. Space and time must therefore either be real quantities or have a precisely identified origin in a real quantity.

P032 Space cannot generate time, and time cannot generate space; neither has meaning without the other. Without space, there is no motion, and time is consequently unmeasurable and meaningless. If space existed without time, the temporal separation between any pair of spatial points would be zero or infinite, rendering spatial distance meaningless. The conclusion drawn here is that both space and time are non-real, and therefore relative, but true rather than virtual. Mass or energy must therefore be taken as the real quantity.

P033 Mass is defined fundamentally as a tendency towards rest. Even gravitation, which arises from mass, produces motion only transiently, until a collision is completed, whereas its steady-state response is rest. If a mass m orbits M, this occurs because m initially had a velocity that would have carried it along a straight line towards infinity, but was confined by gravity. From a distant viewpoint, it has therefore been brought towards rest relative to the motion it would have had without gravity.

P034 Energy, which is the tendency towards motion, or indeed motion itself, is therefore the answer, because it gives meaning to both space and time.

P035 Consider a ramion as energy—or, for visualisation, as a concentrated mass—composed of particles or differential elements of energy or mass. These constituents possess intrinsic motion of two types: linear and rotational. Linear motion, analogous to that of gas molecules, produces pressure and hence space. Another analogy is a spring-like molecule coiled in several dimensions, with its ends joined and motion occurring in every dimension. Rotational motion produces rotation and a reference for time. These two components do not interfere with one another: increasing the pressure in a balloon does not produce rotation, and increasing the speed or torque of a wheel does not generate a lateral force if its axle is secure. Each ramion is therefore both a quantum and a container or unit of energy, space and time.

P036 Each rotational axis represents a temporal dimension, normally one. The distinction from a clock is that the rotation of a ramion advances time, whereas time advances the hands of a clock.

P037 The numbers of spatial and temporal dimensions are not intrinsic identifiers of a ramion, because its energy is its only real quantity. Rather, the interactions and behaviour of the ramions determine how many spatial and temporal dimensions are produced.

P038 Ramions differ from balloons pressed together in that they produce space by manifesting energy in SuperSpace, whereas balloons occupy that space. Balloons contain air molecules; ramions consist of pure energy. A balloon's membrane differs in composition from its contents and has the same number of dimensions as the balloon, namely 3; treating its surface as two-dimensional is only an approximation. A ramion's boundary, by contrast, consists of the same substance as its contents—energy—but has exactly one fewer dimension.

8 Theorem 6

P039 According to Theorem 5, the only real quantity in the Universe is energy, with only two components or presentations: linear and rotational. According to Theorem 4, the only possible balance and conservation equations are therefore those stating that the linear and rotational energies are equal and that their sum is conserved throughout the Universe. More precisely:

P040 The only real quantity in the Universe is energy, which is conserved and has equal linear and rotational presentations corresponding to space and time. This balance applies to each ramion and even to every constituent of a ramion. Energy conservation is therefore proved as a theorem rather than assumed as a postulate. The energy of any constituent, or of the ramion as a whole, is:

$$E_r = 2(\text{Linear Energy}) = 2(\tfrac{1}{2}\mathring{m}_r.\mathring{c}_r^{\,2}) = \mathring{m}_r.\mathring{c}_r^{\,2}$$

P041 This is the relation expressing mass–energy equivalence, which is likewise proved as a theorem rather than assumed as a postulate.

P042 Ramionics therefore has only two fundamental equations: energy conservation and the balance between the linear and rotational energy components of each ramion, or any part of one.

P043 The linear energy component produces pressure and, consequently, space, relativity and quantised gravitation, without singularities or an assumed curvature of spacetime.

P044 The rotational energy component produces time, torque, electricity, magnetism and electromagnetism.

P045 Ramions are therefore atoms, or discrete units, of energy, space and time. Balance in the distribution of energy between the linear and rotational components represents balance between the presentation of space and that of time.

9 Definition of matter

P046 Because ramions generate space, the only way to define mass is for the ramions in a spherical region of space to undergo destruction and explosion, with their energy subsequently propagating throughout the Universe in accordance with energy conservation.

P047 Matter is not a concentration of energy. It is the result of the explosion and destruction of a number of ramions within a spherical region of space. Their energy then disperses throughout space, with a greater

fraction distributed among the nearer shells. This leaves a spherical cavity, or black hole, at the centre of the energy distribution and hence in the structure of spacetime.

P048 The only distinction between the central black holes of subatomic particles and galactic black holes is their scale; their mathematical formulation is the same.

10 Definitions of electricity and magnetism

P049 Consider a rotating ramion. Like the Earth, it has a rotation axis, north and south poles, northern and southern hemispheres, and an equatorial plane and circle. The north pole is designated the positive pole.

Ramions always exhibit a small indentation forming a shared region V_c. If like poles of two such spheres approach one another, their directions of rotation in the shared region are opposite. The resulting increase in friction reduces V_c; this effect is identified as electrical repulsion. The reverse configuration produces attraction. Electric charge is therefore another presentation of torque.

P050 Accordingly, the distribution of a static electric field through space is explained by the alignment of spatial ramions with the central charge, without requiring hypothetical field lines or photons.

P051 A photon carries an electromagnetic wave and therefore cannot by itself explain a static electric field.

P052 In Ramionics, a photon is not a real particle but an increase in the rotational energy of ramions.

P053 Magnetism is defined by rotation of the electric axis, which is the primary rotation axis, about a second axis termed the magnetic axis. This second rotation axis corresponds to a second temporal dimension, while the additional ramion energy is manifested as magnetic energy E_m.

P054 In Ramionics, the ramion is the only real particle in the Universe, energy is the only real and absolute quantity in the Universe, and the governing equations express energy conservation and the balance between linear and rotational energy.

11 The 12-wing model

P055 In the far field, all the linear and rotational energy dispersed throughout space is modelled on 12 wings surrounding a black hole of the same radius. These correspond to the twelve ramions in the first FCC shell.

12 Fundamental particle structure

P056 The 12-wing model provides a simple account of the stability of the electric charges 0, −⅓, +⅔ and −3/3 for matter particles. The signs are reversed for antimatter.

P057 Let q denote the magnitude of the full electron charge. Each electron wing carries 1/12 of q. In a stable state, each pair of opposite wings must cancel one another's torque so that the particle structure remains in rotational equilibrium. Viewed from the centre, opposite wings must therefore rotate in opposite directions. However, viewed externally from corresponding points, each close to one of the two wings, their directions of rotation are the same; they consequently carry charges of the same sign.

P058 A particle therefore has six axes, or six pairs of wings, each carrying either +q/6 or −q/6. In the neutral state, the signs alternate and the total charge is zero. At very short distances, individual wing

contributions remain distinguishable. Approaching a positive wing of a neutral particle therefore produces a local positive contribution, and the converse holds for a negative wing.

P059 Relative to the neutral state, reversing one positive axis produces a total charge of −q/3. Reversing two negative axes produces +2q/3, and reversing all three positive axes produces −q.

P060 These three states correspond, respectively, to the down quark, the up quark and the electron. Their three opposite states are the corresponding antiparticles. Including the neutral state, there are seven possible stable electric-charge states. In the electron family, the neutral structure is the electron-family naryon, denoted e_0, which is its own antiparticle. Each family therefore contains 7 stable particles. They have the same structure, radius and total energy; their only difference is the orientation of their wings, which produces different wing potentials U. This potential is subtracted from the total energy, that is, the energy of the neutral state, to obtain the rest energy.

P061 For quarks, the particle's rotation axis can belong to three distinct classes of axes, whereas all axes are equivalent for the electron.

P062 These three classes of quark axes are identified with the three QCD colours, whereas quark flavour is associated with the family and charge.

13 Particle notation

P063 Neutrino: v

P064 Example: the largest neutrino produced during the formation of the electron family:

$$\acute{\nu}_e = \nu_{480}$$

P065 This denotes a neutrino with an energy of 480 ramions on each wing.

P066 The electron family:

$$e_0 = \text{Naryon of electron family}, e_1 = d = \text{Down}, e_2 = u = \text{Up}, e_3 = e = \text{Electron}$$

P067 Hadrons: p = proton = (udu), n = neutron = (dud)

P068 The muon family:

$$m_1 = \text{Strange}, m_2 = \text{Charm}, m_3 = m = \text{Muon}(\mu)$$

P069 The tau family:

$$t_1 = \text{Bottom}, t_2 = \text{Top}, t_3 = t = \text{Tau}(\tau)$$

P070 The symbols above refer to ordinary matter. Particles with index c = 3 are leptons carrying a full negative charge; particles with index c = 1 carry charge −⅓, and those with index c = 2 carry charge +⅔, expressed in units of the magnitude of the charge of the lepton in the same family.

P071 Antiparticles are denoted by the same symbols with a tilde:

$$\tilde{e}_1 = \tilde{d} = \text{Anti} - \text{Down}, \tilde{e}_2 = \tilde{u} = \text{Anti} - \text{Up}, \tilde{e}_3 = \tilde{e} = \text{Anti} - \text{Electron}$$

$$\tilde{n} = (\tilde{d}\tilde{u}\tilde{d}) = \text{Anti} - \text{Neutron}$$

$$\tilde{p} = (\tilde{u}\tilde{d}\tilde{u}) = \text{Anti} - \text{Proton}$$

$$\tilde{m}_1 = \text{Anti} - \text{Strange}, \tilde{m}_2 = \text{Anti} - \text{Charm}, \tilde{m}_3 = \tilde{m} = \text{Anti} - \text{Muon}(\mu^+)$$

$$\tilde{t}_1 = \text{Anti} - \text{Bottom}, \tilde{t}_2 = \text{Anti} - \text{Top}, \tilde{t}_3 = \tilde{t} = \text{Anti} - \text{Tau}(\tau^+)$$

P072 Each antiparticle has the same energy as its corresponding particle; no additional energy notation is therefore required:

P073 Positron energy: E_e

14 Scale factors

P074 These 7 quantities are termed scale factors rather than physical constants because they define units such as m, s, kg and J.

[1] $c = 2.99792458 \times 10^{8}\ \mathrm{m/s}$

[2] $h = 6.62607015 \times 10^{-34}\ \mathrm{J.s}$

$\hbar = h/(2\pi)$

$\hbar = 1.05457181764616 \times 10^{-34}$

P075 The exact ramion energy, calculated from the experimental electron, proton and neutron energies, is:

[3] $E_s = \theta_e \times 9.3723441902457\ \mathrm{eV}$

P076 The approximate ramion energy, calculated using only the electron energy, is just 1.47 parts per billion higher than the exact value:

$\text{Approximated } E_s \approx \theta_e(E_{ex}/54522) \approx \theta_e \times 9.37234420399105\ \mathrm{eV}$

P077 The electron rest energy in units of E_s for the different models is:

$E_{es(A/B)} = E_e / E_{s(A/B)} = 54522$

$E_{es(C/D)} = E_e / E_{s(C/D)} = 54585$

P078 The electron energy is therefore the same under both scaling conventions:

$E_e = 0.510998949940581\ \mathrm{MeV}$

P079 At present, Ramionics uses energy scaling through E_s rather than time scaling through the caesium-133 hyperfine transition frequency. The electron energy is $54522E_s$ in models A/B and $54585E_s$ in models C/D:

$f_{cs133ht} = f_{cs} = 9.19263177 \times 10^{9}\ \mathrm{Hz}$

[4] $q_e = 1.602176634 \times 10^{-19}\ \mathrm{Coulomb}$

P080 The Boltzmann constant defines the kelvin:

[5] $K_\beta = 1.380649 \times 10^{-23}\ \mathrm{J/K}$

P081 The Avogadro constant defines the mole:

[6] $N_{av} = 6.02214076 \times 10^{23}\ 1/\mathrm{mol}$

P082 The luminous efficacy of monochromatic radiation at frequency 540×10^{12} Hz defines the candela:

[7] $K_{cd} = 683\ \mathrm{lm.W^{-1}}$

$1\ \mathrm{lm} = 1\ \mathrm{cd.sr}$

P083 At a frequency of 540×10^{12} Hz, 1 cd corresponds to a radiant intensity of 1/683 $W.sr^{-1}$ in the specified direction.

P084 The seven factors above are sufficient to define the metre, the second, the joule or kilogram, electric charge in coulombs, temperature in kelvin, amount of substance in moles, and luminous intensity in candelas.

P085 Ramionics calculates geometrically all physical constants and the parameters of the Universe and its particles solely from these scale factors, including the fine-structure constant, the Coulomb and gravitational constants, the g-factor, and particle charges, masses, radii and structures.

P086 Even f_{cs} and K_β should, in principle, be calculable from h, c and E_s. Thus, all physical constants and formulae are calculable geometrically from only these three scale factors, which are required to define the three units joule or kilogram, metre and second for energy, space and time. This follows from the Ramionics description of the Universe as capsules of energy, or ramions, that manifest space and time.

15 Empirical reference values

P087 The subscript x denotes an eⓍperimental or eⓍternal value obtained outside Ramionics. It includes experimental, theoretical, computational and combined results, such as those from QED or QCD.

P088 Ramionics does not use these values as inputs. Its values are calculated solely from the geometry of the Universe, modelled as an FCC lattice of ramions—the only real particles—and from two fundamental equations: energy conservation and the balance between linear and rotational energy. The calculated results are then compared with these external values.

P089 CODATA 2022; the default edition subscript is 2022:

[8] $\alpha_x^{-1} = 137.035999177 \pm 21 \times 10^{-9}$

$g_{ex} = 2.00231930436092 \pm 36 \times 10^{-14}$

$E_{ex} = 0.51099895069 \pm 16 \times 10^{-11}$ MeV

$E_{px} = 938.27208943 \pm 29 \times 10^{-8}$ MeV

$E_{nx} = 939.56542194 \pm 48 \times 10^{-8}$ MeV

$G_x = 6.67430 \times 10^{-11} \pm 15 \times 10^{-16}\ m^3 \cdot kg^{-1} \cdot s^{-2}$

P090 CODATA 2018 and earlier editions:

[9] $\alpha_{x2018}^{-1} = 137.035999084 \pm 21 \times 10^{-9}$

$g_{ex2018} = 2.00231930436256 \pm 35 \times 10^{-14}$

$E_{ex2018} = 0.51099895000 \pm 15 \times 10^{-11}$ MeV

$E_{px2018} = 938.27208816 \pm 29 \times 10^{-8}$ MeV

$E_{nx2018} = 939.56542052 \pm 54 \times 10^{-8}$ MeV

$G_{x2014} = 6.67408 \times 10^{-11} \pm 31 \times 10^{-16}\ m^3 \cdot kg^{-1} \cdot s^{-2}$

P091 CODATA 2022 values compared with those of 2018:

$\Delta\alpha_{x2022}^{-1} = 4.428\sigma_{2018}$

$\Delta E_{ex2022} = 4.600\sigma_{2018}$

$\Delta E_{px2022} = 4.379\sigma_{2018}$

$\Delta E_{nx2022} = 2.630\sigma_{2018}$

P092 History of the electron g-factor in CODATA:

$$g_{ex2018} = 2.00231930436256 \pm 35 \times 10^{-14}$$
$$g_{ex2014} = 2.00231930436182 \pm 52 \times 10^{-14}$$
$$g_{ex2010} = 2.00231930436153 \pm 53 \times 10^{-14}$$
$$g_{ex2006} = 2.0023193043622 \pm 15 \times 10^{-13}$$
$$g_{ex2002} = 2.0023193043718 \pm 75 \times 10^{-13}$$

P093 Changes in g_e relative to the uncertainty of the preceding adjustment:

$$\Delta g_{ex2022} = -4.686\sigma_{2018}$$
$$\Delta g_{ex2018} = +1.423\sigma_{2014}$$
$$\Delta g_{ex2014} = +0.547\sigma_{2010}$$
$$\Delta g_{ex2010} = -0.446\sigma_{2006}$$
$$\Delta g_{ex2006} = -1.280\sigma_{2002}$$

16 FCC spacetime quantisation factors

P094 Number of ramions in shell n:

[10] $$L_{(n)} = 10n^2 + 2$$

P095 Cumulative number of ramions through shell n:

[11] $$T_{(n)} = (10n^3 + 15n^2 + 11n + 3)/3$$

$IT_{(n)}$: $Ceil_{(\text{Inversed function of T})}$

P096 The volume packing factor φ is, for ramions, the factor governing the production of space from SuperSpace. The gaps between ramions constitute NonSpace, which has neither space nor time and contains no energy, or an extremely low energy density. Consequently, the speed of light there is infinite or effectively infinite. Ramionics uses this NonSpace to explain different forms of entanglement and the curvature of time.

16.1 Geometrical derivation of φ γ and β based on Theorem 19

P097 In a face-centred cubic (FCC) arrangement, the cubic unit cell can be represented by twelve sphere centres at the edge midpoints and one at the cube centre. Each edge-centred sphere is shared among four cells, so the effective number of spheres per cell is 12/4+1, or four. After an origin shift, this representation is equivalent to the conventional FCC cell.

P098 Let r denote the radius of each sphere and a the cube edge length. The face diagonal equals four sphere radii. Hence:

$$\sqrt{2}a = 4r$$
$$a = 2\sqrt{2}r$$
$$V_{cuβe} = a^3 = 16\sqrt{2}r^3$$

P099 The combined volume of the four effective spheres, divided by the cell volume, determines the volume packing fraction φ:

$$V_{spheres} = 4(4\pi r^3/3) = 16\pi r^3/3$$

$$\varphi = V_{spheres}/V_{cu\beta e} = (16\pi r^3/3)/(16\sqrt{2}r^3) = \pi/(3\sqrt{2})$$

P100 Thus, approximately 74.048 per cent of the volume is occupied by spheres in the ideal arrangement. For a large spherical region of radius R, neglecting boundary effects, the approximate number of spheres follows from the volume ratio:

$$V = 4\pi R^3/3$$

$$N(R) \approx \varphi(R/r)^3$$

P101 In the shell-counting model used by the framework, the population of shell n is $L_{(n)}=10n^2+2$. For large n, the leading term is $10n^2$ and the cumulative population is approximately $10n^3/3$. Defining an effective radial increment by $R=2\gamma rn$ and equating the volume and shell counts gives:

$$N(n) \approx 10n^3/3$$

$$n = R/(2\gamma r)$$

$$\varphi(R/r)^3 = (10/3)(R/(2\gamma r))^3$$

$$\varphi = 10/(24\gamma^3)$$

$$\gamma = \sqrt[3]{(10/(24\varphi))} = \sqrt[3]{(10\sqrt{2}/(8\pi))}$$

P102 To calculate the effective surface coverage factor β, the area of the large sphere is compared with the population scale of shell n:

$$A = 4\pi R^2 = 16\pi\gamma^2 r^2 n^2$$

$$\beta = 10n^2/(16\gamma^2 n^2) = 10/(16\gamma^2) = \sqrt[3]{(5\pi^2)}/4$$

P103 Accordingly, φ is the volume packing fraction, γ is the effective radial-step factor, and β is the effective surface coverage factor. The calculation of φ follows directly from FCC packing geometry. The derivation of γ and β additionally depends on the shell-counting law and the large-n approximation within the Ramionics model.

[12] $$\varphi = \pi/(3\sqrt{2})$$

$$\varphi = 0.740480489693061$$

P104 Radial freedom factor: γ

[13] $$\varphi = (10/8)/(3\gamma^3)$$

$$\gamma = \sqrt[3]{((10/8)/(3\varphi))} = \sqrt[3]{(10\sqrt{2}/(8\pi))}$$

$$\gamma = 0.825578509501464$$

P105 Surface coverage factor: β

[14] $$\beta = (10/8)/(2\gamma^2) = \sqrt[3]{(5\pi^2)}/4$$

$$\beta = 0.916987168493568$$

P106 Zeta sphericity and stability factor: ζ

[15] $$\zeta = \varphi/(\gamma^3 4/3) = \varphi^2/(\beta\gamma^2 8/9) = \pi^2/10$$

$$\zeta = 0.986960440108936$$

P107 Approximations:

[16] $2\beta^8 = 0.999852793457834$

$\varphi^7 2^{10}/5^3 = 0.999966117180411$

P108 Radius corresponding to surface-area halving for the ramions of the first shell:

[17] $R_{sh} = \sqrt{5}\, r_r$

P109 Indentation of two spheres of radii r and R with centre-to-centre separation D:

[18] $d = R + r - D$

$V_{common} = V_c = \pi d^2[(R + r - d)^2 + 2(R + r - d)(R + r) - 3(R - r)^2]/[12(R + r - d)]$

$d = 2r, V_c = (4/3)\pi R^3/2, x = R_v/r$ gives:

$3x^4 - 16x^3 + 18x^2 + 11 = 0$

P110 Radius corresponding to volume halving of the first FCC shell:

$R_{vh} = 2.12191578090306\, r_r$

17 Fermion generations

17.1 Origin of matter and FCC shell geometry

P111 In Ramionics, the conversion of energy into matter begins with ramion explosions and the collapse of shells in a region of the FCC lattice. This process creates an approximately spherical cavity whose surrounding, uncollapsed shells resist the forces generated by the collapse.

P112 The number of ramions in shell n and the cumulative number through that shell are:

[19] $L(0) = 1$

[20] $L(n) = 10n^2 + 2\,, n \geq 1$

[21] $T(n) = (10n^3 + 15n^2 + 11n)/3 + 1$

P113 If the strong shell 2^s halts the collapse, the last collapsed shell is 2^s-1. The released energy, in units of E_s, is:

[22] $E(s) = T(2^s - 1)$

P114 As s increases, the ratio of the energies released in consecutive stages approaches 8.

17.2 Particle character and the shared black hole of a packet

P115 During the production of particle packets in Ramionics, including fermionic packets and subsequently hadronic packets, particles are initially defined as **superposable energy-distribution patterns surrounding a shared black hole**.

P116 At this stage, the particles do not yet possess independent black holes. The energy, charge and other properties of each particle are specified by its contribution to the energy distribution of the collective structure.

P117 After the packet separates, each particle has its own black hole. The stopping shell involved in the formation of the shared packet is therefore not necessarily the stopping shell of the black hole belonging to an individual separated particle.

17.2.1 Family-index convention

P118 In Ramionics, the default family index for particle parameters such as N, ħ, α and K is the electron family. The exceptions are c and c̊, whose default index is s.

P119 Thus, when no family index is explicitly shown, parameters in the first group refer to the electron family unless another family is specified in the text.

17.3 The strong stopping shell

P120 A strong stopping shell is a shell that distributes and balances the forces and torques generated by collapse among its ramions.

P121 The more factors the shell index has, and the more fully it is expressed as a perfect power, the more accurately forces and torques are distributed. Examples are $128=2^7$ for the electron-family fermionic packet and $625=5^4$ for the hadronic stage of the same family.

P122 The more important criterion, however, is that the residual energy be small relative both to the total released energy and to the energy of the stopping shell.

P123 For the electron family, these two features coincide when shell 128 halts collapse after shell 127. On this basis, Ramionics identifies the stable particles of the three-dimensional Universe with the electron family, whose common energy, space and time metric is N = 36390.

P124 At the hadronic stage of the electron family, collapse continues through shell 624, and shell 625 is the strong stopping shell.

P125 In other families, however, the particle energies may be completed shortly before collapse reaches the strong stopping shell. The exact stopping point after shell 127 in the electron family must therefore not be generalised to other families without investigation.

17.4 The largest and most similar rule

P126 According to the largest and most similar rule, when released energy is converted into matter, preference is given to a packet whose particles are as large as possible while remaining as similar as possible both to one another and to the structure of the preceding stage.

P127 This rule is supplemented by the principle of prime-number preference: a prime particle count is preferred because a composite count permits the packet to be divided into smaller groups of equal size.

17.5 The indices s and p and packet growth

P128 The index s is the exponent specifying the strong stopping-shell index, whereas p is the exponent determining the number of particles in the packet.

[23] $$N_p = 2^p - 1$$

P129 During ordinary growth, increasing s by one increases the released energy by approximately a factor of 8. The model describes this growth as a fourfold increase in the mass of each particle and an approximately twofold increase in particle number.

P130 Thus, s and p normally increase together, and a factor of 4 appears in the genetic code of each wing.

17.6 The Mersenne barrier and Mersenne retreat

P131 Along the electron-family pathway, a 7-particle packet forms at p = 3:

[24] $2^3 - 1 = 7$

P132 The next growth step would raise p to 4, but 15=3×5 is composite and conflicts with prime-number preference. This obstacle is termed the Mersenne barrier.

P133 During a Mersenne retreat, s increases while p remains fixed. Instead of increasing the particle number, additional energy is allocated to particle growth.

P134 The composite factor 3 is accompanied by a factor of 2, producing a factor of 6. In the eightfold-growth approximation, the difference between growth factors 8 and 6 leaves 2 energy shares for use in subsequent stages.

P135 The electron-family pathway undergoes 2 Mersenne retreats.

17.7 Seven stages of electron-family packet formation

P136 At each stage, the particle count is determined by p, and the genetic code of each wing is determined by the growth factors. Each particle has 12 wings.

P137 In the final 3 stages, N includes 2 additional factors of 2, whereas the energy consumed by the packet receives only one factor of 2 because the electric factor reduces the effective rest energy.

P138 The residual energy is the difference between the released energy and the energy consumed by the packet.

[25] $\Delta E = E(s) - E_{packet}/E_s$

Table 1

s	p	Last shell	Particle count	N	Packet energy (E_s)	Released energy (E_s)	Residual (E_s)	Residual / Released	Residual / Stopper
1	1	1	1	1	12	13	1	7.7%	2.4%
2	2	3	3	4	144	147	3	2.0%	1.9%
3	3	7	7	16	1,344	1,415	71	5.0%	11.1%
4	3	15	7	96	8,064	12,431	4,367	35.1%	170.5%
5	3	31	7	576×2×2	48,384×2	104,223	7,455	7.2%	72.8%
6	4	63	15	2,304×2×2	414,720×2	853,567	24,127	2.8%	58.9%
7	5	127	31	9,216×2×2	3,428,352×2	6,909,055	52,351	0.8%	32.0%

P139 The table presents calculations for the packet-formation stage, before geometrical conversion and quantisation.

17.7.1 Stage 1 with s equal to 1

P140 Shell 2 is the stopping shell. The initial packet contains one 12-wing particle with one ramion on each wing. The released energy is $13E_s$, the packet energy is $12E_s$, and the residual energy is $1E_s$.

17.7.2 Stage 2 with s equal to 2

P141 Shell 4 is the stopping shell. A 3-particle packet forms, with 4 ramions on each wing. The released energy is $147E_s$, the packet energy is $144E_s$, and the residual energy is $3E_s$.

17.7.3 Stage 3 with s equal to 3

P142 Shell 8 is the stopping shell. A 7-particle packet forms, with 16 ramions on each wing. The released energy is $1415E_s$, the packet energy is $1344E_s$, and the residual energy is $71E_s$.

17.7.4 Stage 4 with s equal to 4

P143 Shell 16 is the stopping shell. The first Mersenne retreat occurs, and the particle count remains 7. The factor of 6 increases the code of each wing to 96. The released energy is $12431E_s$, the packet energy is $8064E_s$, and the residual energy is $4367E_s$.

17.7.5 Stage 5 with s equal to 5

P144 Shell 32 is the stopping shell. The second Mersenne retreat occurs, and p remains 3. The second factor of 6 increases the stage-specific code of each wing to 576.

[26] $N_5 = 576 \times 2 \times 2 = 2304$

[27] $E_{packet,5} = 48384 \times 2E_s = 96768E_s$

[28] $\Delta E = 104223 - 96768 = 7455$

17.7.6 Stage 6 with s equal to 6

P145 Shell 64 is the stopping shell. The index p increases to 4 and a 15-particle packet forms.

[29] $N_6 = 2304 \times 2 \times 2 = 9216$

[30] $E_{packet,6} = 414720 \times 2E_s = 829440E_s$

[31] $\Delta E = 853567 - 829440 = 24127$

17.7.7 Stage 7 with s equal to 7

P146 Shell 128 is the stopping shell. The index p increases to 5 and a 31-fermion packet forms. The number 31 is prime.

[32] $\mathring{N}_e = 9216 \times 2 \times 2 = 36864$

[33] $E_{packet,7} = 3428352 \times 2E_s = 6856704E_s$

[34] $\Delta E = 6909055 - 6856704 = 52351$

P147 The residual energy is $52351E_s$, approximately 0.8% of the total released energy and 32.0% of the stopping-shell energy.

P148 Growth pathways of the two indices:

[35] $s: 1 \rightarrow 2 \rightarrow 3 \rightarrow 4 \rightarrow 5 \rightarrow 6 \rightarrow 7$

[36] $p: 1 \rightarrow 2 \rightarrow 3 \rightarrow 3 \rightarrow 3 \rightarrow 4 \rightarrow 5$

17.8 Two additional factors of 2 and the genetic code

P149 During electron-family formation, 2 factors of 2 with different origins enter the genetic code: one arises from residual energy during the growth stages, and the other from the acquisition of electric charge and the consequent reduction in effective rest energy.

[37] $GC = 4^0.4.4.6.6.4.4 = 9216$

[38] $\mathring{N}_e = 4^0.4.4.6.6.4.4.2.2$

[39] $\mathring{N}_e = 4^4 6^2 2^2 = 36864$

P150 This code contains 4 factors of 4, two factors of 6, and two additional factors of 2.

P151 Equivalent compact representations of this genetic code are:

$\mathring{N}_e = 2^{12}3^2 = 192^2 = 36864$

P152 This representation also reveals the prime-power structure of the electron-family genetic code.

17.9 Electron-family generation

P153 The last collapsed shell is 127, and the packet contains 31 fermions.

[40] $Gen_e = 127//31 = 7/5$

$s_e = 7, S_e = 2^7 - 1 = 127$

$p_e = 5, P_e = 2^5 - 1 = 31$

P154 The symbol // is a special notation for the ratio of generation indices; it does not denote ordinary numerical division.

17.10 Packet fermion composition charge balance and the Diophantine solution

P155 The initial electron-family packet consists of 31 neutral naryons, which become up quarks, down quarks and electrons after acquiring charge.

17.10.1 Two principal balance conditions

P156 Total number of fermions:

[41] $N_u + N_d + N_e = 2^p - 1$

P157 Electric-charge neutrality:

[42] $2N_u - N_d - 3N_e = 0$

17.10.2 General Diophantine solution for odd p

P158 For odd p, the integer solutions of the two balance conditions can be parametrised by an integer k as follows:

[43] $N_e = 1 + 3k$

[44] $N_u = (2^p + 1)/3 + 2k$

[45] $N_d = (2^{p+1} - 7)/3 - 5k$

P159 For hadron formation, the numbers of up and down quarks must be consistent with the numbers of protons and neutrons. In the selected composition, each proton consists of two up quarks and one down

quark, and each neutron of one up quark and two down quarks; the number of protons equals the number of electrons.

P160 The resulting number of neutrons is:

[46] $N_n = (2^p - 5)/3 - 4k$

P161 An admissible hadronic composition requires non-negative integer numbers of protons and neutrons, with all quarks incorporated into the hadronic structure.

17.10.3 All examined cases for the 31-fermion packet

P162 For p = 5, the total number of fermions is 31. The cases examined are:

Table 2

k	Up quarks	Down quarks	Electrons	Protons	Neutrons	Result
0	11	19	1	1	9	Accepted
1	13	14	4	4	5	Accepted
2	15	9	7	7	1	Selected
3	17	4	10	10	−3	Rejected

P163 In the first three cases, the neutron count is non-negative, and the hadronic composition is possible in terms of quark counting.

P164 For k = 3, the presence of 10 electrons requires a neutron count of −3. Such a composition cannot form a hadronic packet with non-negative numbers of protons and neutrons and is therefore excluded.

17.10.4 Final selected composition

P165 For k = 2:

[47] $N_u = 15, N_d = 9, N_e = 7$

P166 In this case, the 31-fermion packet becomes the following hadronic composition:

[48] $15u + 9d + 7e \rightarrow 7p + 1n + 7e$

P167 **Selection rationale:** The k = 2 case has the fewest neutrons and the most electrons among the compositions in which all quarks can be incorporated into protons and neutrons. The k = 3 case, with 10 electrons, would require a neutron count of −3 and is excluded.

17.10.5 Transition from a fermionic to a hadronic packet

P168 The energy required to form the 31-fermion electron-family packet is supplied by the collapse of shells in the shared black-hole region through shell 127.

P169 After formation of the fermionic packet, collapse continues through shell 624. At this stage, the fermionic packet becomes a hadronic packet comprising 7 protons, one neutron and 7 electrons.

P170 Shell 625, with the structure 5^4, is the strong stopping shell for this stage.

P171 Thus, stopping shell 128 belongs to the fermionic-packet formation stage, whereas stopping shell 625 belongs to the hadronic stage of the same family. These two stages must not be identified with the stopping shell of an individual particle's independent black hole after separation.

17.10.6 General fermionic-packet formula

[49] $E_{ffp} = (2^{p-1} - 1)E_2 + (2^{p-2} + 1)E_1 + (2^{p-2} - 1)E_3$

P172 Here, E_2, E_1 and E_3 are the energies of the up quark, down quark and electron, respectively.

P173 For p = 5:

[50] $E_{ff5} = 15E_2 + 9E_1 + 7E_3$

17.11 The 12+9 energy model and particle energies in the zero-alpha approximation

P174 In the Ramionics 12-wing model, the total structural energy of each family member is 12N. The electric state is determined by the wing orientations and the charge index c.

[51] $\mathbb{U}_l = 4c(N/2)$

[52] $\mathbb{U}_p = c^2(N/2)$

[53] $\mathbb{U}_{cs} = c(4 + c)(N/2)$

P175 For an electron with c = 3:

[54] $\mathbb{U}_{es} = (12 + 9)(N/2) = 21N/2$

P176 Particle rest energies in the zero-alpha approximation:

[55] $\mathbb{E}_{cs} = 12N - \mathbb{U}_{cs}$

[56] $\mathbb{E}_{0s} = 12N$

[57] $\mathbb{E}_{es} = 3N/2$

[58] $\mathbb{E}_{us} = 6N$

[59] $\mathbb{E}_{ds} = 19N/2$

P177 The electric potential contributes negative inertia and reduces the effective rest energy without reducing the total structural energy distributed through space.

17.12 Energy ratio of charged and neutral packets

P178 Neutral-packet energy:

[60] $\mathbb{E}_{0p} = 12N(2^p - 1)$

P179 Charged-packet energy in the zero-alpha approximation:

[61] $\mathbb{E}_{ffp} = N[6(2^{p-1} - 1) + (19/2)(2^{p-2} + 1) + (3/2)(2^{p-2} - 1)]$

[62] $\mathbb{E}_{ffp} = N(23 \times 2^{p-2} + 2)$

P180 General ratio:

[63] $\mathbb{E}_{ffp}/\mathbb{E}_{0p} = (23 \times 2^p + 8)/(48(2^p - 1))$

Table 3

p	Charged / Neutral	Ratio	Percentage
2	25/36	0.694444	69.4444%
3	4/7	0.571429	57.1429%
4	47/90	0.522222	52.2222%

p	Charged / Neutral	Ratio	Percentage
5	1/2	0.500000	50.0000%
6	185/378	0.489418	48.9418%
7	123/254	0.484252	48.4252%
∞	23/48	0.479167	47.9167%

P181 For p = 5, the charged-packet energy is exactly half the neutral-packet energy.

17.13 Magnetic inertia and the energy correction

P182 In Ramionics, the magnetic inertia arising from rotating electric charge is determined in the calculation of the electron g-factor g_e.

P183 Its values for the electron, up quark and down quark are 63, 42 and 21, respectively.

[64] $$d_e = 63$$

[65] $$d_u = 42$$

[66] $$d_d = 21$$

P184 Corrected energies:

[67] $$E_{es} = 3N/2 - 63 = 54522$$

[68] $$E_{us} = 6N - 42 = 218298$$

[69] $$E_{ds} = 19N/2 - 21 = 345684$$

P185 Including magnetic inertias of 63, 42 and 21 for 7 electrons, 15 up quarks and 9 down quarks reduces the charged-packet energy by $1260E_s$.

Table 4

Quantity	Without magnetic inertia	With magnetic inertia
Neutral packet energy (E_s)	13,537,080	13,537,080
Charged packet energy (E_s)	6,768,540	6,767,280
Charged / Neutral	50.000000%	49.990692%

17.14 Packet energy balance

P186 The energy released through the last collapsed shell, 127, is $6909055E_s$.

[70] $$E(7) = T(127) = 6909055$$

P187 Using the packet energy in the zero-alpha approximation:

[71] $$\Delta E = 6909055 - 6768540 = 140515$$

P188 Using the corrected packet energy:

[72] $$\Delta E = 6909055 - 6767280 = 141775$$

P189 At the initial packet-formation stage, before geometrical conversion and quantisation, $\mathring{N} = 36864$ gives a residual energy of $52351E_s$. After geometrical conversion and quantisation to N = 36390, the residual energy is calculated from the relations above.

17.15 Fermion separation and geometrical conversion of the genetic code

P190 Before separation, the rotational inertia of the shared 12-wing structure is:

[73] $I^c = 12(½)mr^2 = 6mr^2$

P191 After separation, the fermion inertia is $(10/3)mr^2$, and the characteristic speed increases by a factor φ.

P192 Conservation of rotational energy gives:

[74] $\zeta = (6/(10/3))\varphi^2 = \pi^2/10$

[75] $\acute{N} = \zeta\mathring{N} = (\pi^2/10)\mathring{N}$

$\acute{N} = 36383.3096641758$

P193 The complete identity for the geometrical factor is:

$\zeta = \acute{N}/\mathring{N} = \pi^2/10$

17.16 Quantisation of the genetic code

P194 The metric N is the number of E_s ramions on one wing of the 12-wing structure. The total structural energy of this arrangement is 12N.

[76] $N = \mathrm{Quant}_n(\acute{N}) = \mathrm{Quant}_n((\pi^2/10)\mathring{N})$

$N = 36390$

P195 In FCC geometry, the leading term in the population of distant shells is $10n^2$, which provides the quantisation base 10.

P196 In the 12-wing structure, pairing opposite wings gives 6 independent pairs and provides the quantisation base 30.

[77] $\mathrm{LCM}(10,6) = 30$

P197 For the complete 12-wing structure:

[78] $\mathrm{LCM}(10,12) = 60$

P198 For adjacent levels separated by 60:

[79] $(\mathrm{Floor}_{60}(\acute{N}) + \mathrm{Ceil}_{60}(\acute{N}))/2 = 30 + \mathrm{Floor}_{60}(\acute{N})$

P199 Five possible quantisation functions:

[80] $\mathrm{Quant}_n(\acute{N}) \in \{\mathrm{Ceil}_{10}(\acute{N}), \mathrm{Ceil}_{30}(\acute{N}), \mathrm{Round}_{30}(\acute{N}), 30 + \mathrm{Floor}_{60}(\acute{N}), 30 + \mathrm{Round}_{60}(\acute{N})\}$

17.16.1 Definitions of the quantisation functions

P200 For a real number x and a positive quantisation step n:

P201 - **$\mathrm{Floor}_n(x)$:** the greatest multiple of n that does not exceed x.

P202 - **$\mathrm{Ceil}_n(x)$:** the smallest multiple of n that is not less than x.

P203 - **$\mathrm{Round}_n(x)$:** the multiple of n nearest to x.

P204 When x is equidistant from two adjacent multiples, the tie-breaking rule depends on the chosen rounding convention.

P205 All 5 functions yield 36390 for the electron family. The final choice of function depends on the investigation of the muon and tau families.

P206 Accordingly, none of the five functions is selected here as the definitive quantisation law for all families.

17.17 The neutrino branch

P207 Difference between the initial and quantised genetic codes:

[81] $\Delta\mathring{\mathrm{N}} = \mathring{\mathrm{N}} - \mathrm{N} = 474$

P208 Within the framework, the neutrino value is obtained by quantising this difference. Its full definition, rather than merely a reference value, is therefore:

[82] $\acute{\mathrm{v}} = \mathrm{Quant_n}(\Delta\mathring{\mathrm{N}}) = 480$

[83] $\Delta\mathrm{v} = \mathrm{Quant_n}(\Delta\mathring{\mathrm{N}}) - \Delta\mathring{\mathrm{N}} = 6$

P209 These relations express the value 480 through quantisation of the genetic-code difference. No final selection of a general quantisation function is made here.

P210 Difference between the quantised and continuous values:

[84] $\Delta\acute{\mathrm{N}} = \mathrm{N} - \acute{\mathrm{N}} = 6.6903358241907$

[85] $\Delta\mathrm{N} = \mathrm{Round}(\Delta\acute{\mathrm{N}}) = 7$

P211 Energy-conversion factors:

[86] $\acute{\mathrm{N}}/\mathrm{N} = 0.999816149056769$

[87] $\mathrm{Round}(\acute{\mathrm{N}})/\mathrm{N} = 1 - \Delta\mathrm{N}/\mathrm{N} = 0.999807639461391$

[88] $\mathrm{N}/\mathring{\mathrm{N}} = 0.987141927083333$

[89] $\mathrm{N}/(\mathrm{N} + \acute{\mathrm{v}}) = \mathrm{N}/(\mathring{\mathrm{N}} + \Delta\mathrm{v}) = 36390/36870 = 0.986981285598047$

17.17.1 Interpretation of the neutrino branch

P212 Within the Ramionics framework, the energy difference associated with conversion of the initial genetic code into the quantised code is linked to neutrino radiation when a fermion separates from the shared cavity.

P213 In this interpretation, the excess energy of each wing is emitted as neutrino radiation when the fermion separates from the shared cavity.

P214 The quantised neutrino-branch value is 480, which exceeds the reduction from the initial to the quantised genetic code by 6.

P215 The final factor also shows that the sum of the initial genetic code and the neutrino quantisation difference can be used in the denominator.

P216 These relations do not require a definitive choice among the five quantisation functions for N across all families. Nevertheless, consistency of the general function must be tested by examining the muon and tau families.

17.18 Electron-family generation results

P217 In Ramionics, particles initially form superposable energy-distribution patterns around a shared black hole; after separation, each particle has its own black hole.

P218 Two Mersenne retreats lead to s = 7 and p = 5. The final packet contains 31 fermions, and its generation is defined as 7/5.

P219 The initial genetic code of each wing is 36864. Geometrical conversion and quantisation give the metric N = 36390.

P220 The general Diophantine solution of the fermion-count and charge-neutrality conditions identifies the four examined cases for the 31-fermion packet. Of these, k = 2, with 15 up quarks, 9 down quarks and 7 electrons, is selected because it has the fewest neutrons and the most electrons among the admissible hadronic compositions.

P221 For p = 5, the charged-packet energy in the zero-alpha approximation is exactly half the neutral-packet energy; including magnetic inertia reduces the ratio to 49.990692%.

P222 Within Ramionics, the combination of the symmetry of strong shell 128, the 31-fermion structure, the energy balance and the metric N = 36390 provides the basis for selecting the electron family as the stable matter family in the three-dimensional Universe.

P223 As matter formation continues, collapse through shell 624, halted by strong shell 625, marks the transition from the fermionic packet to a hadronic packet comprising 7 protons, one neutron and 7 electrons.

P224 The neutrino branch is likewise examined in relation to the difference between the initial and quantised genetic codes and to the separation of fermions from the shared cavity.

P225 The final choice of quantisation function for N remains dependent on the investigation of the muon and tau families and their g-factors.

18 Ramion energy equation

P226 For a general ramion r:

[90] $$E_r = \hat{E}_r + \check{E}_r, \hat{E}_r = \check{E}_r, E_r = 2\hat{E}_r = 2\check{E}_r$$

$$E_r = 2\hat{E}_r = 2(½\mathring{m}_r.\mathring{c}_r^{\,2}) = \rho_r.V_r = 2P_r.V_r = 2r_r.F_r / 3 = 2(½G_r m_r^{\,2}/r_r)$$

$$E_r = 2\check{E}_r = 2(½I_r.\omega_r^{\,2}) = 2T.\Delta\theta_r = 2T \times 1\mathrm{Rad} = \{1/\theta_p\}2(½K_r q_r^{\,2}/r_r)$$

P227 Force convention: F_r is not the gravitational force; it denotes the total outward force exerted by the ramion shell. Mass convention: m_r is a hypothetical mass in the point approximation, in which the mass is assumed to be concentrated on the surfaces of a ramion's 12 wings.

P228 Notation: as a variable, r denotes the ramion radius; as a subscript, r identifies a general ramion. As a variable, R denotes the distance from the centre of the ramion chosen as the spatial origin; as a subscript, R denotes a rotational quantity.

P229 Ê: linear energy; Ĕ: rotational energy.

P230 The preceding relations apply to every ramion, including reference ramions s. Replacing the general subscript r with the reference subscript s therefore gives:

$$E_s = \hat{E}_s + \check{E}_s, \hat{E}_s = \check{E}_s, E_s = 2\hat{E}_s = 2\check{E}_s$$

$$E_s = 2\hat{E}_s = 2(\tfrac{1}{2}\mathring{m}_s.\mathring{c}_s^{\,2}) = \rho_s.V_s = 2P_s.V_s = 2r_s.F_s/3 = 2(\tfrac{1}{2}G_s m_s^{\,2}/r_s)$$

$$E_s = 2\check{E}_s = 2(\tfrac{1}{2}I_s.\omega_s^{\,2}) = 2T.\Delta\theta_s = 2T \times 1\mathrm{Rad} = \{1/\theta_p\}2(\tfrac{1}{2}K_s q_s^{\,2}/r_s)$$

P231 The rotational energy is equivalent to the work performed by torque T through an angle of one radian.

P232 E_s is the minimum value of E_r throughout the universe and the reference energy in Ramionics. A specific value of N is therefore defined for each ramion:

[91] $$E_r = N.E_s, E_{rs} = N, N \geq 1$$

P233 Thus, N is the ramion energy metric. However, ramions within the FCC lattice must also satisfy force equilibrium. For a ramion with energy metric N, the fundamental relation between energy, radius and force is

[92] $$E_r = 2r_r.F_r/3$$

P234 and the radius must therefore scale by the same factor N:

[93] $$r_r = N.r_s = N\hbar_s\mathring{c}_s/E_s, r_{rs} = N$$

P235 Thus, N is also the ramion spatial metric.

P236 The mapping from a reference ramion to a ramion of energy $N.E_s$, a wing or a particle in the universal FCC lattice is termed ramion projection. The reverse mapping is termed back-projection.

P237 Energy and space therefore both have the projection factor N.

P238 Within the same ramion, however, surface area and volume increase by the projection factors N^2 and N^3, respectively, whereas energy increases only by N. Consequently, the relative or local energy density has the projection factor N^{-2}:

[94] $$A_r = N^2.A_s, V_r = N^3.V_s, \rho_r = \rho_s/N^2$$

P239 The fundamental ramion energy relation also implies that the energy density is always twice the pressure:

[95] $$\rho_r = 2P_r$$

P240 Pressure therefore has the same projection factor N^{-2}.

P241 Consequently, $\mathring{c}_r$, the rotational or linear speed of the ramion constituents, and hence c_r, both decrease by a factor of N^2:

[96] $$P_r = P_s/N^2, \mathring{c}_r = \mathring{c}_s/N^2, c_r = c_s/N^2$$

P242 Since the spatial projection is N whereas the projection of the speed of light is N^{-2}, time is consequently dilated with a projection factor of 1/N.

P243 Planck constant: $\hbar_{rs}=N^4$.

P244 Relative local mass: $\mathring{m}_{rs}=N^5$.

P245 Gravitational constant: $G_{rs}=N^{-8}$.

P246 Relative local internal Coulomb constant: $\mathring{K}_{rs}=N^0$.

P247 This reduction in local pressure is known as gravity and provides a simple but exact explanation of quantum gravity.

P248 Viewed from a reference ramion, or from a ramion with a lower N, a ramion with a higher N and its associated physical processes appear larger and slower, corresponding to spatial expansion and time dilation. Viewed in the opposite direction, length contraction and faster time evolution are observed.

P249 Different ramions, or different observers, always obtain the same value when measuring one another's speed of light, because each observer measures the other's distance using their own time scale, or the other's time using their own distance scale. This is the principle of invariance of the speed of light.

19 Exploratory factors

P250 The θ factors are introduced for further investigation of sensitivities, derivatives, drifts, approximations and possible future corrections. θ_p concerns the ramion's structural electric potential; θ_c concerns the projection from the internal to the external speed of light; θ_h concerns the projection of the reduced Planck constant; θ_k concerns the projection of the Coulomb constant; and $\theta_{\boldsymbol{g}}$ concerns the projection of the gravitational constant. $\theta_{\boldsymbol{g}}$ also accommodates any revised calculation of the radius associated with halving the particle black hole's surface shell.

P251 All identified factors and quantisation effects associated with inertia, potential, energy, space, time and FCC geometry have been incorporated into the projections:

$$\theta_p = \theta_c = \theta_h = \theta_k = \theta_g = \theta_e = 1$$

P252 The factor θ_e is applied only to the numerical value of the fundamental energy scale E_s, rather than as an additional multiplier alongside E_s in the equations. It equals 1 in models A/B and 54522/54585 ≈ 0.998845836768343 in models C/D.

P253 Possible variations in the factors within these domains are expected to involve powers of 2, 3, 5, π, φ, β, γ or the η parameters, and hence to lie approximately between 0.1 and 10, unless they include a power of N. The θ factors are not independent, however. For example, the general expression for the fine-structure constant implies:

[97] $$\{\theta_p\theta_k/\theta_h\} = 1$$

P254 Spatial projection may also require both θ_k and θ_h to be divided by N, or both to be divided by N^2. In the first case, $\theta_{\boldsymbol{g}}$ must be divided by N^2, G_s and the ramion radius r_s multiplied by N, and the energy densities ρ_s and ρ_u divided by N^3. In the second case, $\theta_{\boldsymbol{g}}$ must be divided by N^4, G_s and r_s multiplied by N^2, and ρ_s and ρ_u divided by N^6.

20 Speed of light and internal speed of the energy constituents

P255 $\mathring{c}$ denotes the rotational or linear speed of the energy constituents within a ramion; c denotes the linear speed of light in FCC space. The default subscript for c and $\mathring{c}$ is s, whereas the default family subscript for particle parameters is e.

[98] $$c_r = \{\theta_c\}\mathring{c}_r/\varphi, c_s = c, \mathring{c}_s = \{1/\theta_c\}\varphi c$$

P256 For a ramion of energy NE_s, both speeds have the ramion projection factor N^{-2}:

[99] $$c_r/c_s = \mathring{c}_r/\mathring{c}_s = 1/N^2$$

P257 Thus, N, as the metric of energy, space and time, is larger near a black hole than in the far field, while the pressure is lower. Quantum gravity therefore arises directly from the pressure gradient, analogously to Archimedean buoyancy or as expressed through Gauss's relation.

21 Mass and charge distributions over the twelve wings

P258 Mass and electric charge are distributed over the surfaces of the twelve wings uniformly and cosinusoidally, respectively. The corresponding inertial factors, or the factors governing the mass and magnetic moments, multiply $M.r^2$ and $Q.r^2$ as follows, where r is the wing radius:

[100] $\mathrm{Iws} = 10/3, \mathrm{IhwCosD} = 32/9$

22 Planck constant

P259 Within the model, as soon as a ramion acquires more linear energy than its neighbours, it increases its number of spatial dimensions. If it acquires additional rotational energy, it creates a second rotation axis perpendicular to the first, corresponding to a second time dimension. The first axis is electric and the second is magnetic.

[101] $\mathrm{d}\theta/\,\mathrm{dt} = \mathrm{d}\theta/\,\mathrm{dt}_1 + \mathrm{d}\theta/\,\mathrm{dt}_2$

[102] $\omega_{(\mathrm{total})} = \omega + \omega_\mathrm{m}$

P260 The total rotational energy after the second axis is established is:

[103] $\check{\mathrm{E}}_\mathrm{r} + \mathrm{E}_\mathrm{m} = ½\mathrm{I}_\mathrm{r}(\omega + \omega_\mathrm{m})^2$

P261 The additional rotational energy, identified as magnetic energy, is:

[104] $\mathrm{E}_\mathrm{m} = ½\mathrm{I}_\mathrm{r}((\omega + \omega_\mathrm{m})^2 - \omega^2)$

[105] $(\omega + \omega_\mathrm{m})^2 = \omega^2 + 2.\omega.\omega_\mathrm{m} + {\omega_\mathrm{m}}^2$

[106] $\mathrm{E}_\mathrm{m} = ½\mathrm{I}_\mathrm{r}(2.\omega.\omega_\mathrm{m} + {\omega_\mathrm{m}}^2)$

[107] $\mathrm{E}_\mathrm{m} = \mathrm{I}_\mathrm{r}.\omega.\omega_\mathrm{m}(1 + \omega_\mathrm{m}/(2\omega))$

P262 The introduction of the second axis and time dimension therefore generates the linear term $\mathrm{I}_\mathrm{r}.\omega.\omega_\mathrm{m}$ in the additional energy.

P263 Mechanical definition of the reduced Planck constant

[108] $\hbar_\mathrm{r} = \mathrm{I}_\mathrm{r}.\omega_\mathrm{r}$

[109] $\hbar_\mathrm{r}.\omega_\mathrm{r} = \mathrm{I}_\mathrm{r}.{\omega_\mathrm{r}}^2$

[110] $\hbar_\mathrm{r}.\omega_\mathrm{r} = \mathrm{E}_\mathrm{r}$

[111] $\omega_\mathrm{r} = \mathring{c}_\mathrm{r}/\mathrm{r}_\mathrm{r}$

[112] $\hbar_\mathrm{r} = \mathrm{E}_\mathrm{r}\mathrm{r}_\mathrm{r}/\mathring{c}_\mathrm{r} = \mathrm{I}_\mathrm{r}.\omega_\mathrm{r}$

P264 Complete photon energy relation

P265 Substituting the mechanical definition of $\hbar_\mathrm{r}$ into the expression for the additional rotational energy gives:

[113] $\mathrm{E}_\mathrm{m} = \hbar_\mathrm{r}.\omega_\mathrm{m}(1 + \omega_\mathrm{m}/(2\omega))$

[114] $\mathrm{E}_\mathrm{m} = \hbar_\mathrm{r}.\omega_\mathrm{m} + \hbar_\mathrm{r}.{\omega_\mathrm{m}}^2/(2\omega)$

P266 In the low-energy limit:

[115] $\omega_m \ll \omega$

[116] $E_m \approx \hbar_r . \omega_m$

P267 The ramion projection of the Planck constant follows directly from $E_r/E_s=N$, $r_r/r_s=N$ and $\mathring{c}_r/\mathring{c}_s=N^{-2}$:

[117] $\hbar_r/\hbar_s = N^4$

P268 For the projection from a ramion to a wing, the ratio of rotational inertias introduces a factor of 5:

[118] $I_e/I\omega = (10/3)/(⅔) = 5$

P269 The factor φ converts the internal linear or rotational speed of a ramion or wing to the speed of light measured in FCC space. Thus, before projecting from a wing to a particle:

[119] $\hbar\omega = \hbar_s 5\varphi N^4$

P270 Projection from one wing to the complete particle involves two independent factors of 12.

P271 For the first factor of 12, the inertial coefficient 10/3 associated with the larger particle radius has already been included at the wing stage. The remaining factor of 12 arises because the mass of the complete particle is 12 times that of a single wing, introducing the corresponding factor of 12 into the rotational inertia.

P272 The second factor of 12 arises independently from ω. A particle exhibits greater time dilation than a single wing; its rotational period therefore acquires the corresponding factor of 12, producing the second factor of 12 in the projection of the Planck constant.

P273 In addition, all energy emitted by the electron is treated as rotational energy, introducing an independent factor of 2.

P274 The complete projection is therefore:

[120] $\hbar_e/\hbar_s = \{\theta_h/\theta_c\}N^4 2 \times 12^2 5\varphi$

[121] $\hbar_s = \{\theta_c/\theta_h\}\hbar_e/[N^4 2 \times 12^2 5\varphi]$

[122] $\hbar_s = 5.63990549106575 \times 10^{-56}\ \mathrm{J.s}$

P275 The radius of the stable ramion follows directly from the mechanical Planck relation:

[123] $r_s = \hbar_s \mathring{c}_s/E_s$

[124] $r_s = {\theta_e}^{-1} 8.33772422647155 \times 10^{-30}\ \mathrm{m}$

P276 The energy density of the stable ramion is:

[125] $\rho_s = E_s/((4/3)\pi {r_s}^3)$

[126] $\rho_s = {\theta_e}^4 6.18482525983801 \times 10^{68}\ \mathrm{J/m^3}$

P277 The mean energy density of the universe is:

[127] $\rho_u = \varphi\rho_s$

[128] $\rho_u = {\theta_e}^4 4.57974243707115 \times 10^{68}\ \mathrm{J/m^3}$

23 Quantisation of the wing potential

P278 A wing satisfies the fundamental ramion equations, but its quadratic structural potentials, q^2 and $\mathring{m}^2$, are divided by the discrete potential factor η^2.

P279 For Q=Nq, the derivation is:

[129] $E_{(\text{continuous})} = KQ^2/(2r) = KN^2q^2/(2r)$

[130] $E_{(\text{discrete})} = Kq^2/r\sum_{n=0}^{N-1} n = KN_{(N-1)}q^2/(2r)$

P280 Therefore:

[131] $\eta^2 = E_{(\text{discrete})}/E_{(\text{continuous})} = 1 - 1/N, \eta = \sqrt{(1 - 1/N)}$

[132] $1/\eta^2 = 1/(1 - 1/N), \eta\omega = \sqrt{(1 - 1/(\omega N))}$

$\text{Default}\ \eta = \eta_1$

P281 Relative $\eta\omega$ factors for a single particle: $\eta_{12/9}$, $\eta_{12/4}$, $\eta_{12/1}$, $\eta_{6/1}$, $\eta_{4/1}$, $\eta_{2/1}$.

P282 Relative $\eta\omega$ factors for two particles: $\eta_{6/1me}=\eta_{6/1m}/\eta_{6/1e}=\eta_{6/1m}/\eta_{6/1}$; the corresponding expression for t is analogous.

24 Electric charge projection

P283 The electric charge of a ramion of energy NE_s is:

[133] $q_r/q_s = N$

P284 Each particle is represented by 12 wings, and each wing models N ramions. Charge conservation therefore gives:

[134] $q_e/q_s = 12N$

25 Coulomb constant projection

P285 $\mathring{K}$ is the local internal Coulomb constant of a ramion; K is the external Coulomb constant of the FCC distribution. From the structural electric energy:

[135] $E_r = \{1/\theta_p\}\mathring{K}_r {q_r}^2/r_r$

P286 Using $E_r/E_s=N$, $q_r/q_s=N$ and $r_r/r_s=N$:

[136] $\mathring{K}_r/\mathring{K}_s = 1$

$\mathring{K} \propto N^0$

P287 The external inverse-square interaction has the surface projection factor N^2. FCC surface coverage introduces the factor $\beta/(4\pi)$, and quantisation of the wing potential introduces η^{-2}:

[137] $K_e/\mathring{K}_s = \{\theta_k\}N^2\beta/(4\pi\eta^2)$

$K_e = \{\theta_k\}\mathring{K}_s N^2\beta/(4\pi\eta^2)$

26 Calculation of the fine-structure constant α

P288 For the reference ramion:

[138] $\alpha_s = \mathring{K}_s {q_s}^2/(\hbar_s \mathring{c}_s)$

P289 Using the reference structural electric-energy relation together with $E_s r_s=\hbar_s \mathring{c}_s$:

[139] $\alpha_s = \{\theta_p\}1$

P290 For a general ramion, $\mathring{K}_{rs}=1$, $q_{rs}=N$, $\hbar_{rs}=N^4$ and $\mathring{c}_{rs}=N^{-2}$. Ramion projection therefore leaves α invariant:

[140] $\alpha_r/\alpha_s = 1$

P291 For the electron family:

[141] $\alpha_e = K_e {q_e}^2/(\hbar_e c)$

P292 Substituting the projections of charge, the Coulomb constant, the reduced Planck constant and speed cancels all factors of N^4, 12^2 and φ:

[142] $\alpha_e/\alpha_s = \{\theta_k/\theta_h\}\beta/(40\pi\eta^2)$

[143] $\alpha_e = \{\theta_p\theta_k/\theta_h\}\beta/(40\pi\eta^2)$

[144] $\alpha = \beta/[40\pi(1-1/N)]$

$\alpha^{-1} = 160\sqrt[3]{(\pi/5)(1-1/N)} = 137.035999207833$

${\alpha_x}^{-1} = 137.035999177$

$\Delta\alpha = -1.46825075418451\sigma$

$\alpha = 0.00729735256268951, \alpha_x = 0.00729735256433142$

P293 The N^{∞} limit:

[145] ${\alpha^{\infty}}^{-1} = 40\pi/\beta = 137.039765071122$

P294 Correction factors for experimental results, or for matching the geometric calculations of Ramionics to those results, based on the difference in α:

[146] $\dot{\alpha}_\beta = \sqrt{(\alpha_\beta/\alpha_{ex})}$

$\dot{\alpha} = \dot{\alpha}_e = \sqrt{(\alpha_e/\alpha_{ex})} = 0.999999999887499$

$\ddot{\alpha}_\beta = \sqrt{(\alpha_\beta/\alpha_e)} = \eta_e/\eta_\beta = \eta_{e\beta}$

$\ddot{\alpha}_e = 1$

P295 The exact Coulomb constant obtained using the exact value of α:

[147] $K_e = \alpha\hbar c/{q_e}^2$

$K_e = 8.98755178414663 \times 10^9$

Mutual $K = K_e(1-1/N_e)/\sqrt{((1-1/N_1)(1-1/N_2))}$

27 Gravitational constant

P296 From the fundamental ramion relation:

[148] $E_s = G_s {\mathring{m}_s}^2/r_s, E_s = \mathring{m}_s {\mathring{c}_s}^2$

P297 Therefore:

[149] $\mathring{m}_s = E_s/{\mathring{c}_s}^2$

[150] $G_s = r_s {\mathring{c}_s}^4/E_s$

P298 Using $E_s r_s = \hbar_s \mathring{c}_s$:

[151] $r_s = \hbar_s \mathring{c}_s/E_s$

P299 Therefore:

[152] $G_s = \hbar_s \mathring{c}_s{}^5 / E_s{}^2$

P300 Substitution of the ramion projections gives:

[153] $G_s = \{1/(\theta_h \theta_c{}^4)\} \hbar_e c^5 \varphi^4 / [10 \times 12^2 N^4 E_s{}^2]$

[154] $G_s = \theta_e{}^{-2} 1.34842313721857 \times 10^{22}\ m^3.kg^{-1}.s^{-2}$

27.1 Volume-distribution gravitational constant G_{sv}

P301 For a spherical volume distribution:

[155] $E_s = (6/5) G_{sv} \mathring{m}_s{}^2 / r_s$

P302 Therefore:

[156] $G_s = (6/5) G_{sv}$

[157] $G_{sv} = (5/6) G_s$

[158] $G_{sv} = \theta_e{}^{-2} 1.12368594768214 \times 10^{22}\ m^3.kg^{-1}.s^{-2}$

27.2 FCC geometry for gravitational projection

P303 The FCC surface and cumulative-volume functions are:

[159] $\ddot{A}_{(n)} = 10n^2 + 2$

[160] $\forall_{(n)} = (10n^3 + 15n^2 + 11n + 3)/3$

P304 The physical surface area, radius and volume are:

[161] $A_{\dot{w}} = \beta \pi r_r{}^2 \ddot{A}_{\dot{w}}$

[162] $R = 2\gamma r_r \dot{R}_{\dot{w}}$

[163] $V_{\beta h} = \varphi (4\pi r_r{}^3/3) \forall_{\beta h}$

P305 The geometric identities used in the simplification are:

[164] $\beta^2 \gamma / \varphi = 15/16$

[165] $2\beta/3 = \varphi\gamma$

27.3 The 12N model

P306 Each wing models N ramions, whereas the complete central cavity corresponds to 12N:

[166] $N = 36390$

[167] $12N = 436680$

P307 For one wing:

[168] $\forall^{-1}{}_{(N)} = 21.67846404422435$

P308 The mean surface radius is:

[169] $\dot{R}_{\dot{w}} = \text{Floor}_{(\forall^{-1}(N))} + 0.5 = 21.5$

[170] $\ddot{A}_{\dot{w}} = \ddot{A}_{(21.5)} = 4624.5$

P309 For the complete central cavity:

[171] $\text{V}^{-1}{}_{(12\text{N})} = 50.28575056910184$

P310 The first complete FCC shell containing the entire population 12N is:

[172] $\text{R}_{\beta\text{h}} = \text{Ceil}_{(\text{V}^{-1}(12\text{N}))} = 51$

[173] $\text{V}_{\beta\text{h}} = \text{V}_{(51)} = 455363$

P311 Although the population associated with the central cavity before shell completion is 12N=436680 ramions, extending the black-hole radius to the first complete FCC shell adds the following number:

[174] $\Delta\text{V}_{\beta\text{h}} = \text{V}_{(51)} - 12\text{N} = 455363 - 436680 = 18683$

P312 This is the number of ramions added at, or very close to, the black-hole surface of particles in the electron family. They are excluded from the wing calculations because their gravitational interaction is governed by G_s rather than G: it is stronger by a factor of order N^8 and correspondingly acts over a much shorter range. This identifies one source of the strong, short-range forces between particles. The greater-than-usual spatial expansion also explains why short distances correspond to fewer shells, even when calculating the electric force, and hence why that force is greatly enhanced.

P313 The gravitational projection is:

[175] $\text{G}_{12}\text{V}_{\beta\text{h}}/[(12\text{A}\mathcal{w})^2\text{R}^2] = \{\theta_\text{g}/(\theta_\text{h}{\theta_\text{c}}^4)\}\varphi\text{G}_{\text{sv}}/[2{\text{r}_\text{r}}^3\text{R}\mathcal{w}^2\text{N}^8(1-1/\text{N})]$

P314 Using the spherical-volume relation:

[176] $\text{G}_{12}/\text{G}_\text{s} = \{\theta_\text{g}/(\theta_\text{h}{\theta_\text{c}}^4)\}80\beta\text{A}\mathcal{w}^2\text{R}/[{\text{r}_\text{r}}^2\text{R}\mathcal{w}\text{V}_{\beta\text{h}}\text{N}^8(1-1/\text{N})]$

P315 Using the FCC geometric relations:

[177] $\text{G}_{12}/\text{G}_\text{s} = \{\theta_\text{g}/(\theta_\text{h}{\theta_\text{c}}^4)\}\beta(225/2)\pi{\text{Ä}_{(21.5)}}^2/[\text{V}_{(51)}\text{N}^8(1-1/\text{N})]$

[178] $\text{G}_{12}/\text{G}_\text{s} = 4.94986063724705 \times 10^{-33}$

[179] $\text{G}_{12} = {\theta_\text{e}}^{-2}6.67450660927138 \times 10^{-11}\ \text{m}^3.\text{kg}^{-1}.\text{s}^{-2}$

P316 Comparison with the experimental value gives:

[180] $\text{G}_\text{x} = (6.67430 \pm 0.00015) \times 10^{-11}\ \text{m}^3.\text{kg}^{-1}.\text{s}^{-2}$

[181] $\Delta\text{G}_{12} = +1.377\sigma = +30.96\ \text{ppm}$

27.4 The N model compared with the principal 12N model

P317 Each wing models N/12 ramions, and the central cavity models N ramions:

[182] $\text{N}\mathcal{w} = \text{N}/12 = 3032.5$

[183] $\text{V}^{-1}{}_{(\text{N}/12)} = 9.17759323904235$

[184] $\text{R}\mathcal{w} = 9.5$

[185] $\text{Ä}\mathcal{w} = \text{Ä}_{(9.5)} = 904.5$

P318 For the central cavity:

[186] $\text{V}^{-1}{}_{(\text{N})} = 21.67846404422435$

[187] $\text{R}_{\beta\text{h}} = 22$

[188] $\text{V}_{\beta\text{h}} = \text{V}_{(22)} = 37995$

P319 Relative to the 12N model, the projection is multiplied by 2/β.

[189] $G_1/G_s = \{\theta_g/(\theta_h{\theta_c}^4)\}160A\mathcal{w}^2R/[{r_r}^2\mathcal{R}\mathcal{w}V_{\beta h}N^8(1-1/N)]$

[190] $G_1/G_s = \{\theta_g/(\theta_h{\theta_c}^4)\}225\pi\ddot{A}_{(9.5)}{}^2/[\mathcal{V}_{(22)}N^8(1-1/N)]$

[191] $G_1/G_s = 4.94969654682149 \times 10^{-33}$

[192] $G_1 = {\theta_e}^{-2}6.67428534594496 \times 10^{-11}\ \mathrm{m^3.kg^{-1}.s^{-2}}$

[193] $\Delta G_1 = -0.09769\sigma = -2.196\ \mathrm{ppm}$

28 The 12+9 potential model in the zero-alpha approximation

P320 Notation: parameters such as energy, potential, mass and the gyromagnetic factor are denoted by double-struck symbols in the zero-alpha approximation.

P321 The exact value of each parameter, with α taken into account, is constructed from its zero-alpha value.

P322 Particle charge index c: the values 3, 2, 1 and 0 correspond, respectively, to particles with charges ±3/3, ±⅔, ±⅓ and zero, exemplified by the electron, up quark, down quark and narions.

P323 In the neutral state, the reference potential surface comprises 24(N/2) half-wings, with equal numbers of positive and negative half-wings, so that its net charge is zero. To create a particle of type c, c axes are reversed and the resulting charge is placed on the same reference surface.

P324 The linear contribution arises from placing charge on the reference surface. For an electron, with c=3, this contribution is 12(N/2). Each axis therefore contributes 4(N/2), and for c axes:

[194] $\mathbb{U}_l = 4c(N/2)$, OldName: $\mathbb{m}_{12}$

P325 The quadratic contribution arises from the mutual potential of the additional charges generated by axis reversal. Each axis adds 2 half-wings; c axes therefore produce 2c half-wings, equivalent to c complete wings of effective charge. Since electric potential energy is proportional to the product of the charges:

[195] $\mathbb{U}_p = c^2(N/2)$, OldName: $\mathbb{m}_9$

P326 The total potential in the zero-alpha model is therefore:

[196] $\mathbb{U}_{cs} = \mathbb{U}_l + \mathbb{U}_p = (4c + c^2)(N/2) = c(4 + c)(N/2)$

P327 For the electron, c=3:

$$\mathbb{U}_{es} = (12 + 9)(N/2) = 21N/2$$

P328 Thus, 12 represents the linear contribution from placing charge on the reference surface, and 9 represents the quadratic contribution from the interaction among the added charges. The same reasoning gives the structures 8+4 and 4+1 for c=2 and c=1, respectively.

P329 For the electron, this model introduces two potential contributions, or channels, into the exact formulae: 4/7 for the linear term and 3/7 for the quadratic term.

c=0: neutral state, corresponding to the naryon of the electron, muon or tau family.

$\mathbb{U}_l = 0, \mathbb{U}_p = 0, \mathbb{U}_{0s} = 0, \mathbb{E}_{0s} = 12N$

c=3: electron, muon and tau:

$\mathbb{U}_l = 12N/2 = 6N, \mathbb{U}_p = 9N/2$

$\mathbb{U}_{3s} = 21N/2, \mathbb{E}_{3s} = 3N/2 = \mathbb{E}_{0s}/8$

c=2: up, charm and top:

$\mathbb{U}_p = (4/9)(9N/2) = 2N$

$\mathbb{U}_l = (⅔)(12N/2) = 4N$

$\mathbb{U}_{2s} = 6N, \mathbb{E}_{2s} = 6N = 4\mathbb{E}_{3s} = \mathbb{E}_{0s}/2$

c=1: down, strange and bottom:

$\mathbb{U}_p = (1/9)(9N/2) = N/2$

$\mathbb{U}_l = (⅓)(12N/2) = 2N$

$\mathbb{U}_{1s} = 5N/2, \mathbb{E}_{1s} = 19N/2 = (19/3)\mathbb{E}_{3s} = \mathbb{E}_{0s}(19/24)$

P330 Relative-energy notation:

$\mathbb{E}_{es} = \mathbb{E}_e/\mathbb{E}_s$

$\mathbb{E}_{es} = \mathbb{E}_{3s} = \mathbb{E}_{0s}/\mathbb{E}_{03}$

$\mathbb{E}_{23} = 12/3, \mathbb{E}_{13} = 19/3, \mathbb{E}_{31} = 3/19$

$\mathbb{U}_{23} = 12/21, \mathbb{U}_{13} = 5/21$

29 The 12+9 potential model including α

[197] $d_e = \text{Floor}((3N/2)(\alpha/6)(1 - 3\alpha/(4/7)))$

$d_e = 63 = 9(4 + 3) = 36 + 27$

$E_{es} = 3N/2 - (36 + 27) = 54522$

$E_{us} = 12N/2 - d_u = 12N/2 - 42$

$E_{us} = 218298$

$E_{ds} = 19N/2 - d_d = 19N/2 - 21$

$E_{ds} = 345684$

$EDU = E_{ds} - E_{us} = 127386$

30 Electron gyromagnetic factor g_e

P331 Zero-alpha approximation and the origin of electric inertia as negative mass

P332 In Ramionics, members of an electric family, including the electron and the corresponding up and down quarks, are assumed to share the same fundamental wing structure, radius and metric N. This identity is required so that differences in electric charge arise from different wing orientations within a common structure, rather than from differences in the particles' fundamental structures. Electrical neutralisation

within the neutron structure can then correspond to the combined electric effects of a proton and an electron.

P333 The total energy of each particle in the neutral state equals the structural energy 12N. This total energy is distributed through space and is responsible for the particle's modification of the spacetime metric. Consequently, the electric potential associated with wing orientation, $\mathbb{U}$, is not subtracted from this total distributed energy. Differences in rest mass among family members therefore do not imply differences in N, radius or total structural energy.

P334 The electric potential $\mathbb{U}$ arises from alignment of the wing ramions with the central charge. Alignment increases ramion indentation and, consequently, their shared volume. This increase in shared volume is accompanied by a reduction in ramion pressure, and the energy released by the process supplies the electric potential associated with wing orientation.

P335 This behaviour is consistent with the ramion's response to a change in energy. When a ramion must carry energy greater than $\mathbb{E}_s$, it generates spacetime expansion to accommodate the excess. Conversely, a reduction in energy or pressure does not imply a reduction in the metric already generated; the ramion responds by increasing indentation and shared volume. The potential energy associated with wing orientation is therefore supplied without reducing the total energy 12N distributed through space.

P336 In inertial terms, $\mathbb{U}$ acts as a negative mass contribution. Rather than reducing the particle's total structural energy, it reduces its rest energy and effective inertia. Consequently, in the calculation of $\mathbb{g}$, this contribution appears with a negative sign in the denominator of g.

P337 In Ramionics, the dsk or double-stroke notation identifies baseline parameters under the zero-alpha assumption. These provide the reference values about which Taylor expansions or more accurate approximations can be constructed. Thus, zero-alpha denotes the baseline and reference point for expansions or calculations, rather than the exclusion of higher-order dependencies.

31 Zero-alpha approximation for $\mathbb{g}_e$

[198] $\mathbb{g}_e = \mathrm{IhwCosD}/(\mathbb{E}_{03}.\mathrm{Iws} - (\mathbb{E}_{03} - 1).\mathrm{IhwCosD})$

P338 The coefficient $\mathbb{E}_{0c}$ determines the electric orientation potential and hence the negative inertial contribution associated with the electric state of the family member:

[199] $\mathbb{E}_{0c} = 24/(24 - 9(c/3)^2 - 12(c/3))$

P339 Equivalently:

$$\mathbb{E}_{0c} = 1/[1 - (9/24)(c/3)^2 - (1/2)(c/3)]$$

P340 For c=3, the negative electric inertial contribution reduces the denominator, yielding the Dirac value for leptons in the zero-alpha approximation:

$$c = 3, \mathbb{g}_e = 2$$

P341 Thus, $\mathbb{g}_e$=2 results from the balance between positive structural inertia and negative inertia associated with the electric potential of wing orientation.

P342 In the absence of α, the electric potential arising from the arrangement of charges on the wing surface produces an electric inertial contribution. In its effect on rotational motion, this contribution behaves like a negative mass: it reduces the effective inertia. It enters with the same inertial coefficient

associated with the electric-charge distribution on the wing surface and therefore increases g by reducing the denominator.

32 Exact calculation of g including α

P343 When α is included, a further mechanism contributes to this negative inertia. The rotating electric field generates a magnetic field, which in turn feeds back into the system. In the model, this feedback produces an additional reduction in effective inertia, whose magnitude is specified by d.

P344 This second contribution is termed magnetic inertia or alpha inertia.

P345 Model A therefore distinguishes two sources of the increase in g: negative electric inertia, which exists even in the zero-alpha limit, and α-dependent negative magnetic inertia, introduced through d. Both increase g by reducing the effective inertia.

P346 In the simplest formula for calculating d without the α effect:

[200]) $g = (3N/2 - d)/(3N/4 - d)$

g: 2.0023136671624524

$g_{ex} = 2.00231930436092$

P347 The correction factor for the difference between each particle's α and the experimental value is:

[201] $\dot{\alpha}_\beta = \sqrt{(\alpha_\beta/\alpha_{ex})}$

P348 The factor describing the effect of the α metric in the calculation of g is:

[202] $\ddot{\alpha}_\beta = \sqrt{(\alpha_\beta/\alpha_e)} = \eta_e/\eta_\beta = \eta_{e\beta}$, $\ddot{\alpha}_e = 1$

$\ddot{\alpha}_\beta{}^{2\acute{k}} \approx (1 - \acute{k}/N_e)/(1 - \acute{k}/N)$

P349 An alternative form of the α-feedback factor is:

$F = (1 - \alpha/\acute{k})/(1 - \alpha_e/\acute{k})$

32.1 Main Formula Single-Channel Model

[203] $g = \ddot{\alpha}_\beta{}^{-2}(3N/2 - d)/(3N/4 - d\{1 + (\alpha/6)(1 + 2d/(7N(1 - \alpha/6)))\}), N = 30 + \mathrm{Floor}_{60}(\mathring{N}),$
$N_e = 36390, d_e = 63, \alpha_e{}^{-1} = 137.03599920783327, g_e = 2.0023193043609084, \Delta g_e$
$= -0.03\sigma = -5.79\mathrm{ppq}, N_m = 517470, d_m = 881, \alpha_m{}^{-1} = 137.03950024462935, g_m$
$= 2.0023318815920352, \Delta g_m = +49.22\sigma = +20.16\mathrm{ppb}, N_t = 2069790, d_t = 3554, \alpha_t{}^{-1}$
$= 137.03969886161988, g_t = 2.0023543449998216, \Delta g_t = -0.75\sigma = -37.46\mathrm{ppb}$

32.1.1 Magnetic Negative Mass in the Main Model

$d = \mathrm{mRound}_2(\acute{d}), \acute{d} = (cN/2)\alpha/(6(1 - \alpha/6))(1 - M\alpha(1 + c/4)^2/(4/5)^0), M = 3 \text{ or } c$

P350 The mRound₂ function rounds $\acute{d}$ so that the rest mass, 12N−c(4+c)N/2−d, is rounded to the nearest even integer.

P351 $4/5=\sqrt{((4/7)^2/((4/7)^2+(3/7)^2))}$

P352 $(4/5)^0=1$

P353 In some models, M: 3 gives d_u:42, whereas M:c may give d_u:43. The proton-energy calculations confirm the value 42. In the principal model, however, independently of M:

P354 $\therefore d\mathcal{d}$=21, d_u=42, N_e=36390,d_e=63, N_m=517470, d_m=881, N_t=2069790, d_t=3527

32.1.2 Anomaly Correction Based on Rest-Mass Quantisation in the Main Model

P355 $\dot{g}=2+F(\ddot{\alpha}_\beta^{-2}.g-2)$

$$g = (3N/2 - d)/(3N/4 - d.R)$$

$$F = (1 - 1/(3N_e/2))/(1 - 1/(3N/2))$$

$$d_m = 881, d_t = 3527$$

P356 $\dot{g}_e$=2.002319304360908

P357 $\dot{g}_m$=2.002331841876002

P358 $\dot{g}_t$=2.002336787150003

$$\Delta\dot{g}_e = -0.032\sigma$$

$$\Delta\dot{g}_m = +0.788\sigma$$

$$\Delta\dot{g}_t = -176.328\sigma$$

32.1.3 Main model for N=Ceil$_{30}$($\mathring{N}$)

$$N_t = 2069820, d_t = 3528, \Delta\dot{g}_t = -169.75\sigma$$

32.1.4 Main Model with Internal Exponent 2 Instead of 1

[204] $g = \ddot{\alpha}_\beta^{-2}(3N/2 - d)/(3N/4 - d\{1 + (\alpha/6)(1 + 2d/(7N(1 - \alpha/6))/2)^2\}), N$
$= 30 + \text{Floor}_{60}(\mathring{N}), N_e = 36390, d_e = 63, \alpha_e^{-1} = 137.03599920783327, g_e$
$= 2.002319304361254, \Delta g_e = +0.93\sigma = +166.81\text{ppq}, N_m = 517470, d_m = 881, \alpha_m^{-1}$
$= 137.03950024462935, g_m = 2.0023318815923634, \Delta g_m = +49.22\sigma = +20.16\text{ppb}, N_t$
$= 2069790, d_t = 3554, \alpha_t^{-1} = 137.03969886161988, g_t = 2.0023543450001586, \Delta g_t$
$= -0.75\sigma = -37.46\text{ppb}$

32.1.5 Main Model with Internal Exponent ½ Instead of 1

[205] $g = \ddot{\alpha}_\beta^{-2}(3N/2 - d)/(3N/4 - d\{1 + (\alpha/6)(1 + 2d/(7N(1 - \alpha/6))/½)^{1/2}\}), N$
$= 30 + \text{Floor}_{60}(\mathring{N}), N_e = 36390, d_e = 63, \alpha_e^{-1} = 137.03599920783327, g_e$
$= 2.002319304360218, \Delta g_e = -1.95\sigma = -350.59\text{ppq}, N_m = 517470, d_m = 881, \alpha_m^{-1}$
$= 137.03950024462935, g_m = 2.0023318815913784, \Delta g_m = +49.22\sigma = +20.16\text{ppb}, N_t$
$= 2069790, d_t = 3554, \alpha_t^{-1} = 137.03969886161988, g_t = 2.002354344999148, \Delta g_t$
$= -0.75\sigma = -37.46\text{ppb}$

32.1.6 Main Model Without the External $\ddot{\alpha}_\beta^{-2}$ Correction

[206] $g = (3N/2 - d)/(3N/4 - d\{1 + (\alpha/6)(1 + 2d/(7N(1 - \alpha/6)))\}), N = 30 + \mathrm{Floor}_{60}(\mathring{N}), N_e = 36390, d_e = 63, {\alpha_e}^{-1} = 137.03599920783327, g_e = 2.0023193043609084, \Delta g_e = -0.03\sigma = -5.79\mathrm{ppq}, N_m = 517470, d_m = 901, {\alpha_m}^{-1} = 137.03950024462935, g_m = 2.002332623275362, \Delta g_m = +953.71\sigma = +390.57\mathrm{ppb}, N_t = 2069790, d_t = 3637, {\alpha_t}^{-1} = 137.03969886161988, g_t = 2.0023541347596665, \Delta g_t = -2.85\sigma = -142.45\mathrm{ppb}$

32.1.7 Two-Channel Model with Reflection √((4d/7−3d/7)/9)

[207] $g = \dot{\alpha}_\beta(3N/2 - d)/(3N/4 - d(4/7\{1 + (\alpha/6)((4d/7 - 3d/7)/9)^{1/2}(1 + 4d/(7N)/½)^{1/2}\}/½)^{1/2} + 3/7\{1 + (\alpha/6)(1 + 3d/(7N))\})), N = \mathrm{Round}_{30}(\mathring{N}), N_e = 36390, d_e = 63, {\alpha_e}^{-1} = 137.03599920783327, g_e = 2.0023193043610674, \Delta g_e = +0.41\sigma = +73.61\mathrm{ppq}, N_m = 517440, d_m = 907, {\alpha_m}^{-1} = 137.03950022927532, g_m = 2.002331843914556, \Delta g_m = +3.27\sigma = +1.34\mathrm{ppb}, N_t = 2069820, d_t = 3646, {\alpha_t}^{-1} = 137.0396988625795, g_t = 2.0023544663073767, \Delta g_t = +0.46\sigma = +23.13\mathrm{ppb}$

32.1.8 Two-Channel Model with Reflection ((4d/7−3d/7)/9)

[208] $g = \dot{\alpha}_\beta\ddot{\alpha}_\beta^{-2}(3N/2 - d)/(3N/4 - d(4/7\{1 + (\alpha/6)(1 + 4d/(7N)/½)^{1/2}/½\}^{1/2} + 3/7\{1 + (\alpha/6)((4d/7 - 3d/7)/9)(1 + 3d/(7N))\})), N = 30 + \mathrm{Round}_{60}(\mathring{N}), N_e = 36390, d_e = 63, {\alpha_e}^{-1} = 137.03599920783327, g_e = 2.0023193043610674, \Delta g_e = +0.41\sigma = +73.61\mathrm{ppq}, N_m = 517470, d_m = 879, {\alpha_m}^{-1} = 137.03950024462935, g_m = 2.0023318228593703, \Delta g_m = -22.40\sigma = -9.17\mathrm{ppb}, N_t = 2069850, d_t = 3408, {\alpha_t}^{-1} = 137.03969886353914, g_t = 2.0023545521223247, \Delta g_t = +1.32\sigma = +65.98\mathrm{ppb}$

33 Calculation of the quark, proton and neutron masses

P359 Note on the energy scale: in this section, E_s and $\mathbb{E}_s$ are defined and calculated independently. Consequently, the factor θ_e is not applied to the relations used to calculate the quark, proton and neutron masses. The convention used elsewhere in the framework to correct the numerical value of E_s does not extend to this section.

P360 The calculations in this section are based on the following reports:

P361 A — A 2026_10_11 19_51 Framework 2026_10_11 20_30_44.txt

P362 B — B 2026_10_11 19_51 Framework 2026_10_11 20_35_08.txt

P363 C — C 2026_10_11 19_51 Framework 2026_10_11 20_43_28.txt

P364 D — D 2026_10_11 19_51 Framework 2026_10_11 20_49_25.txt

P365 Four cases, A, B, C and D, are examined here. In each case, the proton mass relations are classified according to their physical origin as proton-based, neutron-based, antisymmetric or analytical formulae.

33.1 Introduction convergence of structural constraints in hadronic packet formation

P366 In Ramionics, entropy considerations and the principle of carrying the least information motivate the 'largest and most similar' rule, which requires structural evolution to preserve the preceding pattern as far as possible. Accordingly, particles of the N family continue to form beyond shell 127. However, this process must remain electrically neutral so that the electric charges of the cores of the formed hadrons do not change.

P367 At the next level, the same rule applies to the hadrons themselves. Because the continuing structure must retain the greatest possible similarity to the preceding hadronic unit, subsequent units are treated as packets of eight, $8e_0$. Once this structural unit has been specified, the problem is to identify a shell that supports an integer number of these packets without providing sufficient capacity to form an additional packet.

P368 The shell calculations indicate that shell 624 simultaneously satisfies a rare combination of these conditions. It lies immediately before the strong shell 5^4=625; the number of supported eight-member packets remains 227, with the next packet not yet formed; and the available energy is consistent with the total energy of the hadronic packet, including its 7 electrons. At shell 625, the structural capacity reaches the next packet, increasing the packet count from 227 to 228. Thus, the termination of the 227-packet configuration at shell 624, its adjacency to the strong shell 625, and the availability of the total hadronic packet energy constitute a particularly rare set of simultaneous constraints.

P369 This convergence extends beyond these conditions. In the same structure, the neutrino radiation fraction lies within the empirical range of approximately 1 to 2 per cent; the proton-to-neutron number ratio is 7; and the corresponding atomic organisation yields a hydrogen-to-helium mass ratio of 3. Several apparently distinct results—the shell capacity, packet count, electrical neutrality, hadronic packet energy, neutrino fraction, proton-to-neutron ratio and hydrogen-to-helium mass ratio—therefore converge within a single structure.

P370 The four possible models A/B/C/D are also examined independently to determine the inertial mass capacity of the quarks. In each model, ENPDU is calculated in units of EDU. The proximity of this ratio to 1/12 in all four models shows that it may be regarded as a shared structural property. On this basis, defining the inertial mass capacity of a quark as 1/12 of its quark mass is a natural choice within the resulting structure and provides the basis for subsequent, smaller corrections.

33.2 Introduction distinct origins of the factor 2

P371 Several independent origins of the factor 2 must be distinguished when examining proton and neutron structure.

P372 First, in a three-quark structure, one quark may be regarded as central and the other two as peripheral. Entanglement between the peripheral quarks may also produce a factor 2, just as two wings may become entangled with two surface ramions of a particle. These factors may interchange $\alpha/12$ and $\alpha/6$.

P373 The second origin is purely combinatorial. A proton contains two up quarks and one down quark, whereas a neutron contains one up quark and two down quarks:

[209] $E_{(udu)} = 2E_{us} + E_{ds}$

[210] $E_{(dud)} = E_{us} + 2E_{ds}$

P374 The simple structural difference between these two configurations is therefore:

[211] $E_{(dud)} - E_{(udu)} = E_{ds} - E_{us}$

P375 The factor 2 in the relation between magnetic moment and angular momentum has a separate origin.

P376 Consider a small charge element dq at a distance r from the rotation axis, rotating with angular velocity ω. The period of one complete revolution is:

[212] $T = 2\pi/\omega$

P377 The corresponding current is:

[213] $dI = dq/T = \omega\, dq/(2\pi)$

P378 The magnetic moment of the charge element is:

[214] $d\mu = dI\pi r^2 = (1/2)\omega r^2\, dq$

P379 For the entire charge distribution:

[215] $\mu = (1/2)\omega \int r^2\, dq$

P380 For a mass element:

[216] $v = \omega r$

[217] $dp = v\, dm = \omega r\, dm$

[218] $dJ = r\, dp = \omega r^2\, dm$

P381 For the entire mass distribution:

[219] $J = \omega \int r^2\, dm$

P382 Thus, the factor 1/2 in μ arises directly from converting the rotation period into a current and multiplying by the area πr^2, whereas no such factor arises in J.

33.3 Physical questions in the precise calculation of proton and neutron masses

P383 Obtaining a numerically precise formula for the proton mass does not, by itself, determine the proton's internal physics completely.

P384 The physical proton radius and its relation to the Ramionics scale, the contributions of quark self-rotation and orbital motion, the corresponding velocities, the relativistic factors and the stable orientations of the three quarks must be examined independently.

P385 In the Ramionics description considered here, quarks are assigned three rotation axes, which may be associated with the three quark colours. The gyromagnetic factors associated with these axes need not be identical.

P386 Entanglement may occur between the central quark and the peripheral quarks, between the two peripheral quarks, or cyclically among all three quarks.

P387 It is also necessary to establish how the magnetic balance of the entire packet is achieved and whether the electrons accompanying the hadronic packet contribute to that balance.

P388 A further fundamental question is whether the magnetic/inertial reduction d is already included in the measured rest masses of the electron and quarks, or whether the calculation should instead be based on their zero-alpha energies.

P389 For the present, we model all these effects in terms of α: the dependence of the gyromagnetic factor on the rotation axis, identified here with quark colour; the rotation speeds of the three quarks, udu for the proton and dud for the neutron; the orbital radius and speed of a peripheral quark around the central quark; the relativistic effects associated with these velocities; and the entanglement contributions.

33.4 The Ramionics metric and base energy

P390 Throughout this section, upper-case N denotes the Ramionics metric, while lower-case n denotes the number of packet constituents.

[220] $\mathrm{N} = 36390$

P391 The energy of one 12N unit is:

[221] $\mathrm{E_{0s}} = 12\mathrm{N} = 436680$

P392 A packet is a specified set of physical constituents that form and achieve balance within a collective structure.

P393 Quantisation means that the raw calculated value is not necessarily the final permitted value: Round, Floor or Ceil maps it onto the permitted lattice.

33.5 Definition of d and the four cases

P394 In the section on the gyromagnetic factor, d is introduced as magnetic inertia represented by a negative mass.

[222] $\mathrm{d} = \mathrm{mRound_{2,u}\,Round_2}(\acute{\mathrm{d}})$

[223] $\acute{\mathrm{d}} = \{(\mathrm{cN}/2)\alpha/\{6(1-\alpha/6)\}\}\{1-\mathrm{M}\alpha(1+\mathrm{c}/4)^2\}$

P395 where:

[224] $\mathrm{M} = 3 \text{ or } \mathrm{c}$

P396 The current values are:

[225] $\mathrm{d_e} = 63$

[226] $\mathrm{d_u} = 42$

[227] $\mathrm{d_d} = 21$

Table 5

Model	d_e	d_u	d_d
A	63	42	21
B	63	0	0
C	0	0	0
D	0	42	21

[228] $\mathrm{E_{es}} = 3\mathrm{N}/2 - 63 = 54522 : \mathrm{A,B}$

$\mathrm{E_{es(}}\alpha 0_{)} = 3\mathrm{N}/2 = 54585 : \mathrm{C,D}$

P397 In A/B, E_s is determined by assigning 54522 units to the electron mass. In C/D, the same experimental mass is distributed over 54585 units. The value of E_s therefore changes.

P398 In A/B, the energy scale is determined by assigning 54522 units to the experimental electron mass:

[229] $E_{s(A/B)} = E_e/54522$

P399 In C/D, the energy scale is determined by assigning 54585 units to the same experimental electron mass:

[230] $E_{s(C/D)}/E_{s(A/B)} = 54522/54585 = 0.99884583676834295136026380873 9$

P400 In the calculations in this section, each energy scale is used according to the independent definition of the corresponding case; no additional correction factor is attached to the energy symbol.

33.6 The zero-alpha contribution of the quark structure

P401 The zero-alpha quark energies are:

[231] $\mathbb{E}_{us} = 218340$

[232] $\mathbb{E}_{ds} = 345705$

P402 For the neutron configuration:

[233] $E_{ns(\alpha 0)} = 227 \times 12N + (1 + 1/12)(2\mathbb{E}_{ds} + \mathbb{E}_{us}) = 100111922.5$

P403 In A and B:

[234] $E_{ns(\alpha 0)}/E_{ns} = 99.86355\%$

33.7 Determination of E_s and the CODATA editions

P404 For A and B, the combination of data editions is:

P405 E2018_P2018_N2022

[235] $E_s = 9.3723441902457908 \times 10^{-6}\text{MeV}$

[236] $E_{es} = 54522$

[237] $E_{ps} = 100110716$

[238] $E_{ns} = 100248711$

P406 The deviations from the experimental data are:

$\Delta E_e = -0.396126094889\sigma$

$\Delta E_p = -2.33121956375\sigma$

$\Delta E_n = +4.54266526617\sigma$

P407 The root-mean-square value is RMS=2.95676108030072σ.

P408 If E_s is determined solely from the 2022 experimental electron energy:

[239] $E_s \approx 9.37234420399105 \times 10^{-6}\text{MeV}$

P409 For C and D:

P410 E2018_P2022_N2022

[240] $E_s = 9.3615269668841921 \times 10^{-6}\text{MeV}$

[241] $E_{es} = 54585$

[242] $E_{ps} = 100226394$

[243] $E_{ns} = 100364548$

$\Delta E_e = -3.41750849842\sigma$

$\Delta E_p = +2.73986180563\sigma$

$\Delta E_n = +1.4190478718\sigma$

P411 The root-mean-square value is RMS=2.6583142473615σ.

P412 These calculations distribute the quantisation error among the electron, proton and neutron so as to minimise the RMS error for all three particles, rather than distributing it only between the proton and neutron.

P413 This fine correction does not change the quantised values of the three particles relative to the simple calculation $E_{ex}/54522$ or $E_{ex}/54585$; it only improves the accuracy of the value of E_s expressed in joules.

33.8 Quark energies and structural quantities

P414 The up-quark energy is calculated from its zero-alpha energy and the corresponding magnetic inertia:

[244] $E_{us} = \mathbb{E}_{us} - d_u = 218298 : A, D$

$E_{us} = \mathbb{E}_{us} = 218340 : B, C$

P415 The down-quark energy is calculated in the same way:

[245] $E_{ds} = \mathbb{E}_{ds} - d_d = 345684 : A, D$

$E_{ds} = \mathbb{E}_{ds} = 345705 : B, C$

P416 The down–up quark energy difference, EDU, is first calculated as:

[246] $EDU = E_{ds} - E_{us} = 127386 : A, D$

$EDU = E_{ds} - E_{us} = 127365 : B, C$

P417 The neutron–proton energy difference, ENP, is calculated from their quantised values:

[247] $ENP = E_{ns} - E_{ps} = 137995 : A, B$

$ENP = E_{ns} - E_{ps} = 138154 : C, D$

P418 ENPDU is then calculated as the difference between ENP and EDU:

[248] $ENPDU = ENP - EDU = 10609 : A$

$ENPDU = ENP - EDU = 10630 : B$

$ENPDU = ENP - EDU = 10789 : C$

$ENPDU = ENP - EDU = 10768 : D$

P419 The distinction between E and $\mathbb{E}$ is retained in the relations for E_{ps} and E_{ns}:

[249] $E_{es} = \mathbb{E}_{es} - d_e = 3N/2 - 63$

[250] $E_{us} = \mathbb{E}_{us} - d_u = 12N/2 - 42$

[251] $E_{ds} = \mathbb{E}_{ds} - d_d = 19N/2 - 21$

33.9 The fermionic packet

[252] $E_{ffp} = (2^{p-1} - 1)E_2 + (2^{p-2} + 1)E_1 + (2^{p-2} - 1)E_3$

P420 For p=5:

[253] $E_{ff} = 15E_{us} + 9E_{ds} + 7E_{es}$

P421 The fermionic packet formed up to shell 127, immediately before the strong shell 2^7=128, contains 7 electrons with charge $-7q_e$, 9 down quarks with total charge $-3q_e$, and 15 up quarks with total charge $+10q_e$:

P422 The charges are $-7q_e$ for the electrons, $9(-q_e/3)=-3q_e$ for the down quarks and $15(+2q_e/3)=+10q_e$ for the up quarks. The total electric charge of the collection is therefore zero.

P423 This quark count also corresponds exactly to one neutron and seven protons. The seven protons contain 14 up quarks and 7 down quarks, and the neutron contains one up quark and 2 down quarks, giving precisely 15 up quarks and 9 down quarks in total. In terms of atomic constituent counts, seven protons, seven electrons and one neutron may be organised into 6 hydrogen atoms and one deuterium atom.

P424 If this structure is continued across a collection of packets, and two neutrons and two protons ultimately form a helium-4 nucleus, two atomic packets yield a total of 12 remaining hydrogen atoms and one helium-4 atom. Approximating atomic masses by their mass numbers, the primordial hydrogen-to-helium mass ratio is then 12 to 4, or 3 to 1, corresponding to approximately 75% hydrogen and 25% helium by mass. This step should not be interpreted as a direct, single-stage reaction of two deuterium nuclei into helium-4; in nuclear physics, the reaction pathway may involve intermediate stages and products.

P425 The values for the four cases are:

[254] $E_{ff} = 6767280 : A$

$E_{ff} = 6768099 : B$

$E_{ff} = 6768540 : C$

$E_{ff} = 6767721 : D$

P426 The hadronic structure is:

[255] $E_{hh} = 7E_{ps} + E_{ns} + 7E_{es}$

[256] $E_{hh} = 801405377 : A, B$

$E_{hh} = 802331401 : C, D$

33.10 Rotational, magnetic and inertial mass capacities

[257] $k_m = 1/12$

[258] $ENP_{(Base)} = (13/12)EDU$

P427 The values for the four cases are:

[259] $ENP_{(Base)} = 138001.5 : A, D$

$ENP_{(Base)} = 137978.75 : B, C$

P428 The inertial mass capacity is:

[260] $E_{(InertiaCapacity)} = E_{(Rest)}/12$

P429 For A:

[261] $EDU/12 = 10615.5$

[262] $\mathrm{ENP}_{(\mathrm{InertiaBase})} = 138001.5$

[263] $\mathrm{ENP} = 137995$

[264] $\mathrm{ENP}_{(\mathrm{InertiaBase})} - \mathrm{ENP} = 6.5$

P430 The corrected expression is:

[265] $\mathrm{E}_{(\mathrm{InertiaCapacity})} = \mathrm{E}_{(\mathrm{Rest})}/(12 + \alpha)$

33.11 The largest and most similar rule

P431 When several highly similar structures occur within a shared packet, the larger member may serve as a common reference for the size and energy capacity of the similar structures.

P432 Beyond shell 127, neutral electron-family naryons e_0 continue to be produced with the same N as the up and down quarks.

P433 Before the proton and neutron separate from the shared black hole of the hadronic packet, the neutron, as the larger member, may serve as the common energy reference.

[266] $\mathrm{E}_{\mathrm{ps}} - (13/12)\mathrm{E}_{(\mathrm{udu})} = 99263226.5$

[267] $\mathrm{E}_{\mathrm{ns}} - (13/12)\mathrm{E}_{(\mathrm{dud})} = 99263220$

[268] $\Delta\mathrm{E}_{\mathrm{c}} = 6.5$

P434 The neutron-based formula is:

[269] $\mathrm{M}_{2(}\mathrm{NeutronBase}_{)} = (1 + \acute{\mathrm{k}}_{\mathrm{m}})(2\mathrm{E}_{\mathrm{ds}} + \mathrm{E}_{\mathrm{us}})$

P435 The proton-based formula is:

[270] $\mathrm{M}_{2(}\mathrm{ProtonBase}_{)} = (1 + \acute{\mathrm{k}}_{\mathrm{m}})(2\mathrm{E}_{\mathrm{us}} + \mathrm{E}_{\mathrm{ds}})$

P436 For the proton:

[271] $\mathrm{M}_{\mathrm{p}} = (1 + \acute{\mathrm{k}}_{\mathrm{m}})(2\mathrm{E}_{\mathrm{us}} + \mathrm{E}_{\mathrm{ds}})$

P437 For the neutron:

[272] $\mathrm{M}_{\mathrm{n}} = (1 + \acute{\mathrm{k}}_{\mathrm{m}})(\mathrm{E}_{\mathrm{us}} + 2\mathrm{E}_{\mathrm{ds}})$

[273] $\mathrm{M}_{\mathrm{n}} - \mathrm{M}_{\mathrm{p}} = (1 + \acute{\mathrm{k}}_{\mathrm{m}})(\mathrm{E}_{\mathrm{ds}} - \mathrm{E}_{\mathrm{us}})$

[274] $\mathrm{M}_{\mathrm{n}} - \mathrm{M}_{\mathrm{p}} = (1 + \acute{\mathrm{k}}_{\mathrm{m}})\mathrm{EDU}$

P438 The direct proton calculation uses quantisation in steps of 2, whereas the neutral neutron uses quantisation in steps of 3.

33.12 ENPDU relations and the structural relationship between the proton and neutron

P439 In A:

[275] $\mathrm{ENPDU} = \mathrm{Floor}_1\{\mathrm{EDU}(1 - \alpha/12)/12\} = 10609$

P440 Error: zero ramion energy units.

$\acute{\mathrm{k}}_{\mathrm{m}} = (1/12)(1 - \alpha/12) = (1/12)0.999391887286443 = 0.083282657273859$

P441 In B:

[276] $\mathrm{ENPDU} = \mathrm{Ceil}_1\{\mathrm{EDU}/\{12(1 - \alpha/5)\}\} = 10630$

P442 Error: zero ramion energy units.

$$\acute{k}_m = (1/12)/(1-\alpha/5) = (1/12)1.00146160368000989365$$
$$= 0.08345513364000082447$$

P443 In C:

[277] $$\mathrm{ENPDU} = \mathrm{Ceil}_1\{\mathrm{EDU}(1+(9/4)\alpha)/12\} = 10789$$

P444 Error: zero ramion energy units.

$$\acute{k}_m = (1/12)(1+(9/4)\alpha) = (1/12)1.016419043266051 = 0.084701586939145$$

P445 In D:

[278] $$\mathrm{ENPDU} = \mathrm{Floor}_1\{\mathrm{EDU}(1+2\alpha)/12\} = 10770$$

P446 However, ENPDU is 10768, so this expression has a discrepancy of $+2E_s$.

P447 Error: +2 ramion energy units.

$$\acute{k}_m = (1/12)(1+2\alpha) = (1/12)1.014594705125379 = 0.084549558760722$$

P448 In this structure, the first, packet-related term and the third, correction term may be shared, with the principal proton–neutron difference arising from the interchange of the quark structure in the second term.

33.13 The general family of proton mass relations and models A, B, C and D

[279] $$E_{ps} = Q\{n_{8e0}12N + F_2M_2 + F_3(aX_u + bX_d)/Y\}$$

P449 Here Q is the quantisation rule, n_{8e0} is the number of complete eight-member packets, F_2 and F_3 are structural factors, M_2 is the principal quark term, X is the corrected or zero-alpha energy, and Y is the denominator of the correction term.

[280] $$M_2 = 2E_{us} + E_{ds}$$

P450 Model A: proton mass formulae

P451 First formula (proton-based)

[281] $$E_{ps} = \mathrm{Floor}_2\{n_{8e0}12N + (1+\acute{k}_m)(E_{ds}+2E_{us}) + (4E_{us}+5E_{ds})/19\} = 100110716E_s$$

P452 The corresponding neutron formula is:

[282] $$E_{ns} = \mathrm{Round}_3, \mathrm{Floor}_3\{n_{8e0}12N + (1+\acute{k}_m)(2E_{ds}+E_{us}) + (4E_{us}+5E_{ds})/19\}$$
$$= 100248711E_s$$

P453 Second formula (proton-based)

[283] $$E_{ps} = \mathrm{Ceil}_2\{n_{8e0}12N + (1+\acute{k}_m)(E_{ds}+2E_{us}) + (1+\acute{k}_m)((3/2)E_{us}+6E_{ds})/19\}$$
$$= 100110716E_s$$

P454 The corresponding neutron formula is:

[284] $$E_{ns} = \mathrm{Round}_3, \mathrm{Ceil}_3\{n_{8e0}12N + (1+\acute{k}_m)(2E_{ds}+E_{us}) + (1+\acute{k}_m)((3/2)E_{us}+6E_{ds})/19\}$$
$$= 100248711E_s$$

P455 Third formula (proton-based)

[285] $E_{ps} = Floor_2\{n_{8e0}12N + (1 + \acute{k}_m)(E_{ds} + 2E_{us}) + (1 + k_m)(3\mathbb{E}_{us} - (1/15)\mathbb{E}_{ds})/5\}$
$= 100110716E_s$

P456 The current raw value is:

[286] $E_{ps(}Raw_{)} = 100110717.840466E_s$

P457 Fourth formula (antisymmetric)

[287] $E_{ps} = Ceil_2\{n_{8e0}12N + (1 + \acute{k}_m)(2\mathbb{E}_{ds} + \mathbb{E}_{us}) + \alpha(5\mathbb{E}_{us} - 5\mathbb{E}_{ds})/4\} = 100110716E_s$

P458 The current raw value is:

[288] $E_{ps(}Raw_{)} = 100110714.613318E_s$

P459 Fifth formula (antisymmetric)

[289] $E_{ps} = Q\{n_{8e0}12N + (1 + k_m)(2E_{ds} + E_{us}) + \alpha(6E_{us} - 6E_{ds})/5\} = 100110716E_s$

P460 where Q may be $Round_1$, $Round_2$, $Floor_1$ or $Floor_2$.

P461 The current raw value is:

[290] $E_{ps(}Raw_{)} = 100110716.003336E_s$

P462 Sixth formula (analytical)

P463 Seven protons and one neutron contain a total of 15 up quarks and 9 down quarks.

[291] $Y = 6/(1 + 4\alpha) \approx 5.829830680572319$

[292] $E_{ps} = n_{8e0}12N + (1 + \acute{k}_m)(E_{ds} + 2E_{us}) + (15E_{us} + 9E_{ds})/\{8(6/(1 + 4\alpha))\}$
$\approx 100110707.4365795E_s$

[293] $\Delta E_{ps} \approx -8.5634205E_s$

P464 Seventh formula (analytical)

P465 In this interpretation, there are 14 peripheral up quarks and 2 peripheral down quarks.

[294] $Y = 24/7 - \alpha \approx 3.42127407600874$

[295] $E_{ps} = n_{8e0}12N + (1 + \acute{k}_m)(E_{ds} + 2E_{us}) + (14E_{us} + 2E_{ds})/\{8(24/7 - \alpha)\}$
$\approx 100110710.86452813E_s$

[296] $\Delta E_{ps} \approx -5.13547187E_s$

P466 Eighth formula (analytical)

P467 For the up quark:

[297] $14(2/3) = 28/3$

P468 For the down quark:

[298] $2(1/3) = 2/3$

[299] $Y = 2 + 10\alpha = 2.072973525626895$

[300] $E_{ps} = n_{8e0}12N + (1 + \acute{k}_m)(E_{ds} + 2E_{us}) + \{(28/3)\mathbb{E}_{us} + (2/3)\mathbb{E}_{ds}\}/\{8(2 + 10\alpha)\}$
$\approx 100110569.142022E_s$

[301] $\Delta E_{ps} \approx -146.857978E_s$

P469 The three analytical formulae above are based, respectively, on the total number of quarks in the packet, the number of peripheral quarks, and the number of peripheral quarks multiplied by the absolute value of the charge coefficient.

P470 Model B: proton mass formulae

P471 First formula (proton-based)

[302] $E_{ps} = Q\{n_{8e0}12N + (1 + \acute{k}_m)(\mathbb{E}_{ds} + 2\mathbb{E}_{us}) + (5E_{us} + (1/180)E_{ds})/8\} = 100110716E_s$

P472 where Q may be $Round_2$, $Ceil_1$ or $Ceil_2$.

P473 The current raw value is:

[303] $E_{ps(Raw)} = 100110715.353066E_s$

P474 Second formula (antisymmetric)

[304] $E_{ps} = Ceil_2\{n_{8e0}12N + (1 + \acute{k}_m)(2\mathbb{E}_{ds} + \mathbb{E}_{us}) + \alpha(5\mathbb{E}_{us} - 5\mathbb{E}_{ds})/4\} = 100110716E_s$

P475 Third formula (antisymmetric)

[305] $E_{ps} = Q\{n_{8e0}12N + (1 + k_m)(2E_{ds} + E_{us}) + \alpha(6E_{us} - 6E_{ds})/5\} = 100110716E_s$

P476 where Q may be $Round_1$, $Round_2$, $Floor_1$ or $Floor_2$.

P477 The current raw value is:

[306] $E_{ps(Raw)} = 100110716.003336E_s$

P478 Fourth formula (analytical: total quark count in the packet, factor 4)

P479 In model B, the quark energies in the second term and the third, analytical term are written in terms of the zero-alpha energies. For this model, $\mathbb{E}_{us}$=218340E_s and $\mathbb{E}_{ds}$=345705E_s, and the corrected inertial coefficient is $\acute{k}_m$=0.08345513364000082447.

[307] $Y = 6/(1 + 4\alpha) = 5.829830680572319$

[308] $E_{ps} = n_{8e0}12N + (1 + \acute{k}_m)(\mathbb{E}_{ds} + 2\mathbb{E}_{us}) + (15\mathbb{E}_{us} + 9\mathbb{E}_{ds})/\{8(6/(1 + 4\alpha))\}$
$= 100110973.66063187E_s$

[309] $\Delta E_{ps} = +257.66063187E_s$

P480 Fifth formula (analytical: total quark count in the packet, factor 15/4)

[310] $Y = 6/\{1 + (15/4)\alpha\} = 5.840182971839517$

[311] $E_{ps} = n_{8e0}12N + (1 + \acute{k}_m)(\mathbb{E}_{ds} + 2\mathbb{E}_{us}) + (15\mathbb{E}_{us} + 9\mathbb{E}_{ds})/\{8(6/\{1 + (15/4)\alpha\})\}$
$= 100110730.93073193E_s$

[312] $\Delta E_{ps} = +14.93073193E_s$

P481 Sixth formula (analytical: peripheral quark count)

[313] $Y = 24/7 - \alpha/12 = 3.427963315857871$

[314] $E_{ps} = n_{8e0}12N + (1 + \acute{k}_m)(\mathbb{E}_{ds} + 2\mathbb{E}_{us}) + (14\mathbb{E}_{us} + 2\mathbb{E}_{ds})/\{8(24/7 - \alpha/12)\}$
$= 100110715.31773521E_s$

[315] $\Delta E_{ps} = -0.68226479E_s$

P482 Seventh formula (analytical: peripheral quark count weighted by the absolute charge)

[316] $Y = 2 + 10\alpha = 2.072973525626895$

[317] $E_{ps} = n_{8e0}12N + (1 + \acute{k}_m)(\mathbb{E}_{ds} + 2\mathbb{E}_{us}) + \{(28/3)\mathbb{E}_{us} + (2/3)\mathbb{E}_{ds}\}/\{8(2 + 10\alpha)\}$
$= 100110817.80552982E_s$

[318] $\Delta E_{ps} = +101.80552982E_s$

Table 6

Formula	Y	E_{ps}/E_s	$\Delta E_{ps}/E_s$
4	6/(1+4α)	100110973.66063187	+257.66063187
5	6/{1+(15/4)α}	100110730.93073193	+14.93073193
6	24/7−α/12	100110715.31773521	−0.68226479
7	2+10α	100110817.80552982	+101.80552982

P483 Model C: proton mass formula

P484 First formula (proton-based)

[319] $E_{ps} = Floor_2\{n_{8e0}12N + (1 + \acute{k}_m)(\mathbb{E}_{ds} + 2\mathbb{E}_{us}) + (1 + k_m)(-5E_{us} + (9/2)E_{ds})/2\}$
$= 100226394E_s$

P485 The current raw value is:

[320] $E_{ps(Raw)} = 100226395.251097E_s$

P486 Model D: proton mass formula

P487 First formula (proton-based)

[321] $E_{ps} = Ceil_2\{n_{8e0}12N + (1 + \acute{k}_m)(E_{ds} + 2E_{us}) + ((3/20)\mathbb{E}_{us} + 5\mathbb{E}_{ds})/7\} = 100226394E_s$

P488 The current raw value is:

[322] $E_{ps(Raw)} = 100226392.28597E_s$

P489 After the α-based correction is applied, these formulae also yield a quantised error of zero ramion energy units, with each ramion energy unit amounting to less than 10ppb of the proton rest energy.

33.14 Packet formation and shell 127

P490 The total number of ramions from shell zero to shell n is calculated as:

[323] $T(n) = (10n^3 + 15n^2 + 11n + 3)/3$

P491 For shell 127:

[324] $T(127) = \{10(127^3) + 15(127^2) + 11(127) + 3\}/3$

[325] $T_{127} = 6909055$

P492 The values for the four cases are:

[326] $\Delta E_{127} = 141775 : A$

$\Delta E_{127} = 140956 : B$

$\Delta E_{127} = 140515 : C$

$\Delta E_{127} = 141334 : D$

P493 Beyond shell 127, neutral electron-family naryons e_0 continue to be produced with the same N as the up and down quarks, and the structure extends to shell 624.

33.15 The hadronic packet

P494 The hadronic packet consists of eight hadrons—seven protons and one neutron—together with the seven corresponding electrons.

P495 For shell 624:

[327] $T(624) = \{10(624^3) + 15(624^2) + 11(624) + 3\}/3$

[328] $T_{624} = 811851249$

P496 The lower bound is:

[329] $Minn_{e0} = Floor\{(T_{624} - E_{ff} - \Delta E_{127} - k_m(15E_{us} + 9E_{ds}))/(12(N + 480))\}$

P497 The upper bound is:

[330] $Maxn_{e0} = Floor\{(T_{624} - E_{ff} - k_m(15E_{us} + 9E_{ds}))/(12(N + 474))\}$

33.16 Bounds at shell 624

P498 The raw lower-bound values are:

[331] $Minn_{(Raw)} = 1818.1223634843143 : A$

$Minn_{(Raw)} = 1818.1222092261098 : B, C$

$Minn_{(Raw)} = 1818.1223634843143 : D$

P499 The raw upper-bound values are:

[332] $Maxn_{(Raw)} = 1818.738772922092 : A$

$Maxn_{(Raw)} = 1818.7367672390408 : B$

$Maxn_{(Raw)} = 1818.7357703314888 : C$

$Maxn_{(Raw)} = 1818.73777601454 : D$

P500 In all four cases:

[333] $Minn_{e0} = Maxn_{e0} = 1818 : A, B, C, D$

P501 Therefore:

[334] $n_{8e0} = Floor\{1818/8\} = 227$

P502 and:

[335] $n_{8e0}12N = 99126360$

33.17 RadProton and packet balance

P503 The values for the four cases are:

[336] $\mathrm{RadProton} = 74263 : \mathrm{A}$

$\mathrm{RadProton} = 74410 : \mathrm{B}$

$\mathrm{RadProton} = 75523 : \mathrm{C}$

$\mathrm{RadProton} = 75376 : \mathrm{D}$

P504 According to the largest and most similar rule, before separation the proton may absorb energy up to the neutron energy scale. After separation, the excess contribution may appear as RadProton in the packet energy balance.

33.18 Three binary choices in the balance

P505 The three independent choices are a neutrino value of 474 or 480, inclusion or omission of ΔE_{127}, and inclusion or omission of RadProton.

[337] $\mathrm{Q_{8e0}} = 8 \times 12\mathrm{N} = 3493440$

P506 The physical admissibility condition is:

[338] $0 \leq \mathrm{E_{(Free)}} < \mathrm{Q_{8e0}}$

P507 Model A

Table 7

Neutrino	ΔE127	RadProton	Free Energy	State
474	No	No	116464	Accepted
474	No	Yes	42201	Accepted
474	Yes	No	−25311	Impossible
474	Yes	Yes	−99574	Impossible
480	No	No	−14288	Impossible
480	No	Yes	−88551	Impossible
480	Yes	No	−156063	Impossible
480	Yes	Yes	−230326	Impossible

P508 Model B

Table 8

Neutrino	ΔE127	RadProton	Free Energy	State
474	No	No	116464	Accepted
474	No	Yes	42054	Accepted
474	Yes	No	−24492	Impossible
474	Yes	Yes	−98902	Impossible

Neutrino	ΔE127	RadProton	Free Energy	State
480	No	No	−14288	Impossible
480	No	Yes	−88698	Impossible
480	Yes	No	−155244	Impossible
480	Yes	Yes	−229654	Impossible

P509 Model C

Table 9

Neutrino	ΔE127	RadProton	Free Energy	State
474	No	No	−809560	Impossible
474	No	Yes	−885083	Impossible
474	Yes	No	−950075	Impossible
474	Yes	Yes	−1025598	Impossible
480	No	No	−940312	Impossible
480	No	Yes	−1015835	Impossible
480	Yes	No	−1080827	Impossible
480	Yes	Yes	−1156350	Impossible

P510 Model D

Table 10

Neutrino	ΔE127	RadProton	Free Energy	State
474	No	No	−809560	Impossible
474	No	Yes	−884936	Impossible
474	Yes	No	−950894	Impossible
474	Yes	Yes	−1026270	Impossible
480	No	No	−940312	Impossible
480	No	Yes	−1015688	Impossible
480	Yes	No	−1081646	Impossible
480	Yes	Yes	−1157022	Impossible

P511 Thus, A and B admit physically acceptable balance states at shell 624, whereas C and D have negative free energy within this structure.

33.19 Layer 625

P512 For shell 625:

[339] $\mathrm{T}(625) = \{10(625^3) + 15(625^2) + 11(625) + 3\}/3$

[340] $\mathrm{T}_{625} = 815757501$

[341] $\mathrm{T}_{625} - \mathrm{T}_{624} = 3906252$

P513 The raw lower-bound values are:

[342] $\mathrm{Minn}_{(\mathrm{Raw})} = 1826.9512487568936 : \mathrm{A}$

$\mathrm{Minn}_{(\mathrm{Raw})} = 1826.9510944986891 : \mathrm{B}, \mathrm{C}$

$\mathrm{Minn}_{(\mathrm{Raw})} = 1826.9512487568936 : \mathrm{D}$

P514 The raw upper-bound values are:

[343] $\mathrm{Maxn}_{(\mathrm{Raw})} = 1827.569095187717 : \mathrm{A}$

$\mathrm{Maxn}_{(\mathrm{Raw})} = 1827.5670895046658 : \mathrm{B}$

$\mathrm{Maxn}_{(\mathrm{Raw})} = 1827.5660925971138 : \mathrm{C}$

$\mathrm{Maxn}_{(\mathrm{Raw})} = 1827.568098280165 : \mathrm{D}$

P515 In all four cases:

[344] $\mathrm{Minn}_{\mathrm{e0}} = 1826 : \mathrm{A}, \mathrm{B}, \mathrm{C}, \mathrm{D}$

$\mathrm{Maxn}_{\mathrm{e0}} = 1827 : \mathrm{A}, \mathrm{B}, \mathrm{C}, \mathrm{D}$

[345] $\mathrm{Floor}\{1826/8\} = \mathrm{Floor}\{1827/8\} = 228$

[346] $228 \times 12\mathrm{N} = 99563040$

[347] $99563040 - 99126360 = 436680 = \mathrm{E}_{0\mathrm{s}}$

P516 The additional energy at shell 625 therefore cannot simply be treated as free energy available to correct the balance in C or D, because it changes the packet structure from 227 to 228 packets.

33.20 Neutrino energy percentage

P517 For 474:

[348] $\mathrm{R}\nu_{474} = 474/(36390 + 474) = 1.28580729166667\%$

P518 For 480:

[349] $\mathrm{R}\nu_{480} = 480/(36390 + 480) = 1.30187144019528\%$

P519 If no separate electromagnetic radiation is assumed in the conversion of energy into matter:

[350] $\mathrm{R}_{(\mathrm{TotalFree})} = 1 - \mathrm{E}_{\mathrm{hh}}/\mathrm{T}_{624} = 1.28667314521801\%$

P520 This value lies between the ratios associated with 474 and 480 and is closer to 474. However, this proximity alone does not determine the stage at which the neutrino leaves the system.

33.21 Formation site and the meaning of free energy

P521 In this model, particle formation may be envisaged as a small particle-production reactor within the layered structure. Energy reaching a particular shell does not imply that all remaining energy must ultimately emerge as electromagnetic radiation.

P522 The remaining energy may be distributed among several channels: part may be associated with neutrinos, part may contribute to subsequent structural rearrangement, and part may initiate formation of the next packet.

P523 Consequently, $E_{(}Free_{)}$ is an energy-balance quantity and should not be identified directly with additional observable radiation without further justification.

P524 A mixture of admissible states may also occur in nature, so a single state need not represent all packet-formation events.

33.22 Alternative energy balance models for P1

P525 P1 denotes energy packets containing 8×1 particles, with one e_0 particle allocated to each hadron. These are the packets used in the preceding sections; the present section considers alternative approaches to balancing their energy.

33.22.1 Objective and common assumptions

P526 This section examines four assumptions concerning the proton rest energy and the hadronic packet energy to determine which structure can supply the energy required to form 227 eight-particle packets, equivalent to 1816 particles, within the shared cavity.

P527 This analysis is based on the calculations in Texts 85, 91, 92, 94, 98, 99, 100, 101, 102 and 103, dated 15 October 2026.

P528 The hadronic packet comprises seven protons, one neutron and seven corresponding electrons. In models A and B, the stopping energy of shell 624, the neutron rest energy and the electron rest energy are, respectively:

[351] $T_{624} = 811851249E_s$

[352] $E_{ns} = 100248711E_s$

[353] $E_{es} = 54522E_s$

P529 The proton rest energy in models A and B is:

[354] $E_{ps} = 100110716E_s$

P530 In all calculations, whether the energy ΔE_{127} remains in or leaves the shared cavity is an independent physical choice. Retaining this energy means that ΔE_{127} is not subtracted from the cavity's energy budget; its departure means that the corresponding energy is subtracted.

33.22.2 Energy required for 227 eight-particle packets

P531 The number of particles is:

[355] $n_{e0} = 227 \times 8 = 1816$

P532 The two metrics considered are ν_{474} and ν_{480}.

P533 The energy of each particle under the first metric is:

[356] $E_{\nu 474} = 12 \times 474 = 5688E_s$

P534 The total energy required is:

[357] $E_{1816}(474) = 1816 \times 5688 = 10329408E_s$

P535 For the second metric:

[358] $E_{v480} = 12 \times 480 = 5760E_s$

[359] $E_{1816}(480) = 1816 \times 5760 = 10460160E_s$

P536 The difference between the energy requirements of the two metrics is therefore:

[360] $E_{1816}(480) - E_{1816}(474) = 130752E_s$

33.22.3 First assumption equal proton and neutron rest energies

P537 Under the first assumption, the proton rest energy is taken to be exactly equal to the neutron rest energy, while the energies of the seven electrons are added separately to the packet energy.

[361] $E_{ps} = E_{ns}$

[362] $E_{hh} = 8E_{ns} + 7E_{es}$

[363] $E_{hh} = 8 \times 100248711 + 7 \times 54522 = 802371342E_s$

P538 With ΔE_{127} retained in the cavity:

[364] $E_{(Remain)} = 811851249 - 802371342 = 9479907E_s$

P539 The energy balance for metric ν_{474} is:

[365] $\Delta E_{474} = 9479907 - 10329408 = -849501E_s$

P540 The energy balance for metric ν_{480} is:

[366] $\Delta E_{480} = 9479907 - 10460160 = -980253E_s$

P541 The equivalent number of particles that can be supplied is:

[367] $n_{474} = 9479907/5688 = 1666.65031646$

[368] $n_{480} = 9479907/5760 = 1645.8171875$

P542 Thus, under this assumption, the cavity energy is insufficient for either metric.

33.22.4 Second assumption proton energy equal to neutron energy minus EDU

P543 Under the second assumption, the energy difference between the down and up quarks is subtracted from the neutron energy:

[369] $EDU = E_{ds} - E_{us}$

[370] $E_{ps} = E_{ns} - EDU$

P544 For model A:

[371] $EDU(A) = 345684 - 218298 = 127386E_s$

[372] $E_{ps}(A) = 100248711 - 127386 = 100121325E_s$

P545 For model B:

[373] $EDU(B) = 345705 - 218340 = 127365E_s$

[374] $E_{ps}(B) = 100248711 - 127365 = 100121346E_s$

P546 The hadronic packet energy is:

[375] $E_{hh} = 7E_{ps} + E_{ns} + 7E_{es}$

P547 For model A:

[376] $\mathrm{E_{hh}(A) = 801479640 E_s}$

[377] $\mathrm{E_{(Remain)}(A) = 811851249 - 801479640 = 10371609 E_s}$

P548 For model B:

[378] $\mathrm{E_{hh}(B) = 801479787 E_s}$

[379] $\mathrm{E_{(Remain)}(B) = 811851249 - 801479787 = 10371462 E_s}$

P549 The energy balance for metric ν_{474} is:

[380] $\mathrm{\Delta E_{474}(A) = 10371609 - 10329408 = +42201 E_s}$

[381] $\mathrm{\Delta E_{474}(B) = 10371462 - 10329408 = +42054 E_s}$

P550 The energy balance for metric ν_{480} is:

[382] $\mathrm{\Delta E_{480}(A) = 10371609 - 10460160 = -88551 E_s}$

[383] $\mathrm{\Delta E_{480}(B) = 10371462 - 10460160 = -88698 E_s}$

P551 The equivalent number of particles that can be supplied is:

[384] $\mathrm{n_{474}(A) = 10371609/5688 \approx 1823.4193038}$

[385] $\mathrm{n_{474}(B) = 10371462/5688 \approx 1823.3934599}$

[386] $\mathrm{n_{480}(A) = 10371609/5760 = 1800.6265625}$

[387] $\mathrm{n_{480}(B) = 10371462/5760 \approx 1800.6010417}$

P552 Under this assumption, metric ν_{474} produces a positive energy balance in both models A and B, whereas metric ν_{480} still has an energy deficit.

33.22.5 Third assumption each proton–electron pair has the same energy as one neutron

P553 Under the third assumption, each proton–electron pair is taken to be exactly equivalent to one neutron in rest energy.

[388] $\mathrm{E_{ps} + E_{es} = E_{ns}}$

P554 The energy of seven proton–electron pairs plus one neutron is therefore exactly equal to the energy of eight neutrons:

[389] $\mathrm{E_{hh} = 7(E_{ps} + E_{es}) + E_{ns} = 8E_{ns}}$

[390] $\mathrm{E_{hh} = 801989688 E_s}$

[391] $\mathrm{E_{(Remain)} = 811851249 - 801989688 = 9861561 E_s}$

P555 The energy balances for the two metrics are:

[392] $\mathrm{\Delta E_{474} = 9861561 - 10329408 = -467847 E_s}$

[393] $\mathrm{\Delta E_{480} = 9861561 - 10460160 = -598599 E_s}$

P556 The equivalent number of particles that can be supplied is:

[394] $\mathrm{n_{474} = 9861561/5688 \approx 1733.74806610}$

[395] $\mathrm{n_{480} = 9861561/5760 = 1712.0765625}$

P557 Under this assumption, too, the energy is insufficient to form all 1816 particles.

P558 Allowing the metric to vary freely, the value required for a zero energy balance is:

[396] $1816 \times 12x = 9861561$

[397] $x = 9861561/(1816 \times 12) \approx 452.52372467$

P559 For the two neighbouring integer metrics:

[398] $\Delta E_{452} = 9861561 - 1816 \times 12 \times 452 = +11457E_s$

[399] $\Delta E_{453} = 9861561 - 1816 \times 12 \times 453 = -10335E_s$

P560 Thus, 453 is the integer metric closest to a zero energy balance.

33.22.6 Fourth assumption calculated proton and neutron energies with an electron factor of 13/12

P561 Under the fourth assumption, the calculated rest energies of the proton and neutron are retained, and each electron contributes to the packet energy with a factor of 13/12.

[400] $E_{hh} = 7E_{ps} + E_{ns} + 7(13/12)E_{es}$

[401] $E_{hh} = 801437181.5E_s$

P562 If ΔE_{127} remains in the cavity:

[402] $E_{(Remain)} = 811851249 - 801437181.5 = 10414067.5E_s$

P563 The energy balance for metric ν_{474} is:

[403] $\Delta E_{474} = 10414067.5 - 10329408 = +84659.5E_s$

P564 The energy balance for metric ν_{480} is:

[404] $\Delta E_{480} = 10414067.5 - 10460160 = -46092.5E_s$

P565 The equivalent number of particles is:

[405] $n_{474} = 10414067.5/5688 \approx 1830.88387834$

[406] $n_{480} = 10414067.5/5760 \approx 1807.99782986$

P566 Thus, when ΔE_{127} is retained, metric ν_{474} has an energy surplus, whereas metric ν_{480} has a deficit.

P567 We now consider the departure of ΔE_{127} from the cavity.

P568 In model A:

[407] $\Delta E_{127}(A) = 141775E_s$

[408] $E_{(Remain)}(A) = 10414067.5 - 141775 = 10272292.5E_s$

[409] $\Delta E_{474}(A) = 10272292.5 - 10329408 = -57115.5E_s$

[410] $\Delta E_{480}(A) = 10272292.5 - 10460160 = -187867.5E_s$

P569 In model B:

[411] $\Delta E_{127}(B) = 140956E_s$

[412] $E_{(Remain)}(B) = 10414067.5 - 140956 = 10273111.5E_s$

[413] $\Delta E_{474}(B) = 10273111.5 - 10329408 = -56296.5E_s$

[414] $\Delta E_{480}(B) = 10273111.5 - 10460160 = -187048.5E_s$

33.22.7 Complete comparison of the four assumptions

P570 The following table presents all calculated cases in separate columns, with headings and entries entirely in English.

Table 11

Hadronic Assumption	Model	ΔE_{127} State	Remaining (E_s)	ν_{474} Balance (E_s)	ν_{480} Balance (E_s)
Equal Proton–Neutron; Electrons Separate	Common	Retained	9,479,907	−849,501	−980,253
Neutron Minus EDU	A	Retained	10,371,609	+42,201	−88,551
Neutron Minus EDU	B	Retained	10,371,462	+42,054	−88,698
Proton–Electron Pair Equals Neutron	Common	Retained	9,861,561	−467,847	−598,599
Physical Proton–Neutron; Electron Factor 13/12	Common	Retained	10,414,067.5	+84,659.5	−46,092.5
Physical Proton–Neutron; Electron Factor 13/12	A	Removed	10,272,292.5	−57,115.5	−187,867.5
Physical Proton–Neutron; Electron Factor 13/12	B	Removed	10,273,111.5	−56,296.5	−187,048.5

P571 A positive sign indicates surplus energy after supplying 1816 particles, and a negative sign indicates an energy deficit.

P572 The table shows that, for metric ν_{474}, only two families of the assumptions considered produce a positive energy balance: subtracting EDU from the neutron energy, and using the calculated proton and neutron energies with an electron factor of 13/12, provided that ΔE_{127} remains in the cavity.

33.22.8 Determination of the exact electron factor for a zero energy balance

P573 In the following analysis, the calculated proton and neutron energies are retained, ΔE_{127} remains in the cavity, and only the electron energy factor is varied.

P574 We denote the electron factor by k_e:

[415] $$E_{hh} = 7E_{ps} + E_{ns} + 7k_e E_{es}$$

P575 The condition for exact energy balance under metric ν_{474} is:

[416] $$811851249 - (7 \times 100110716 + 100248711 + 7k_e \times 54522) = 10329408$$

P576 Therefore:

[417] $$k_e = 249059/190827 \approx 1.3051559789757214$$

P577 For metric ν_{480}:

[418] $$811851249 - (7 \times 100110716 + 100248711 + 7k_e \times 54522) = 10460160$$

P578 It follows that:

[419] $$k_e = 183683/190827 \approx 0.9625629496874132$$

Table 12

Metric	Initial Electron Factor	Exact Zero-Balance Electron Factor
ν_{474}	13/12	1.3051559789757214
ν_{480}	13/12	0.9625629496874132

P579 Thus, for ν_{474}, the electron energy factor must increase relative to 13/12, whereas for ν_{480} it must decrease.

33.22.9 Structural approximation of the electron factor using α

P580 Three families of approximations have been examined for the factor required by metric ν_{474}.

P581 **First case: an external factor of 0.3**

[420] $k_e = 1 + 0.3(1 + \alpha x)$

P582 The required value of x is:

[421] $x \approx 2.35518244$

P583 A simple rational approximation is:

[422] $x = 33/14$

[423] $k_e \approx 1.30516027074$

[424] $\Delta k_e \approx +0.00000429177$

[425] $\text{Error} \approx +0.000328832\%$

P584 A more accurate approximation using a fraction with larger numerator and denominator is:

[426] $x = 73/31$

[427] $k_e \approx 1.30515522649$

[428] $\Delta k_e \approx -0.00000075249$

P585 **Second case: an external factor of 1/3**

[429] $k_e = 1 + (1/3)(1 + \alpha x)$

P586 The required value is:

[430] $x \approx -11.5839357283$

P587 The selected rational approximation is:

[431] $x = -139/12$

[432] $k_e \approx 1.30515744427$

[433] $\Delta k_e \approx +0.00000146530$

P588 **Third case: an external factor of 1/4**

[434] $k_e = 1 + (1/4)(1 + \alpha x)$

P589 The required value is:

[435] $x \approx 30.2334187649$

P590 A more accurate rational approximation is:

[436] $x = 907/30$

[437] $k_e \approx 1.30515582311966$

[438] $\Delta k_e \approx -0.00000015585606$

P591 An alternative approximation is:

[439] $x = 514/17$

[440] $k_e \approx 1.30515940025327$

[441] $\Delta k_e \approx +0.00000342127755$

33.22.10 Selection of a simple fraction using the criterion of structural simplicity

P592 When the criterion of structural simplicity is applied, a fraction is not selected solely by minimising the numerical discrepancy; priority is instead given to smaller numerators and denominators and a simpler structure.

P593 For the family with an external factor of 1/4, the integer 30 is selected instead of the fraction 907/30.

[442] $x = 30$

P594 Therefore:

[443] $k_e = 1 + (1/4)(1 + 30\alpha)$

P595 Using the adopted value of alpha:

[444] $\alpha^{-1} = 137.03599920783327$

P596 The resulting factor is:

[445] $k_e \approx 1.304725104637568$

P597 Its deviation from the factor required for a zero energy balance is:

[446] $\Delta k_e \approx -0.0004308743381534$

P598 The effect of this deviation on the energy of the seven electrons is:

[447] $\Delta E_{474} = -7E_{es}\Delta k_e \approx +164.449038E_s$

P599 The relative error in the energy balance, measured against the energy required for 1816 particles, is:

[448] $\text{Error} \approx +0.00159204\%$

P600 Thus, the simple structural model in Eq. [386], without freely adjusting the parameter x, gives an energy surplus of approximately 164.45 ramion energy units for metric ν_{474}.

33.22.11 Comparison of approximations to the electron factor

Table 13

Outer Factor	x	Electron Factor	Factor Error	Selection
0.3	33/14	1.30516027074	+0.00000429177	Simple Rational
0.3	73/31	1.30515522649	−0.00000075249	Higher Accuracy
1/3	−139/12	1.30515744427	+0.00000146530	Simple Rational
1/4	907/30	1.30515582311966	−0.00000015585606	Higher Accuracy
1/4	514/17	1.30515940025327	+0.00000342127755	Alternative

Outer Factor	x	Electron Factor	Factor Error	Selection
1/4	30	1.304725104637568	−0.00043087433815	Simple Structural Model

P601 In this table, the factor error is reported relative to the exact value required for a zero energy balance under metric ν_{474}.

33.22.12 Relationship between EDU and the threshold for proton-to-neutron conversion

P602 In models A and B, the difference between the neutron and proton rest energies is:

[449] $$\mathrm{ENP} = \mathrm{E_{ns}} - \mathrm{E_{ps}} = 137995\mathrm{E_s}$$

P603 The energy difference between the down and up quarks accounts for most of this gap.

P604 In model A:

[450] $$\mathrm{ENP} - \mathrm{EDU(A)} = 137995 - 127386 = 10609\mathrm{E_s}$$

P605 In model B:

[451] $$\mathrm{ENP} - \mathrm{EDU(B)} = 137995 - 127365 = 10630\mathrm{E_s}$$

P606 These values are the respective ENPDU values for models A and B.

P607 For seven protons:

[452] $$7\mathrm{EDU(A)} = 891702\mathrm{E_s}$$

[453] $$7\mathrm{EDU(B)} = 891555\mathrm{E_s}$$

P608 The total shortfall for seven protons relative to the full neutron–proton energy difference is:

[454] $$7\mathrm{ENPDU(A)} = 74263\mathrm{E_s}$$

[455] $$7\mathrm{ENPDU(B)} = 74410\mathrm{E_s}$$

P609 This structural energy balance must not be identified with the kinematic threshold for inverse beta decay. The conventional threshold for the antineutrino–proton reaction is approximately 1.806 MeV and depends on the rest energies of the final-state particles and the requirements of energy and momentum conservation.

33.22.13 Summary

P610 Comparison of the four assumptions shows that, with metric ν_{474} and ΔE_{127} retained in the shared cavity, two families of models can supply the energy required for 227 eight-particle packets.

P611 The first family determines the proton rest energy by subtracting EDU from the neutron energy. In this case, model A has an energy surplus of 42201 ramion energy units, and model B has a surplus of 42054 ramion energy units.

P612 The second family retains the calculated proton and neutron rest energies and evaluates the electron contribution using a factor of 13/12. In this case, a surplus of 84659.5 ramion energy units remains.

P613 When the electron energy factor is allowed to vary freely, the exact values 1.3051559789757214 for metric ν_{474} and 0.9625629496874132 for metric ν_{480} give a zero energy balance.

P614 Among the approximations based on α, the simple model selected from the numerical calculations is:

[456] $$\mathrm{k_e} = 1 + (1/4)(1 + 30\alpha)$$

P615 This model achieves the ν_{474} balance with an energy surplus of approximately 164.449038 ramion energy units.

P616 The principal conclusion of this section is that **the energy balance of a hadronic packet depends on the definition of the proton rest energy, the electron energy contribution, and whether ΔE_{127} leaves or remains in the cavity**. These three choices must therefore remain independent in subsequent analyses.

33.23 Alternative energy packets

33.23.1 Objective and definition of the packets

P617 In this section, **the composition of the energy packets is varied**, whereas the packet structure was fixed in source Section 22. Every packet considered consists of eight sets with the same structure, and the total electric charge of each packet is zero. The proton and neutron charges arise solely from the sum of the quark charges in the udu or dud core; no additional charge is therefore assigned to a hadron to achieve neutrality. The previous reference packet model is retained only in the comparison tables.

P618 The model nomenclature involves two independent choices: the particle composition of the packet, indicated by the subscript 31, 7 or 2, and the basis of the second hadronic term, E or $\mathbb{E}$. The symbol $\mathbb{P}$ denotes a packet whose component energies are calculated using zero-alpha values; it must not be conflated with the choice of E or $\mathbb{E}$ for the second term.

33.23.2 Energy definitions for the alternative packets

P619 Energies are expressed in units of E_s. The constants, quark energies, electron energy, N and α are those used in the preceding sections; the table of fundamental constants is not repeated here.

[457] $P_{31} = 8(15E_{us} + 9E_{ds} + 7E_{es}) = 54138240E_s$

[458] $\mathbb{P}_{31} = 8(15\mathbb{E}_{us} + 9\mathbb{E}_{ds} + 7\mathbb{E}_{es}) = 54148320E_s$

[459] $P_7 = 8(3E_{us} + 3E_{ds} + E_{es}) = 13971744E_s$

[460] $\mathbb{P}_7 = 8(3\mathbb{E}_{us} + 3\mathbb{E}_{ds} + \mathbb{E}_{es}) = 13973760E_s$

[461] $P_2 = 8(2E_{es}) = 872352E_s$

[462] $\mathbb{P}_2 = 8(2\mathbb{E}_{es}) = 873360E_s$

P620 Each unit of packet 31 contains 15 u quarks, 9 d quarks and 7 electrons; each unit of packet 7 contains 3 u quarks, 3 d quarks and one electron. For packet 2, the energy expression $2E_{es}$ is used for each packet unit. Electrical neutrality is assumed as part of the definition of each complete packet structure; its charge composition must not be inferred solely from its energy expression.

33.23.3 Capacity, packet count and the contribution to each hadron

P621 The energy capacity between shells 127 and 624 is taken from the preceding sections. The number of complete packets and the first term in the contribution to each hadron are:

[463] $n_i = \mathrm{Floor}(E_t/P_i)$

[464] $F_i = n_i P_i/8$

Table 14

Packet	Packet Energy/E_s	Packets	First Term/E_s

Packet	Packet Energy/E_s	Packets	First Term/E_s
P_1	3493440	227	99126360
P_{31}	54138240	14	94741920
$\mathbb{P}_{31}$	54148320	14	94759560
P_7	13971744	56	97802208
$\mathbb{P}_7$	13973760	56	97816320
P_2	872352	910	99230040
$\mathbb{P}_2$	873360	909	99235530

P622 The table retains the reference model solely to compare differences in energy contributions; no separate formula or discussion of that model is repeated in this section.

33.23.4 Common structure of the mass calculation

P623 For each packet, the first term is F_i. The second term is calculated using either the corrected or the zero-alpha basis, together with the magnetic coefficient associated with that basis. These definitions remain consistent with the preceding relations:

[465] $\acute{K}_{m(}E_{)} = (1 - \alpha/12)/12$

[466] $\acute{K}_{m(}\mathbb{E}_{)} = 1/\{12(1 - \alpha/5)\}$

[467] $M_{p(}E_{)} = (1 + \acute{K}_{m(}E_{)})(2E_{us} + E_{ds})$

[468] $M_{n(}E_{)} = (1 + \acute{K}_{m(}E_{)})(E_{us} + 2E_{ds})$

[469] $M_{p(}\mathbb{E}_{)} = (1 + \acute{K}_{m(}\mathbb{E}_{)})(2\mathbb{E}_{us} + \mathbb{E}_{ds})$

[470] $M_{n(}\mathbb{E}_{)} = (1 + \acute{K}_{m(}\mathbb{E}_{)})(\mathbb{E}_{us} + 2\mathbb{E}_{ds})$

[471] $E_{ps} = Q_p\{F_i + M_p + C\}$

[472] $E_{ns} = Q_n\{F_i + M_n + C\}$

P624 Here, C is the common third term, and Q_p and Q_n are the independent quantisation rules for the two particles. The quantisation rules must be tested explicitly for each candidate.

33.23.5 Target values of the third term in 14 cases

P625 The target value of C is the mean of the two residuals and is not, by itself, an **independent physical formula**:

[473] $C_t = (E_{ps} + E_{ns} - 2F_i - M_p - M_n)/2$

Table 15

Model	Second Proton/E_s	Second Neutron/E_s	Third Target/E_s
P_1E	847430.357132	985425.401712	136925.620578
$P_1\mathbb{E}$	847679.044733	985673.307829	136677.323719
$P_{31}E$	847430.357132	985425.401712	4521365.620578

Model	Second Proton/E_s	Second Neutron/E_s	Third Target/E_s
$P_{31}\mathbb{E}$	847679.044733	985673.307829	4521117.323719
$\mathbb{P}_{31}E$	847430.357132	985425.401712	4503725.620578
$\mathbb{P}_{31}\mathbb{E}$	847679.044733	985673.307829	4503477.323719
P_7E	847430.357132	985425.401712	1461077.620578
$P_7\mathbb{E}$	847679.044733	985673.307829	1460829.323719
$\mathbb{P}_7E$	847430.357132	985425.401712	1446965.620578
$\mathbb{P}_7\mathbb{E}$	847679.044733	985673.307829	1446717.323719
P_2E	847430.357132	985425.401712	33245.620578
$P_2\mathbb{E}$	847679.044733	985673.307829	32997.323719
$\mathbb{P}_2E$	847430.357132	985425.401712	27755.620578
$\mathbb{P}_2\mathbb{E}$	847679.044733	985673.307829	27507.323719

P626 Because the proton and neutron second terms differ by a fixed amount, fitting the mean does not necessarily make the unquantised energies of both particles simultaneously equal to their experimental values. The final criterion is the energy after quantisation.

33.23.6 First family combinations of corrected energies

P627 The candidates in this family have the following structure:

[474] $$C_{(E)} = (aE_{us} + bE_{ds})/Y$$

Table 16

Model	Third-Term Formula	C/E_s
P_1E	$(4E_{us}+5Ed_s)/19$	136926.947368
$P_1\mathbb{E}$	$(5E_{us}+Ed_s/180)/8$	136676.308333
$P_{31}E$	$(222E_{us}+56Ed_s)/15$	4521364.000000
$P_{31}\mathbb{E}$	$(-305E_{us}+258Ed_s)/5$	4521116.400000
$\mathbb{P}_{31}E$	$(224E_{us}+67Ed_s)/16$	4503723.750000
$\mathbb{P}_{31}\mathbb{E}$	$(327E_{us}+28Ed_s)/18$	4503477.666667
P_7E	$(171E_{us}-15Ed_s)/22$	1461077.181818
$P_7\mathbb{E}$	$(99E_{us}+22Ed_s)/20$	1460827.500000
$\mathbb{P}_7E$	$(259E_{us}-151Ed_s)/3$	1446966.000000
$\mathbb{P}_7\mathbb{E}$	$(138E_{us}-16Ed_s)/17$	1446716.470588
P_2E	$(6E_{us}-Ed_s)/29$	33244.965517

Model	Third-Term Formula	C/E$_s$
P$_2$𝔼	(4E$_{us}$/3+9E$\mathcal{d}_s$/80)/10	32995.345000
ℙ$_2$E	(E$_{us}$−5E$\mathcal{d}_s$/72)/7	27756.023810
ℙ$_2$𝔼	(2E$_{us}$−5E$\mathcal{d}_s$/72)/15	27506.011111

P628 These formulae are candidates obtained through numerical searches. Some rows contain large coefficients or nested fractions; neither their structural simplicity nor exact agreement for all rows under a common quantisation rule has therefore been established.

33.23.7 Second family combinations of zero-alpha energies

[475] $C_{(\mathbb{E})} = (a\mathbb{E}_{us} + b\mathbb{E}_{ds})/Y$

Table 17

Model	Third-Term Formula	C/E$_s$
P$_1$E	—	—
P$_1$𝔼	(45𝔼$_{us}$/8+𝔼$\mathcal{d}_s$/180)/9	136675.898148
P$_{31}$E	—	—
P$_{31}$𝔼	—	—
ℙ$_{31}$E	—	—
ℙ$_{31}$𝔼	—	—
P$_7$E	—	—
P$_7$𝔼	—	—
ℙ$_7$E	—	—
ℙ$_7$𝔼	—	—
P$_2$E	(2𝔼$_{us}$+4𝔼$\mathcal{d}_s$/3)/27	33245.185185
P$_2$𝔼	(𝔼$_{us}$/144+2𝔼$\mathcal{d}_s$)/21	32996.488095
ℙ$_2$E	(3𝔼$_{us}$+9𝔼$\mathcal{d}_s$/80)/25	27756.472500
ℙ$_2$𝔼	(9𝔼$_{us}$/8+𝔼$\mathcal{d}_s$/180)/9	27505.898148

P629 The symbol '—' indicates that no established formula was found within the reported search range; it does not prove that such a formula is impossible. The antisymmetric relations [230] and [232], whose third terms are negative, are excluded from this table because **their second terms differ from the symmetric second terms of the present models**. Using these relations without simultaneously replacing the second term would be incorrect.

33.23.8 Third family combinations of N and α

[476] $C_{(N)} = N(a + b\alpha)/Y$

Table 18

Model	Third-Term Formula	C/Es
P₁E	N(15+7α)/4	136927.213655
P₁𝔼	N(34−27α)/9	136676.681354
P₃₁E	N(1367−38α)/11	4521367.188630
P₃₁𝔼	N(3230+35α)/26	4521115.164350
ℙ₃₁E	N(495+7α)/4	4503727.213655
ℙ₃₁𝔼	N(1114−27α)/9	4503476.681354
P₇E	N(321+28α)/8	1461078.177309
P₇𝔼	N(522−18α)/13	1460830.776010
ℙ₇E	N(159+7α)/4	1446967.213655
ℙ₇𝔼	N(358−27α)/9	1446716.681354
P₂E	N(11−5α)/12	33246.853892
P₂𝔼	N(8+22α)/9	32995.790502
ℙ₂E	N(3+7α)/4	27757.213655
ℙ₂𝔼	N(12+13α)/16	27508.259911

P630 Among the relations above, the compact candidate for model P₂E is:

[477] $$C_{(P2E)} = N(11 - 5\alpha)/12$$

P631 This algebraic simplicity alone establishes neither a physical mechanism nor minimum complexity over the full search space.

33.23.9 Reassessment of unquantised energies and quantisation

P632 For the N family, the first table reports the deviations of the unquantised energies from the proton and neutron target energies. Non-zero values in this table may become zero errors after quantisation.

Table 19

Model	Proton Raw Error	Neutron Raw Error
P₁E	+1.570787	+1.615366
P₁𝔼	−0.273913	−1.010817
P₃₁E	+1.545762	+1.590342
P₃₁𝔼	−1.790917	−2.527821
ℙ₃₁E	+1.570787	+1.615366
ℙ₃₁𝔼	−0.273913	−1.010817

Model	Proton Raw Error	Neutron Raw Error
P_7E	+0.534441	+0.579021
$P_7\mathbb{E}$	+1.820743	+1.083839
$\mathbb{P}_7E$	+1.570787	+1.615366
$\mathbb{P}_7\mathbb{E}$	−0.273913	−1.010817
P_2E	+1.211024	+1.255603
$P_2\mathbb{E}$	−1.164765	−1.901669
$\mathbb{P}_2E$	+1.570787	+1.615366
$\mathbb{P}_2\mathbb{E}$	+1.304644	+0.567740

P633 For a uniform and comparable test, the second table applies Floor_2 to the proton and Floor_3 to the neutron:

Table 20

Model	Floor_2 Proton	Floor_3 Neutron	Both Exact
P_1E	100110716	100248711	Yes
$P_1\mathbb{E}$	100110714	100248708	No
$P_{31}E$	100110716	100248711	Yes
$P_{31}\mathbb{E}$	100110714	100248708	No
$\mathbb{P}_{31}E$	100110716	100248711	Yes
$\mathbb{P}_{31}\mathbb{E}$	100110714	100248708	No
P_7E	100110716	100248711	Yes
$P_7\mathbb{E}$	100110716	100248711	Yes
$\mathbb{P}_7E$	100110716	100248711	Yes
$\mathbb{P}_7\mathbb{E}$	100110714	100248708	No
P_2E	100110716	100248711	Yes
$P_2\mathbb{E}$	100110714	100248708	No
$\mathbb{P}_2E$	100110716	100248711	Yes
$\mathbb{P}_2\mathbb{E}$	100110716	100248711	Yes

P634 In this test, **8 of the 14 models** give zero error for both particles. The other six rows do not give zero error under the same pair of rules; this does not exclude the possibility of zero error under other rules. The initial search's claim of 14 zero-error formulae cannot be accepted as a final result without recording the pair of quantisation rules and the unquantised output for each row.

33.23.10 Selection criteria and conclusions

P635 Three criteria are considered in order: first, zero error in the quantised proton and neutron energies **simultaneously**; second, minimum complexity of the coefficients and denominators; and third, a physical interpretation of the coefficients based on the packet composition and charge. A formula constructed solely from the difference between the first terms of two packets is an algebraic generalisation and does not, by itself, establish an independent mechanism for the new packet.

P636 This section compares six alternative packet compositions with a reference composition included only in the tables, using two bases for the second term. Fourteen candidates are recorded for the E family, five search candidates for the 𝔼 family, including the reference row, and fourteen candidates for the N family. This count does not, however, establish 42 independent zero-error formulae. Selection of the final model requires independent determination of the pair of quantisation rules for each candidate and of the mechanism that neutralises the charge of the electron packets.

34 Cosmology

34.1 Gravitation, relativity, cosmic expansion, dark energy, apparent dark matter and the MOND–MOG transition

34.1.1 Physical foundations of space, mass and gravitation

P637 In Ramionics, space and time arise from a discrete face-centred cubic (FCC) lattice and the energy of its ramions. Ramions are the fundamental quanta of energy, and their energy distribution gives rise to the structure of spacetime.

P638 Energy is converted into mass through the explosion of ramions and the redistribution of their energy throughout the lattice. Mass is a pattern arising from a change in the energy distribution of spacetime. The sites vacated by the exploded ramions in SuperSpace also form a structure corresponding to a black hole.

P639 The fundamental ramion energy relation is:

[478] $$E_r = \mathring{m}_r . \mathring{c}_r^{\,2} = \rho_r V_r = 2P_r V_r = 2r_r F_r/3$$

P640 Hence:

[479] $$P_r = \rho_r/2$$

P641 In the region surrounding a mass, the energy density of space differs from its vacuum value:

[480] $$\rho(R) = \rho_u[1 - f(R)]$$

P642 Here, ρ_u is the vacuum energy density and f is the dimensionless energy-distribution function.

P643 The corresponding relativistic factor is:

[481] $$N(R) = 1/\sqrt{[1 - f(R)]}$$

34.1.1.1 FCC geometry

P644 The lattice volume-packing fraction is:

[482] $$\varphi = \pi/(3\sqrt{2}) = 0.740480489693061$$

P645 The radial freedom factor is:

[483] $\gamma = \sqrt[3]{(10\sqrt{2}/(8\pi))} = 0.825578509501464$

P646 The surface-coverage factor is:

[484] $\beta = \sqrt[3]{(5\pi^2)/4} = 0.916987168493568$

P647 The factor β enters surface calculations, whereas φ enters volume calculations for the lattice.

34.1.2 Derivation of gravitation from the pressure gradient

P648 Spatial variations in the energy pressure around a mass generate a radial force:

[485] $F = -V\,dP/\,dR$

P649 Using the pressure–energy-density relation gives:

[486] $F = -(V/2)\,d\rho/\,dR$

P650 The corresponding acceleration is:

[487] $g = -c^2/(2\rho)\,d\rho/\,dR$

P651 Substitution of the energy-distribution function yields:

[488] $g = c^2/[2(1-f)]\,df/\,dR$

P652 In the weak-field limit:

[489] $g \approx (c^2/2)\,df/\,dR$

P653 Within this framework, gravitation is derived from the gradient of the spacetime energy distribution.

34.1.3 Gravitational field in the absence of cosmic expansion

34.1.3.1 Energy-distribution function

P654 To examine the initial field, we consider a function with a Newtonian core and exponential damping:

[490] $f(R) = (R_s/R)\mathrm{Exp}[-(R/R_d)^k]$

P655 The Schwarzschild radius is:

[491] $R_s = 2GM/c^2$

P656 At distances small compared with the damping scale:

[492] $f(R) \approx R_s/R$

34.1.3.2 Field-energy integral

P657 The radial integral is:

[493] $I = \int_{R_s}^{\infty} R^2 f(R)\,dR$

P658 Substituting the damping function gives:

[494] $I = R_s \int_{R_s}^{\infty} R.\,\mathrm{Exp}[-(R/R_d)^k]\,dR$

P659 The analytical result is:

[495] $I = (R_s {R_d}^2/k)\Gamma[2/k, (R_s/R_d)^k]$

P660 Under the condition:

[496] $R_s \ll R_d$

P661 the following approximation is obtained:

[497] $I \approx (R_s {R_d}^2/k)\Gamma(2/k)$

P662 The corresponding energy is:

[498] $E \approx 2\pi\rho_u I$

P663 Including the energy-balance factor gives:

[499] $E \approx 2\pi\rho_u z I$

34.1.3.3 Equivalence of the discrete and continuous gravitational-energy calculations

P664 In Ramionics, the energy associated with a change in the ramion distribution can be calculated either by discrete counting of FCC shells or by continuous integration of the energy density. This section examines the consistency of the coefficients obtained by the two methods in the continuum limit.

P665 The energy associated with the change in distribution per ramion is:

[500] $\Delta E_1 = E_s f/2$

P666 The number of ramions in shell n, and its large-n approximation, are:

[501] $L(n) = 10n^2 + 2$

[502] $L(n) \approx 10n^2$

P667 The total energy in the large-shell approximation is therefore:

[503] $\Delta E \approx 5E_s \sum_n n^2 f(n)$

P668 The geometrical relation for the shell radius and the corresponding change of variable are:

[504] $R = 2\gamma n r_s$

[505] $n^2\, dn = R^2\, dR/(8\gamma^3 {r_s}^3)$

P669 Thus, in the continuum approximation:

[506] $\Delta E \approx [5E_s/(8\gamma^3 {r_s}^3)] \int_0^\infty R^2 f(R)\, dR$

P670 The background energy density and the FCC geometrical identity are:

[507] $\rho_u = \varphi E_s/[(4\pi/3){r_s}^3]$

[508] $1/(8\varphi\gamma^3) = 3/10$

P671 The discrete energy coefficient therefore becomes the continuous coefficient:

[509] $5E_s/(8\gamma^3 {r_s}^3) = 2\pi\rho_u$

P672 Hence:

[510] $\Delta E \approx 2\pi\rho_u \int_0^\infty R^2 f(R)\, dR$

P673 This relation is consistent with the field-energy integral in the continuum limit. This equivalence does not imply exact equality between a finite sum and an integral; boundary corrections and corrections for small shells must be examined separately. Furthermore, this geometrical transformation alone does not determine the origin of the energy-balance factor z.

34.1.3.4 Damping scale

P674 The geometrical function is:

[511] $$F(k) = \Gamma(2/k)/k$$

P675 An equivalent expression is:

[512] $$F(k) = ½\Gamma(1 + 2/k)$$

P676 Hence:

[513] $$I \approx R_s {R_d}^2 F(k)$$

P677 and:

[514] $$R_d = \sqrt{[I/(R_s F(k))]}$$

34.1.3.5 Extremum and stationary point of the function

P678 The stationarity condition is:

[515] $$F'(k) = -\Gamma(1 + 2/k)\psi(1 + 2/k)/k^2 = 0$$

P679 Consequently:

[516] $$\psi(1 + 2/k) = 0$$

P680 The numerical solution is:

[517] $$k_{opt} = 4.332453928522$$

P681 The function value at this point is:

[518] $$F_{min} = 0.442801597205$$

P682 The maximum damping scale for a fixed value of the integral is:

[519] $$R_{d(max)} = \sqrt{[I/(0.442801597205 R_s)]}$$

P683 This result applies to the single-function model and provides the basis for selecting the fixed Newtonian damping exponent in the two-branch model. The damping exponent of the modified branch is determined independently.

34.1.4 Radial correction due to cosmic expansion

P684 In an expanding universe, the effective radial distance may differ from the original geometrical distance.

P685 The radial mapping is:

[520] $$\bar{R} = R/[1 - (R/R_u)^{km1}]^{km2}$$

P686 Its domain is:

[521] $$0 < R < R_u$$

P687 At small distances:

[522] $$\bar{R} \approx R$$

P688 The modified field function is:

[523] $$f(R) = [R_s/\bar{R}(R)]Exp[-(\bar{R}(R)/R_d)^k]$$

34.1.5 Relativity, the Schwarzschild radius and the Newtonian limit

P689 The Schwarzschild radius is:

[524] $R_s = 2GM/c^2$

P690 In the Schwarzschild metric, with the appropriate sign convention:

[525] $g_{tt} = 1 - R_s/R$

P691 The time-dilation factor is:

[526] $N_{gr} = 1/\sqrt{(1 - R_s/R)}$

P692 In the Newtonian limit:

[527] $f(R) \approx R_s/R$

P693 Hence:

[528] $|g| \approx GM/R^2$

34.1.5.1 Relativistic projection of the parameters

P694 In Ramionics, an increase in the local ramion energy by a factor N is accompanied by changes in the geometrical and dynamical scales.

P695 The local radius scales as N, the surface area as N^2 and the volume as N^3; consequently, the local energy density and pressure scale as $1/N^2$.

P696 Under the Ramionics projection convention, mass scales as N^5, the Planck constant as N^4 and the gravitational constant as $1/N^8$.

34.1.6 Friedmann equations, cosmic expansion and the vacuum-energy-density discrepancy

34.1.6.1 Friedmann equations and the energy density of space

P697 One of the largest discrepancies in orders of magnitude in physics is that between the vacuum energy density estimated in quantum field theory and the dark-energy density inferred from cosmological observations. Depending on the assumptions used in the calculation, the discrepancy can approach 120 orders of magnitude.

P698 The first Friedmann equation for a homogeneous and isotropic universe is:

[529] $H^2 = (8\pi G/3)\rho_m - kc^2/a^2 + \Lambda c^2/3$

P699 The second Friedmann equation is:

[530] $\ddot{a}/a = -(4\pi G/3)(\rho_m + 3P/c^2) + \Lambda c^2/3$

P700 Here, H is the expansion rate, ρ_m is the mass density equivalent to the energy density, P is pressure, a is the scale factor, k is the spatial-curvature parameter and Λ is the cosmological constant.

P701 For a spatially flat universe, the critical mass-equivalent density is:

[531] $\rho_c = 3H^2/(8\pi G)$

P702 The critical energy density is:

[532] $u_c = \rho_c c^2 = 3H^2c^2/(8\pi G)$

P703 In standard cosmology, these relations connect the expansion rate to the total effective density and the other geometrical and cosmological components.

P704 In Ramionics, the fundamental energy density of the FCC lattice is calculated from the energies and volumes of the ramions and is distinct from the Friedmann critical density.

34.1.6.2 Ramion entanglement and the closure of the universe

P705 In Ramionics, the universe is a network of entangled ramions rather than a collection of free, independent components.

P706 If any ramion is taken as the centre of the universe, the most distant ramions define the surface of an imaginary sphere. However, ramions on this surface are entangled with their symmetric counterparts on the opposite side. The surface is therefore not a free boundary of the universe; **the universe is confined within itself**.

P707 The Friedmann equations account for spatial curvature, but do not explicitly include this particular mechanism of entanglement and microscopic FCC closure.

P708 For this reason, Ramionics does not directly identify the fundamental ramion energy density with the critical density obtained from the Friedmann equations.

34.1.6.3 Geometrical and topological derivation of the relation between the universe radius and the Hubble radius

P709 In the FCC lattice, the number of ramions in shell n and the total number up to that shell are, respectively:

[533] $L(n) = 10n^2 + 2$

[534] $T(n) = (10n^3 + 15n^2 + 11n + 3)/3$

P710 In the limit of a very large number of shells:

[535] $L(n) \approx 10n^2$

[536] $T(n) \approx (10/3)n^3$

P711 The one-sided geometrical radius of the lattice is:

[537] $R_n = 2\gamma r_s n$

P712 The factor γ is derived from the ratio of the volume occupied by ramions to the volume of the equivalent sphere:

[538] $\varphi = 10/(24\gamma^3)$

P713 Hence:

[539] $\gamma = \sqrt[3]{[10/(24\varphi)]} = 0.825578509501464$

P714 The increase in the number of ramions between consecutive shells is:

[540] $\Delta L = L(n+1) - L(n) = 20n + 10$

P715 For large n, the relative increase in the number of ramions in the shell is:

[541] $\Delta L/L \approx 2/n$

P716 Since the number of ramions in a shell is proportional to the square of the length scale, the relative increase in the linear scale is half the relative increase in area:

[542] $\Delta a/a \approx \frac{1}{2}\Delta L/L \approx 1/n$

P717 The fundamental lattice-growth time is:

[543] $t_s = r_s/c$

P718 The expansion rate is therefore:

[544] $H \approx (\Delta a/a)/t_s \approx c/(nr_s)$

P719 Using the one-sided geometrical radius gives:

[545] $H \approx 2\gamma c/R_n$

P720 In the entangled structure of Ramionics, the outermost shell is not a free boundary and is connected to the symmetric side of the universe. The effective two-sided radius of this structure is defined as:

[546] $R_u = 2R_n = 4\gamma n r_s$

P721 Consequently:

[547] $H \approx 4\gamma c/R_u$

P722 This derivation associates the factor 4γ with two geometrical factors: a factor of 2 in the equivalent FCC radius and a factor of 2 in the definition of the effective radius of the entangled universe.

34.1.6.4 Independent derivation from force and dynamical analysis

P723 In the force analysis of Ramionics, the internal pressure of each ramion is half its energy density. The total ramion force is obtained from the surface pressure:

[548] $F_s = P_s A_s = 3E_s/(2r_s) = 3m_s c^2/(2r_s)$

P724 After the force is divided into three contributions—surface, internal and external—the difference in ramion counts between consecutive shells gives the following net expansion contribution:

[549] $F_{exp,n} \approx (20n/3)F_s$

P725 Summing this force up to the outermost shell and dividing by the total number of ramions gives the mean residual force per ramion:

[550] $F_{exp} \approx F_s/n_u$

P726 The corresponding acceleration is:

[551] $a_{exp} = F_{exp}/m_s = 3c^2/(2n_u r_s)$

P727 Using the geometrical relation for the universe radius:

[552] $R_u = 2\gamma n_u r_s$

P728 the expansion acceleration is:

[553] $a_{exp} = 3\gamma c^2/R_u$

P729 To convert the mean acceleration into a Hubble rate, the mean radial position of the ramions is calculated from the FCC shell-counting law:

[554] $\bar{n} = \sum_{n=1}^{n_u} nL(n) \,/\, \sum_{n=1}^{n_u} L(n) \approx 3n_u/4$

P730 Hence:

[555] $\bar{R} = 3R_u/4$

P731 Using the characteristic propagation time across the universe:

[556] $t_u = R_u/c$

P732 the mean velocity resulting from the acceleration is:

[557] $\bar{v}_{exp} = a_{exp} t_u = 3\gamma c$

P733 The Hubble law evaluated at the mean distance also gives:

[558] $\bar{v}_{exp} = H.\bar{R} = (3/4)H.R_u$

P734 Equating these expressions yields:

[559] $H = 4\gamma c/R_u$

P735 Thus, under their respective stated assumptions, the force–dynamical analysis and the geometrical–topological analysis lead to the same relation.

P736 In the force analysis, the factor 4 results from combining the acceleration coefficient 3 with the mean-radius factor 3/4; in the topological analysis, it arises from two geometrical factors of 2.

P737 Methodological note: these derivations rely on specific model assumptions, including division of the force of each ramion into three contributions, selection of the characteristic time R_u/c, and the definition of the effective radius of the entangled universe. They therefore demonstrate consistency between two approaches within Ramionics, while the independent validity of these assumptions still requires physical investigation.

34.1.6.5 Hubble radius and universe radius

P738 The Hubble radius is defined by:

[560] $R_h = c/H_0$

P739 The derived expansion relation gives:

[561] $R_u = 4\gamma R_h$

P740 Hence:

[562] $R_u/R_h = 4\gamma = 3.302314038005856$

P741 Using the local value of the Hubble constant:

[563] $H_0 = 73.50 \pm 0.81\ \text{km.s}^{-1}.\text{Mpc}^{-1}$

P742 the Hubble radius is:

[564] $R_h = 4078.808952381\ \text{Mpc} = 13.3032955331\ \text{Gly}$

P743 The universe radius in the Ramionics model is:

[565] $R_u = 13469.5080618\ \text{Mpc} = 43.9316595906\ \text{Gly}$

P744 The unit Gly denotes one billion light-years.

P745 **In Ramionics, the Hubble radius is directly related to the geometrical radius of the universe, rather than to the fundamental ramion energy density.**

34.1.6.6 Fundamental scale of the universe and residual expansion force

P746 Using the fundamental ramion radius:

[566] $r_s = \theta_e{}^{-1} 8.33772422647155 \times 10^{-30}$ m

P747 and the universe radius:

[567] $R_u \approx 4.155582742 \times 10^{26}$ m

P748 the ratio of these scales is:

[568] $R_u / r_s \approx \theta_e \times 4.984073146 \times 10^{55}$

P749 The geometrical relation for the universe radius gives the number of shells:

[569] $n_u \approx \theta_e \times 3.018533725 \times 10^{55}$

P750 The net expansion force as a fraction of the total force of each ramion is therefore:

[570] $F_{exp} / F_s = 1/n_u \approx \theta_e{}^{-1} 3.312866747 \times 10^{-56}$

P751 In this description, almost all of the fundamental ramion force is balanced within the lattice, leaving only a very small residual contribution on the scale of the universe.

P752 As the universe radius increases, the following relation holds:

[571] $H \propto 1/R_u$

P753 In the limit of an infinite universe, the model predicts decreasing net force, acceleration and expansion rate.

34.1.6.7 Analysis of the vacuum-energy-density discrepancy

P754 Within Ramionics, the enormous vacuum-energy-density discrepancy arises from equating two distinct quantities: the fundamental ramion energy density and the cosmological critical density.

P755 Entanglement and the internal closure of the universe imply that the fundamental lattice energy need not contribute to cosmic expansion in the same way as the energy of a free medium.

P756 The force analysis shows that each ramion's net expansion contribution is very small relative to its fundamental force. The geometrical analysis likewise relates the expansion rate to the number of shells and the universe radius.

P757 In this model, the universe radius is calculated from FCC geometry, whereas the fundamental energy density of space is calculated from the structure of the ramions.

P758 This distinction underlies the resolution of the vacuum-energy-density discrepancy in Ramionics. However, the ratio of residual force to fundamental force alone does not constitute a quantitative demonstration that the discrepancy has been resolved. Such a demonstration requires independent derivations of the gravitational contribution of the lattice energy and of the cosmological evolution equations.

34.1.6.8 Hubble tension

P759 The Hubble tension refers to the discrepancy between the value of the Hubble constant inferred from the cosmic microwave background and the value obtained from local measurements.

P760 In Ramionics, this discrepancy is associated with the FCC surface-coverage factor β:

[572] $H_{0(\mathrm{local})} \approx H_{0(\mathrm{cm}\beta)}/\beta$

P761 Using the reference value:

[573] $H_{0(\mathrm{cm}\beta)} \approx 67.4\ \mathrm{km.s^{-1}.Mpc^{-1}}$

P762 the geometrical correction gives a value close to 73.5 km.s^{-1}.Mpc^{-1}.

P763 This relation is proposed in Ramionics as a geometrical mechanism for explaining the Hubble tension; its validity for cosmological data requires independent testing.

34.1.7 Dark energy and apparent dark matter

P764 In Ramionics, the energy distributed throughout the spacetime lattice provides the physical basis of dark energy.

P765 Variations in this distribution around a mass generate a gravitational field. Additional gravitational effects on galactic and cluster scales are also investigated through changes in the structure of the field.

P766 The geometrical fraction of unoccupied space in the FCC lattice is:

[574] $1 - \varphi \approx 0.2595$

P767 This value is close to the cosmological fraction attributed to dark matter.

P768 In Ramionics, this numerical similarity is used to investigate a geometrical origin for apparent dark matter. Its dynamical connection to acceleration and gravitational lensing must be calculated from the field equations.

34.1.8 MOND and the gravitational acceleration scale

34.1.8.1 History and originator

P769 MOND, an acronym for Modified Newtonian Dynamics, was introduced in 1983 by the Israeli physicist **Mordehai Milgrom**.

P770 Its principal aim was to explain galaxy rotation curves and the discrepancy between the gravitational acceleration calculated from visible matter and that inferred from the motions of stars and gas.

P771 In Newtonian gravity, the orbital speed outside a spherical mass distribution decreases with distance, whereas the rotation curves of many spiral galaxies remain approximately flat in their outer regions.

P772 MOND addresses this discrepancy by modifying the dynamical law at very low accelerations.

34.1.8.2 Fundamental MOND relation

P773 In the usual algebraic formulation of MOND, for systems with suitable symmetry:

[575] $g_n = \mu(g/a_{\mathrm{mon}})g$

P774 Here, g_n is the Newtonian acceleration due to the baryonic mass, g is the actual acceleration in the model, a_{mon} is the characteristic acceleration and μ is the interpolating function.

P775 In the high-acceleration limit:

[576] $\mu(x) \approx 1\ , x \gg 1$

P776 In the low-acceleration limit:

[577] $\mu(x) \approx x\,, x \ll 1$

P777 One commonly used interpolating function is:

[578] $\mu(x) = x/\sqrt{(1 + x^2)}$

P778 The choice of interpolating function affects the details of the transition region.

34.1.8.3 Deep-MOND limit

P779 At very low accelerations:

[579] $g \approx \sqrt{(g_n a_{mon})}$

P780 For a spherical or point mass:

[580] $g_n = GM/R^2$

P781 Hence:

[581] $g_{mon} \approx \sqrt{(GMa_{mon})}/R$

P782 In this limit, the acceleration decreases inversely with distance, whereas the Newtonian acceleration varies inversely with the square of the distance.

34.1.8.4 Orbital speed

P783 The centripetal acceleration for circular motion is:

[582] $g = v^2/R$

P784 In the deep-MOND limit:

[583] $v^4 \approx GMa_{mon}$

P785 This expression is related to the form of the empirical relation between baryonic mass and galaxy rotation speed, known as the baryonic Tully–Fisher relation.

34.1.8.5 MOND transition radius

P786 The characteristic transition radius is:

[584] $R_{mon} = \sqrt{(GM/a_{mon})}$

P787 In isolated systems, Newtonian behaviour is relevant at high accelerations, whereas modified behaviour becomes important at low accelerations.

34.1.8.6 MOND acceleration in Ramionics

P788 In Ramionics, the MOND acceleration scale is related to the local Hubble constant:

[585] $a_{mon} \approx cH_0/6$

P789 Using the adopted Hubble constant gives:

[586] $a_{mon} \approx 1.190162456547 \times 10^{-10}\ \mathrm{m.s^{-2}}$

P790 This value is used to calculate the MOND transition radius in the two-branch model.

34.1.8.7 Domain of application of MOND

P791 MOND is used primarily to study galaxy rotation curves, the baryonic mass–velocity relation and systems with low accelerations.

P792 Its principal regime is defined by accelerations of order 10^{-10} m.s^{-2} or below, rather than by a universal fixed distance.

P793 In the presence of a significant external field, a system may behave differently from an isolated system in the deep-MOND limit. This property is known as the external-field effect.

P794 The original formulation of MOND is not, by itself, a complete relativistic and cosmological theory. The study of galaxy clusters and gravitational lensing requires a more extensive formulation.

34.1.9 MOG and the enhancement of gravity on large scales

34.1.9.1 History and originator

P795 MOG, an acronym for Modified Gravity, was developed by the Canadian physicist **John W. Moffat**.

P796 Its well-known formulation, Scalar–Tensor–Vector Gravity (STVG), was published in 2006.

P797 The theory was developed to investigate the dynamics of galaxies and galaxy clusters, gravitational lensing and other large-scale gravitational phenomena.

P798 Unlike the original formulation of MOND, MOG provides a framework with additional fields and scale-dependent parameters.

34.1.9.2 Physical structure of MOG

P799 In STVG, a vector field and scalar fields are introduced alongside the gravitational metric field.

P800 In the weak-field limit for a point source, the effective acceleration includes a Yukawa term:

[587] $g_{mog} = (GM/R^2)[1 + \alpha_{mog} - \alpha_{mog}(1 + \mu R)\mathrm{Exp}(-\mu R)]$

P801 Here, $\alpha_{mo}\boldsymbol{g}$ is the dimensionless gravitational-enhancement parameter and μ is an inverse-length parameter.

P802 The transition length scale is:

[588] $R\mu = 1/\mu$

34.1.9.3 Short-distance limit

P803 Under the condition:

[589] $\mu R \ll 1$

P804 the Yukawa term approximately cancels the additional enhancement, and the acceleration approaches its Newtonian limit:

[590] $g_{mog} \approx GM/R^2$

34.1.9.4 Large-distance limit

P805 Under the condition:

[591] $\mu R \gg 1$

P806 the exponential term decays, and the acceleration becomes:

[592] $g_{mog} \approx (GM/R^2)(1 + \alpha_{mog})$

P807 In this limit, gravity is enhanced relative to its Newtonian value but retains its inverse-square dependence on distance.

34.1.9.5 MOG enhancement factor in Ramionics

P808 In Ramionics, the enhancement factor is related to the geometrical coefficient γ:

[593] $\alpha_{mog} = 5\pi/\gamma$

P809 Its approximate value is:

[594] $\alpha_{mog} \approx 19.03$

P810 The asymptotic enhancement factor is:

[595] $1 + \alpha_{mog} \approx 20.03$

P811 This value serves as a reference for examining gravitational enhancement on large scales in the Ramionics model.

34.1.9.6 Observational calibrations of the MOG parameter

P812 In some fits of MOG theory, the parameter α specifies the enhancement of the gravitational component relative to the Newtonian limit within the model formulation. Reported values depend on the dataset, mass and fitting assumptions; they are not necessarily independent measurements of a universal constant.

Table 21

Study	Observational sample	Fitted α
Moffat & Rahvar (2013)	THINGS galaxy rotation curves	8.89 ± 0.34
Harikumar et al. (2022)	X-COP clusters, M_{200}	9.12 ± 2.72
Harikumar et al. (2022)	X-COP clusters, M_{500}	9.99 ± 3.40

P813 These values are reported as comparative benchmarks, rather than as constraints imposed in advance on the Ramionics field function. For a consistent comparison with the data, the acceleration-enhancement ratio and its excess contribution are calculated directly from the field:

[596] $A(R, M) = |g(R, M)|/(GM/R^2)$

[597] $\alpha_{eff}(R, M) = A(R, M) - 1$

P814 Such comparisons must respect the parameter definitions used in each study and the radial range over which each fit is valid. The geometrical value $5\pi/\gamma$ in the main text remains an independent Ramionics hypothesis or reference value; these data alone do not validate it.

34.1.9.7 Domain of application of MOG

P815 MOG is used to investigate galaxy dynamics, galaxy clusters and gravitational lensing.

P816 Unlike MOND, the transition scale in the point-source MOG relation is specified directly by the parameter μ.

P817 The effective parameters $\alpha_{mo}\mathcal{G}$ and μ may depend on the mass and scale of the system in different applications of the theory.

P818 For extended mass distributions, the point-source acceleration relation must be generalised by calculating the field generated by the mass distribution.

34.1.9.8 Comparison of MOND and MOG

Table 22

Property	MOND	MOG
Founder	Mordehai Milgrom	John W. Moffat
Initial publication	1983	2006 (STVG)
Main scale	Acceleration	Length and coupling
Main parameters	a_{mon}, μ(x)	$\alpha_{mo}\mathcal{G}$, μ
Newtonian limit	High acceleration	Short distance
Modified regime	Low acceleration	Large distance
Point-mass far-field acceleration	∝1/R	∝1/R²
Main applications	Galaxy dynamics	Galaxies and clusters

P819 In Ramionics, behaviours corresponding to MOND and MOG are investigated using a common modified function.

34.1.10 Two-branch model of the Ramionics gravitational field

P820 To combine Newtonian behaviour at small distances with modified behaviour on large scales, the energy-distribution function is divided into two components.

P821 The Newtonian component is:

[598] $$f_n(\bar{R}_n) = (R_s/\bar{R}_n)\mathrm{Exp}[-(\bar{R}_n/R_{dn})^{kdn}]$$

P822 **The Newtonian damping exponent $k\mathcal{d}_n$ is set to the analytical value 4.332453928522 obtained from Eqs. [454] to (40) and is held fixed in the final Gravity23, Stage39 model. It is therefore not a free parameter in the fit to the MOND and MOG data.**

P823 The common MOND–MOG component is:

[599] $$f_m(\bar{R}_m) = [R_s/(p_m R_{mon})]\mathrm{Ln}[1 + (R_m/\bar{R}_m)^{pm}]\mathrm{Exp}[-(\bar{R}_m/R_{dm})^{kdm}]$$

P824 The total field function is:

[600] $$f(R) = f_n(\bar{R}_n) + f_m(\bar{R}_m)$$

34.1.10.1 Basis for selecting the model and analysis of the Newtonian, MOND and MOG limits

P825 The two-branch function in Eqs. [541] to (123) is chosen to combine a Newtonian core with a logarithmic branch that reproduces MOND behaviour under suitable conditions and permits investigation of behaviour corresponding to MOG on larger scales. To clarify the capabilities and limitations of this choice, we first examine the analytical limits of the two branches. The equations in this subsection continue the sequential equation numbering of the manuscript.

34.1.10.2 Newtonian limit of the first branch

P826 The Newtonian-branch function is the same as Eq. [541]:

[601] $$f_n(\bar{R}_n) = (R_s/\bar{R}_n)\mathrm{Exp}[-(\bar{R}_n/R_{dn})^{kdn}]$$

P827 At distances smaller than the damping scale:

[602] $$\bar{R}_n \ll R_{dn}$$

P828 the exponential factor is approximately unity:

[603] $$\mathrm{Exp}[-(\bar{R}_n/R_{dn})^{kdn}] \approx 1$$

P829 Hence:

[604] $$f_n(\bar{R}_n) \approx R_s/\bar{R}_n$$

P830 If the effect of the radial mapping is also negligible:

[605] $$\bar{R}_n \approx R$$

P831 then:

[606] $$f_n(R) \approx R_s/R$$

P832 In the weak-field limit, using the definition $R_s=2GM/c^2$, the acceleration of this branch becomes:

[607] $$g_n(R) \approx -GM/R^2$$

P833 The first branch therefore reproduces Newton's inverse-square law in this limit. For the total acceleration to be Newtonian, the acceleration contributed by the modified branch must also be small over the same range.

34.1.10.3 Modified branch and radial scales

P834 The common MOND–MOG function is the same as Eq. [542]:

[608] $$f_m(\bar{R}_m) = [R_s/(p_m R_{mon})]\mathrm{Ln}[1 + (R_m/\bar{R}_m)^{pm}]\mathrm{Exp}[-(\bar{R}_m/R_{dm})^{kdm}]$$

P835 Here, R_{mon} is the characteristic MOND radius, R_m is the transition scale from logarithmic to power-law behaviour, and Rd_m is the damping scale of the modified branch. To derive the leading behaviour, we first consider a range in which:

[609] $$\bar{R}_m \ll R_{dm}$$

[610] $$\bar{R}_m \approx R$$

P836 Under this approximation:

[611] $$f_m(R) \approx [R_s/(p_m R_{mon})]\mathrm{Ln}[1 + (R_m/R)^{pm}]$$

34.1.10.4 MOND limit at distances smaller than R_m

P837 If:

[612] $$R \ll R_m$$

P838 then:

[613] $$(R_m/R)^{pm} \gg 1$$

P839 Consequently:

[614] $$\mathrm{Ln}[1 + (R_m/R)^{pm}] \approx p_m \mathrm{Ln}(R_m/R)$$

P840 Thus:

[615] $f_m(R) \approx (R_s/R_{mon})\mathrm{Ln}(R_m/R)$

P841 The radial derivative is:

[616] $df_m/\,dR \approx -R_s/(R_{mon}R)$

P842 and the corresponding acceleration in the weak-field limit is:

[617] $g_m(R) \approx -GM/(R_{mon}R)$

P843 From the definition of the MOND radius:

[618] $R_{mon} = \sqrt{(GM/a_{mon})}$

P844 it follows that:

[619] $|g_m(R)| \approx \sqrt{(GMa_{mon})}/R$

P845 This is the radial dependence of the deep-MOND limit. For this branch to dominate the Newtonian acceleration, R must exceed R_{mon}, in addition to the approximations remaining valid. The appropriate approximate range is therefore:

[620] $R_{mon} \ll R \ll R_m$

P846 Such a range is broad only when R_m exceeds R_{mon}.

34.1.10.5 Large-scale limit and its difference from the MOG inverse-square law

P847 If:

[621] $R \gg R_m$

P848 then:

[622] $(R_m/R)^{pm} \ll 1$

P849 In this limit:

[623] $\mathrm{Ln}[1 + (R_m/R)^{pm}] \approx (R_m/R)^{pm}$

P850 The modified-branch function is therefore approximated by:

[624] $f_m(R) \approx [R_s/(p_m R_{mon})](R_m/R)^{pm}$

P851 Its derivative is:

[625] $df_m/\,dR \approx -[R_s/(R_{mon}R)](R_m/R)^{pm}$

P852 and the corresponding acceleration is:

[626] $|g_m(R)| \approx [GM/(R_{mon}R)](R_m/R)^{pm}$

P853 For the value adopted in the final model:

[627] $p_m = 1/4$

P854 it follows that:

[628] $|g_m(R)| \approx (GM/R_{mon}){R_m}^{1/4}/R^{5/4}$

P855 In this approximation, the modified branch therefore decreases as the inverse 5/4 power of distance, rather than as its inverse square. The logarithmic transition alone thus does not establish the asymptotic MOG limit. To evaluate the actual field behaviour on cluster scales, the complete derivative of the

function, the exponential damping, the radial mapping and the Newtonian contribution must all be calculated.

34.1.10.6 Mass dependence of the transition radius

P856 In the final model, according to Eq. [582]:

[629] $R_m = R_{mon}(M/M_c)^{-1/2}$

P857 Substituting the definition of R_{mon} gives:

[630] $R_m = \sqrt{(GM/a_{mon})}\sqrt{(M_c/M)}$

P858 and simplification yields:

[631] $R_m = \sqrt{(GM_c/a_{mon})}$

P859 Thus, if G, M_c and a_{mon} are constant, R_m is independent of the source mass under this definition, whereas the ratio R_m/R_{mon} decreases as the mass increases. In the table in source Section 18, this ratio is reported as 72.86796, 7.286796 and 0.7286796 for masses of 10^{11}, 10^{13} and 10^{15} solar masses, respectively. The simple MOND regime can therefore be broad for galactic masses, but need not exist for very large masses.

34.1.10.7 Transition function without the logarithmic approximation

P860 Neglecting damping and radial mapping, but retaining the logarithm without approximation when differentiating, the modified-branch acceleration in the weak-field limit is:

[632] $|g_m(R)| \approx [GM/(R_{mon}R)]/[1 + (R/R_m)^{pm}]$

P861 This relation continuously connects the MOND limit to the large-scale power-law limit. At the transition radius:

[633] $|g_m(R_m)| \approx GM/(2R_{mon}R_m)$

P862 Consequently, R_m is a smooth transition scale rather than a discontinuous boundary. **The rationale for the present model** is that it analytically reproduces the Newtonian structure in the first branch and deep-MOND behaviour in the logarithmic branch, while permitting a simultaneous fit to large-scale data and the energy-balance constraint. Nevertheless, reproduction of the enhanced inverse-square MOG law does not follow from this choice alone and must be tested using the complete field function.

P863 In this structure, the two components have independent damping scales.

P864 The first component preserves approximately Newtonian behaviour, while the second describes gravitational transitions on large scales.

34.1.11 Energy balance in the two-branch field

P865 The energy constraint used in the model, with a general upper limit R_{lim}, is:

[634] $E_s(M/m_s)^2/12 = 2\pi\rho_u \int_{R_s}^{R_{lim}} [f_n(R) + f_m(R)]\, R^2\, dR$

P866 The vacuum energy density used in the calculations is:

[635] $\rho_u = 4.57974243707115 \times 10^{68}\ J/m^3$

P867 The integral contribution of the Newtonian branch is:

[636] $I_n = \int_{R_s}^{R_{\mathrm{lim}}} R^2 \, f_n(R) \, \mathrm{d}R$

P868 The contribution of the modified branch is:

[637] $I_m = \int_{R_s}^{R_{\mathrm{lim}}} R^2 \, f_m(R) \, \mathrm{d}R$

P869 The total integral is:

[638] $\mathrm{I} = \mathrm{I_n} + \mathrm{I_m}$

P870 The energy constraint applies to the sum of the two branches, rather than to each branch independently.

P871 **Integration domain:** the symbol R_{lim} in Eqs. [577], (159) and (160) denotes the upper integration limit expressed in terms of the physical radius R. In the **unmapped case**, R_{lim} is ∞; in the **current Stage39 mapped case**, R_{lim} is R_u; and in the **alternative mapping with a Hubble boundary**, R_{lim} would be R_h. The volume element $R^2 dR$ is expressed in terms of the physical radius; divergence of the mapped effective radius at the boundary does not make the physical integration domain infinite.

P872 **Consistency of the energy coefficient with the script:** the density ρ_u in Eq. [578] is eight times the conventional density used in the Gravity23 script. Consequently, rearranging the energy equation [577] and using the script's density makes its coefficient 12 consistent with the script's coefficient 96. These two representations should not be interpreted as distinct energy models.

34.1.12 Mass-dependent radial scales

34.1.12.1 Common transition scale

[639] $\mathrm{R_m} = \mathrm{R_{mon}}(\mathrm{M}/\mathrm{M_c})^{-1/2}$

P873 The parameter M_c sets the transition mass scale.

34.1.12.2 Damping scale of the Newtonian branch

[640] $\mathrm{R_{dn}} = \mathrm{R_h}(\mathrm{M}/\mathrm{M_{dn}})^2$

34.1.12.3 Damping scale of the modified branch

[641] $\mathrm{R_{dm}} = \mathrm{R_h}(\mathrm{M}/\mathrm{M_{dm}})^{\mathrm{pdm}}$

P874 The mass-dependence exponent is:

[642] $\mathrm{p_{dm}} = 3/[2(3 - \mathrm{p_m})]$

P875 For the value:

[643] $\mathrm{p_m} = 1/4$

P876 it follows that:

[644] $\mathrm{p_{dm}} = 6/11$

P877 These scales are distinct from the Schwarzschild radius, MOND radius and Hubble radius, although those radii enter their definitions.

34.1.13 Analytical scaling of the energy

P878 In the two-branch model, the behaviour of the energy integral depends on the radial exponents and the mass dependence of the damping scales.

P879 The Newtonian branch combines an inverse-radius core with exponential damping.

P880 In the MOND–MOG branch, the logarithmic function and transition scale R_m modify the energy behaviour.

P881 The mass exponent 6/11 for $R\mathcal{d}_m$ is associated with the analytical scaling condition for the modified branch.

P882 This structure permits calculation and comparison of the energy contributions of the two branches for different masses.

34.1.14 Nonlinear radial mapping in an expanding universe

34.1.14.1 Physical meaning of the mapping and choice of reference radius

P883 Within the Ramionics framework, cosmic expansion means that the geometrical radius R need not coincide with the effective radius entering the energy distribution function and the calculation of the gravitational field. The radial mapping transforms R into an effective radius $\bar{R}$, thereby incorporating cosmic expansion into the radial dependence of the field. In the current model, this mapping is a structural assumption; it has not yet been derived independently from the full evolution equations of the FCC lattice.

P884 The mapping is chosen so that $\bar{R}$ increases without bound as R approaches the ultimate reference radius from below. The finite geometrical distance corresponding to the selected boundary is thus mapped to infinity in the effective field variable. This divergence does not imply that the physical radius of the universe itself becomes infinite; it is a property of the effective coordinate transformation used in the model.

P885 Two options are considered for the reference radius of this mapping:

P886 - **First option, the radius of the universe R_u:** the effective radius tends to infinity as the geometrical radius approaches R_u from within the domain. This is the default computational assumption in the present version of the Ramionics manuscript.

P887 - **Second option, the Hubble radius R_h:** this alternative places the same limiting behaviour at R_h. The Hubble radius is a scale determined by the expansion rate and is not necessarily the boundary of the universe or the ultimate horizon for receiving light. Its selection therefore requires physical justification and independent calibration.

P888 The current choice of R_u is motivated by the Ramionics assumption that optical signals from objects throughout the universe considered by the model can reach an observer, and that the corresponding gravitational influence must also be able to propagate or become established throughout that domain. On this basis, the effective boundary of the mapping is currently assigned to the radius of the universe rather than to the Hubble radius. Nevertheless, the statement that ‘light from all the stars in the universe has reached us’ is not, in general, an established observational fact; the observable universe is not assumed to be identical to the entire universe. Nor does this argument alone imply that a gravitational influence arrives before the corresponding light signal; that claim requires a propagation model and an independent test of causality.

P889 Accordingly, **the choice of R_u is a testable assumption of the current model, rather than a definitive observational conclusion**. The R_h option is retained for future comparison. Changing the reference radius of the mapping changes the effective radius and its derivative, and hence the calculated acceleration; such a change therefore requires the calculations and fitting procedure to be repeated.

34.1.14.2 Mathematical definition of the current mapping

P890 The general radial mapping is

[645] $\bar{R} = R/[1 - (R/R_u)^{km1}]^{km2}$

P891 The combined mapping parameter is

[646] $\lambda = -k_{m2}\mathrm{Ln}(k_{m1})$

P892 This parameter expresses the joint effect of the two mapping coefficients, but does not replace their separate definitions.

P893 In the two-branch model, radial mapping enters the calculation of each branch. Once the mapping has been defined, the following structural choices are specified independently. Equations [541] and (122) give the current form of the field function; presenting alternative options does not imply that they have been numerically implemented or validated in Stage39.

34.1.14.3 Option 1 The reference radius of the mapping and the integration limit

P894 **Unmapped case:** the effective radius equals the physical radius, and the upper limit of the energy integral is infinity. **Mapped case, current choice:** the mapping boundary is R_u, and the energy integral is evaluated in the physical radial variable R from R_s to R_u. **Mapped case, alternative choice:** the mapping boundary is R_h, and the energy integral extends from R_s to R_h. In both mapped cases, the effective radius increases without bound as the physical radius approaches the selected boundary. This property does not make the upper integration limit in the physical variable R infinite.

P895 The choice of R_u rather than R_h relies on the preceding argument concerning the domain of physical influence in the Ramionics universe. This argument is a model assumption and does not, by itself, empirically establish that R_u is the preferable choice. Changing the boundary requires the field, its radial derivative and the energy integral to be recalculated and refitted.

34.1.14.4 Option 2 Where the radial mapping is applied

P896 In **full mapping**, the effective radius $\bar{R}$ is used in both the principal term of the field function and the damping factor. This is the convention used in equations [541] and (122). For the Newtonian branch, the principal kernel is the ratio $R_s/\bar{R}_n$; for the MOND–MOG branch, it is a logarithmic kernel dependent on $\bar{R}_m$.

P897 In **damping-only mapping**, the principal term of each branch is evaluated using the physical radius R, while $\bar{R}$ is used only in the radial ratio entering the attenuation factor. The two options are therefore not equivalent in their radial derivatives, asymptotic behaviour or energy integrals. The present manuscript adopts full mapping; the damping-only case is retained as an option for testing.

34.1.14.5 Option 3 The attenuation function

P898 Two families of attenuation functions are considered, with dimensionless variable x and positive exponent k:

P899 **Exponential attenuation:**

[647] $D_{exp}(x) = Exp(-x^k)$

P900 **Rational attenuation with a power-law tail:**

[648] $D_{rat}(x) = 1/(1 + x^k)$

P901 In each branch, x is the ratio of the radius used in the damping term to the damping scale of that branch; depending on option 14–4, this radius is R or $\bar{R}$. Both functions approach unity at small radii. At large radii, however, exponential attenuation decreases more rapidly, whereas rational attenuation has a power-law tail. Substituting one for the other can therefore alter the field, acceleration and convergence of the energy integral. The reported Stage39 model uses exponential attenuation in both branches. The attenuation functions for the two branches could also be selected independently in subsequent tests.

34.1.14.6 Option 4 Shared or separate mappings for the Newtonian and MOND–MOG branches

P902 In **shared mapping**, both branches use the same mapping law and parameters. Consequently, $\bar{R}_n$ and $\bar{R}_m$ are equal at the same physical radius. This is the choice adopted by the highest-ranked Stage39 model.

P903 In **separate mapping**, the Newtonian and MOND–MOG branches may have different mapping parameters. Each branch must then be mapped separately, and the derivative of the total field with respect to R must be calculated using the chain rule. Independent mappings do not, in themselves, imply different boundary radii R_u or R_h: the boundary is selected under option 1, whereas the branch-specific parameters are selected under option 4.

34.1.14.7 Combinations of options and computational status

P904 The four choices above define four independent aspects of the model: the mapping boundary; where the mapping is applied; the attenuation family; and whether the branches share a mapping or use separate mappings. For every new combination, the physical constraints, full field derivative, convergence of the energy integral, and MOND and MOG errors must be tested again. **The Stage39 numerical results apply only to the configuration that was actually implemented** and must not be attributed to alternative combinations without rerunning the calculations.

34.1.15 Calculation of the acceleration and the Newtonian ratio

P905 The acceleration is obtained from the radial derivative of the total field function:

[649] $g(R) = c^2/[2(1 - f(R))]\, df(R)/\, dR$

P906 The ratio of the magnitude of the model acceleration to the Newtonian acceleration is

[650] $A(R) = |g(R)|/(GM/R^2)$

P907 In the Newtonian regime, this ratio approaches unity. In the transition regime and at large scales, the contribution of the modified branch changes its value.

34.1.16 Computational measures of the field

P908 The relative percentage error at each point is

[651] $\varepsilon_i = 100[A_i/A_{t,i} - 1]$

P909 The root-mean-square error is

[652] $\mathrm{RMS} = \sqrt{[(1/n)\sum_i \varepsilon_i{}^2]}$

P910 This measure is used to assess the behaviour of the field over the MOND and MOG reference-point sets.

P911 In addition to the acceleration error, the discrepancy in the integrated field energy is calculated so that the dynamical and energetic consistency of the model can be assessed together.

34.1.17 Numerical determination of the field parameters

P912 The parameters of the two-branch model are determined using energy constraints, the analytical structure of the mass scales and the reference acceleration data.

34.1.17.1 Definition of the reference and calculated acceleration in MOND and MOG calibration

P913 The Reference and Calculated entries in the table in this section are not accelerations with physical units. They are **gravitational acceleration enhancement factors relative to the Newtonian acceleration at the same mass and radius**. These factors are dimensionless.

P914 The Newtonian acceleration for source mass M at radius R is

[653] $g_{ne} = GM/R^2$

P915 The acceleration enhancement factor is

[654] $A(R) = |g(R)|/g_{ne} = |g(R)|R^2/(GM)$

P916 The table uses the following definitions:

P917 - **Reference:** the reference acceleration enhancement factor, namely the ratio of the reference acceleration to the Newtonian acceleration.

P918 - **Calculated:** the acceleration enhancement factor calculated from the Ramionics model relative to the same Newtonian acceleration.

P919 - **Error %:** the percentage difference between the calculated and reference values, as defined by equation [592].

P920 - **R/R_{mon}:** the ratio of the radius of the evaluation point to the characteristic MOND radius for the same mass.

P921 - **$M/M_\odot$:** the source mass in solar masses.

P922 For the 10 MOND points, the reference values are factors associated with galactic data and the MOND relation; they should therefore not all be described as direct experimental measurements. For the 10 MOG points, the reference values are taken from the comparison MOG model and are not direct experimental measurements. The independent observational provenance and construction of each point must be documented separately.

34.1.17.2 Combined table of the 20 reference points and model outputs

P923 This table brings together the inputs for the 20 calibration points and the calculated acceleration factors of the highest-ranked Gravity23 model from Stage39. The Reference and Calculated columns contain acceleration enhancement factors, not accelerations in m.s⁻². The calculated values and errors are reproduced from an earlier computational report; no new fitting has been performed for this revision.

Table 23

No.	Dataset	Object	M/M⊙	R/R_{mon}	Reference	Calculated	Error %
1	MOND	DDO 154	$5.000000000000\times10^{8}$	10.45	10.961955	11.857411	+8.17
2	MOND	IC 2574	$2.000000000000\times10^{9}$	8.50	9.014693	9.069552	+0.61
3	MOND	LMC	$3.000000000000\times10^{9}$	4.80	5.325971	5.207749	−2.22
4	MOND	M33	$6.400000000000\times10^{9}$	6.21	6.730096	6.340683	−5.79
5	MOND	NGC 2403	$1.000000000000\times10^{10}$	2.92	3.462499	3.027258	−12.57
6	MOND	NGC 3198	$2.000000000000\times10^{10}$	3.10	3.640064	3.082139	−15.33
7	MOND	Milky Way	$6.000000000000\times10^{10}$	2.98	3.521655	3.462847	−1.67
8	MOND	NGC 2841	$1.000000000000\times10^{11}$	2.31	2.863493	2.750410	−3.95
9	MOND	M31 low	$1.000000000000\times10^{11}$	2.22	2.775610	2.664056	−4.02
10	MOND	M31 high	$1.000000000000\times10^{11}$	2.77	3.314765	3.204319	−3.33
11	MOG	MOG 1	$1.000000000000\times10^{13}$	0.50	1.050000	0.958380	−8.73
12	MOG	MOG 2	$1.000000000000\times10^{13}$	1.00	1.180000	1.303745	+10.49
13	MOG	MOG 3	$1.000000000000\times10^{13}$	1.20	1.250000	1.437428	+14.99
14	MOG	MOG 4	$1.000000000000\times10^{13}$	1.50	1.380000	1.634182	+18.42
15	MOG	MOG 5	$1.000000000000\times10^{13}$	2.00	1.620000	1.953595	+20.59
16	MOG	MOG 6	$1.000000000000\times10^{15}$	0.50	1.050000	0.857555	−18.33
17	MOG	MOG 7	$1.000000000000\times10^{15}$	1.00	1.180000	1.097787	−6.97
18	MOG	MOG 8	$1.000000000000\times10^{15}$	1.20	1.250000	1.189284	−4.86
19	MOG	MOG 9	$1.000000000000\times10^{15}$	1.50	1.380000	1.322898	−4.14
20	MOG	MOG 10	$1.000000000000\times10^{15}$	2.00	1.620000	1.537748	−5.08

34.1.17.3 Numerical interpretation and model accuracy

P924 For the galaxy DDO 154, the reference acceleration factor is 10.961955, meaning that the reference acceleration is approximately 10.96 times the Newtonian acceleration at the same point. The Ramionics model gives a factor of 11.857411, corresponding to a calculated acceleration of approximately 11.86 times the Newtonian value and a relative difference from the reference of approximately +8.17 per cent.

P925 To convert a factor into a physical acceleration, it must be multiplied by the Newtonian acceleration at the corresponding point. The present comparison tests agreement with the MOND and MOG reference sets; it does not, by itself, constitute independent empirical validation of the Ramionics model.

Table 24

Metric	RMS
MOND acceleration	7.376181%
MOG acceleration	12.748308%
Total acceleration (20 points)	10.414591%
Energy	3.938752%
Combined	7.873292%

P926 The largest absolute relative error in the table occurs at point 15, with mass 10^{13} M⊙ and radius $2R_{mon}$, and is approximately 20.59 per cent. The overall RMS acceleration error for the 20 points is 10.414591 per cent.

P927 Gauss–Legendre quadrature was used to control the accuracy of the numerical integration, and the stability of the results was checked by increasing the quadrature order. These calculations adopt the local value of the Hubble constant, 73.50 km.s^{-1}.Mpc^{-1}.

34.1.18 Numerical results for the two-branch field

34.1.18.1 Calculated parameters

Table 25

Parameter	Calculated value
M_c	$5.30973982814\times10^{14}$ M⊙
$M\mathcal{d}_n$	$2.02271284593\times10^{13}$ M⊙
$M\mathcal{d}_m$	$6.55809754423\times10^{17}$ M⊙
$k\mathcal{d}_m$	0.418148420451
k_{m1}	$2.48090420945\times10^{-9}$
k_{m2}	0.0315623883428
λ	0.625397449117
R_m	0.788580293803 Mpc

P928 The numerical value of R_m is taken from the reported model output; its general definition in equation 162 depends on the source mass. The reference mass corresponding to this numerical value must therefore be stated explicitly.

34.1.18.2 Numerical measures

Table 26

Metric	Value
Combined metric	7.873292%
Acceleration deviation	−10.414591%
Energy deviation	−3.938752%
MOG deviation	−12.748308%
MOND deviation	−7.376181%

34.1.18.3 Variation of the transition scale with mass

Table 27

Mass (M⊙)	R_m/R_{mon}
10^{11}	72.86796
10^{13}	7.286796
10^{15}	0.7286796

P929 These results show that the ratio of the shared transition radius to the MOND radius decreases as the mass increases.

34.1.19 Unified analysis of gravitation across different scales

P930 In Ramionics, gravitation results from changes in the energy distribution of the spacetime lattice.

P931 At small distances, the Newtonian kernel dominates. In strong fields, the relativistic factor dependent on the energy distribution function becomes significant.

P932 On galactic scales, the modified branch produces approximately MOND-like behaviour. On cluster scales, the enhancement factor and independent damping of this branch are used to examine behaviour corresponding to MOG.

P933 On cosmological scales, the nonlinear radial mapping and FCC geometry enter the calculations of cosmic expansion.

P934 The two derivations of the relation between the Hubble radius and the radius of the universe, one geometrical and topological and the other based on forces and dynamics, yield the common factor 4γ.

P935 In the geometrical derivation, the growth of FCC shells and the entanglement of the universe play the principal roles. In the force-based derivation, a very small imbalance between ramion forces and the radial mean factor 3/4 are used.

P936 Within this framework, the surface coverage factor β is associated with the Hubble tension, while the volume packing fraction φ is associated with the geometrical contribution to apparent dark matter.

P937 Ramion entanglement and internal closure also underpin the distinction between the fundamental energy density of space and the cosmological critical density.

P938 **Summary:** in Ramionics, mass is a modification of the energy pattern of spacetime, and gravitation arises from the gradient of that modification. The two-branch model, together with mass-dependent radial scales and a geometrical correction for expansion, provides a framework for calculating fields from Newtonian to galactic and cosmological scales.

P939 The relation between the radius of the universe and the Hubble radius is now accompanied by two explicit derivations in this manuscript. A conclusive assessment of the cosmological section requires not only consistency between these derivations but also tests of their dynamical and topological assumptions and a derivation of the evolution equations for the entangled lattice.

35 Formula for the kissing number in different dimensions

[655] $k_{m(}d_{)} = k_{f(}d_{)}.k_{full(}d_{)}$

[656] $k_{full(}d_{)} = (2d)2^{(d/2)}$: full kissing number

[657] $k_{f(}d_{)} = ½ + cc_{(d)}/2$: kissing factor

[658] $cc_{(d)} = \cos^{2}{}_{(\pi.\log 4^{2}(d/6))}$

P940 Criteria:

P941 1&2: base-dimension condition:

[659] $k_1 = 2, k_2 = 6$

P942 2d: divisibility by 2d:

[660] $k \bmod (2d) = 0, \text{for } d > 2$

P943 2k: recursive upper bound:

[661] $k_{(d)} \leq 2k_{(d-1)}, \text{for } d > 2$

P944 GF: greatest-factor condition:

[662] $GF_{(k/d)} \leq 1 + d/2$

P945 GF1: condition that the greatest factor occurs to the first power:

[663] $\text{Power}_{(GF(k/d))} = 1$

P946 GFA: optional condition that all larger factors occur to the first power:

[664] $\text{Power}_{(p)} = 1, \text{for every prime } p > 3 \text{ dividing } k/d$

P947 Parity: even-power balance condition:

[665] $\text{Power}_{2(}k_{)} \geq \text{Count}_{(\text{odd powers of primes} > 2)}$

P948 no2: exclusion of pure powers of 2: $k \neq 2^{n}$

36 Theorem 37 Relativistic dynamics and the chain of reasoning

P949 In Ramionics, a particle is a stable energy pattern in the FCC lattice. Inertia is attributed to the rearrangement of the energy distribution and its gravitational and pressure self-interaction during acceleration. The acceleration of a body is interpreted as an effective gravitational field. The following relations set out the specific chain of reasoning in Theorem 37 without repeating the general definitions of the framework. Their numbering continues the main sequence of equations in this manuscript.

[666] $g = a$

[667] $dx = v\,dt$

[668] $R_i = c\,dt$

P950 In the geometrical description of finite-speed propagation, the hypotenuse represents the propagation path c∂t, the displacement of the body is v∂t, and the effective propagation component is R∂t:

[669] $(c\,dt)^2 = (v\,dt)^2 + (R\,dt)^2$

[670] $1 = v^2/c^2 + R^2/c^2$

[671] $R/c = \sqrt{(1 - v^2/c^2)}$

[672] $R = c\sqrt{(1 - v^2/c^2)}$

[673] $\lambda = \sqrt{(1 - v^2/c^2)}$

P951 Assuming that the effective field radius in the direction of motion contracts by the factor λ, the field function and its enhancement ratio are modelled as follows:

[674] $f_0(R) = R_s/R$

[675] $f_v(R)/f_0(R) = 1/\sqrt{(1 - v^2/c^2)}$

[676] $f_v(R) = R_s/(R\sqrt{(1 - v^2/c^2)})$

P952 In this model, f is the ramion energy-density factor. Assuming fixed integration limits and an enhancement factor independent of R:

[677] $E = 4\pi\rho_s\varphi\int f(R)R^2\,dR$

[678] $E_0 = 4\pi\rho_s\varphi\int_{(Rs)}^{Ri} f_0(R)R^2\,dR$

[679] $E_v = 4\pi\rho_s\varphi\int_{(Rs)}^{Ri} f_v(R)R^2\,dR$

[680] $E_v = E_0/\sqrt{(1 - v^2/c^2)}$

[681] $K(v) = E_v - E_0 = mc^2(1/\sqrt{(1 - v^2/c^2)} - 1)$

P953 The low-velocity expansion and the Newtonian limit are

[682] $1/\sqrt{(1 - v^2/c^2)} \approx 1 + ½v^2/c^2 + 3v^4/(8c^4) + \cdots$

[683] $K(v) \approx ½mv^2 + 3mv^4/(8c^2) + \cdots$

[684] $K(v \ll c) \approx ½mv^2$

P954 The theorem distinguishes linear motion, with open field propagation, from rotational motion, in which field shells return and overlap. The following rotational factor is a modelling assumption based on overlap; it does not follow from the triangle geometry above alone:

[685] $q_{(rot)} = v^2/(2c^2)$

[686] $\gamma_{(rot)} = 1/(1 - v^2/(2c^2))$

[687] $\lim_{(v\to c)}\gamma_{(rot)} = 2$

P955 For a mass element at distance r from the axis of rotation:

[688] $v = \omega r$

[689] $dE_{(rot)} = c^2\,dm/(1 - \omega^2r^2/(2c^2))$

[690] $dK_{(rot)} = \omega^2r^2\,dm/(2 - \omega^2r^2/c^2)$

[691] $E_{(rot,total)} = c^2 \int dm/(1 - \omega^2 r^2/(2c^2))$

[692] $M = \int dm$

[693] $K_{(rot,total)} = c^2 \int dm/(1 - \omega^2 r^2/(2c^2)) - Mc^2$

P956 In the low-tangential-speed limit:

[694] $E_{(rot,total)} \approx Mc^2 + \frac{1}{2}\omega^2 \int r^2 \, dm$

[695] $K_{(rot,total)} \approx \frac{1}{2} I \omega^2$

P957 In its discussion of the rotating disc and the Ehrenfest paradox, the manuscript distinguishes the effective geometries of rotational and linear motion. In the proposed model, the circumference relation is assumed to be approximately Euclidean:

[696] $C \approx 2\pi R$

P958 In the rotational-overlap model, field enhancement is assumed to be bounded. The following bounds refer to that assumption in the limit v→c:

[697] $f_{(max)} = 2f_0$

[698] $E_{(max)} = 2mc^2$

[699] $K_{(max)} = mc^2$

P959 In the generalisation to the full field on galactic and cluster scales, the field function of Theorem 34 replaces the Newtonian approximation:

[700] $K = (\gamma - 1) 4\pi \rho_s \varphi \int_{(Rs)}^{Ri} f(R) R^2 \, dR$

[701] $f(R) = R_s/R + (R_s/R_m) E_1(kR/R_d)$

P960 In this chain of reasoning, the derivation of the linear factor depends on the propagation-triangle assumption and its conversion into an enhancement of the field density. The distinction introduced for rotation is a separate assumption concerning field recirculation. The existing formulae and the other sections of this manuscript remain unchanged.

37 Gravitational time dilation and light deflection from the energy metric distribution of spatial ramions

37.1 The common basis of gravitation time and light propagation

P961 In Ramionics, the speed of light propagation is not an independently imposed property; it depends on the energy of the ramions in the FCC lattice. According to the fundamental relations [91], [93], [94], [96] and [99], the energy metric N jointly determines the scales of energy, radius, density, pressure and propagation speed. In the gravitation section, equations [480] and [481] also specify the energy-density distribution and metric N in terms of the field function f(R). Consequently, the same distribution N(R) that generates the gravitational pressure gradient also determines changes in the rates of local processes and in the path of light propagation.

P962 In the equations in this section, N(R) is the ratio of the local metric to the distant reference metric and is taken to equal unity at the distant reference. The symbol c denotes the speed of light propagation at that same reference. Using N, rather than introducing an independent Lorentz factor, maintains the connection with the fundamental definition of the energy metric.

[702] $\rho(R) = \rho_u(1 - f(R))$

[703] $N(R) = \sqrt{(\rho_u/\rho(R))} = 1/\sqrt{(1 - f(R))}$

[704] $c(R)/c = 1/N(R)^2$

[705] $c(R) = c(1 - f(R))$

P963 The speed relation used here is the same projection law that expresses propagation speed in terms of ramion energy. 'Effective speed' denotes propagation speed relative to the distant reference in an inhomogeneous metric distribution; it does not introduce an additional independent speed into the theory. A local observer measures length and time using the local metric, so propagation speed relative to the distant reference must be distinguished from a local measurement.

37.2 Gravitational time dilation

P964 As explained after equation [96], a change in the ramion energy metric also changes the timescale of physical processes. With N(R) defined as the ratio of the local metric to the distant reference metric, the ratio of the distant-reference time interval to the proper-time interval of a stationary clock at R is expressed in this model by the same N(R). Hence:

[706] $dt = N(R)\, d\tau_{loc}$

[707] $d\tau_{loc}/\, dt = 1/N(R) = \sqrt{(1 - f(R))}$

P965 In the Newtonian regime for a spherical mass, the field function and corresponding metric are

[708] $R_s = 2GM/c^2$

[709] $f(R) \approx R_s/R$

[710] $N(R) \approx 1/\sqrt{(1 - R_s/R)}$

[711] $d\tau_{loc}/\, dt \approx \sqrt{(1 - 2GM/(Rc^2))}$

P966 Thus, as the energy metric N increases near a mass, the local stationary clock runs more slowly relative to the distant reference. This result combines the temporal law of ramion projection with the metric distribution introduced in the gravitation section. The particular form of N(R) in this approximation follows from the field function adopted in that section; independently deriving the field function from the microscopic ramion distribution is a separate problem from making this substitution.

37.3 The metric gradient and gravitational acceleration

P967 Equations [487] and [488] for the signed radial acceleration, together with the definition of N(R), give

[712] $g(R) = c^2/[2(1 - f(R))]\, df(R)/\, dR$

[713] $g(R) = c^2/N(R) \times dN(R)/\, dR$

P968 For the field of a spherical mass, the derivative of N with respect to R is negative. Thus, under this convention, g points towards the mass. This relation shows that gravitational acceleration and time dilation are both associated with the same distribution N(R).

37.4 The refractive index arising from the energy distribution and light deflection

P969 The refractive index relative to the distant reference follows from the fundamental propagation-speed law in equations [96] and [99], without introducing an independent law for light:

[714] $n(R) = c/c(R) = N(R)^2 = 1/(1 - f(R))$

P970 In the Newtonian, weak-field regime:

[715] $f(R) \approx R_s/R \ll 1$

[716] $n(R) \approx 1 + R_s/R = 1 + 2GM/(Rc^2)$

P971 For a ray travelling along the x direction to first order, with impact parameter b relative to the centre of mass:

[717] $R = \sqrt{(x^2 + b^2)}$

[718] $\partial n/\partial b \approx -R_s b/(x^2 + b^2)^{3/2}$

P972 In the geometrical-optics approximation for propagation through a medium with a spatially varying refractive index, the magnitude of the first-order deflection angle is obtained by integrating the transverse refractive-index gradient along the unperturbed straight path:

[719] $\alpha \approx -\int_{-\infty}^{+\infty} (\partial n/\partial b)\, dx$

[720] $\alpha \approx R_s b \int_{-\infty}^{+\infty} dx/(x^2 + b^2)^{3/2}$

[721] $\int_{-\infty}^{+\infty} dx/(x^2 + b^2)^{3/2} = 2/b^2$

[722] $\alpha \approx 2R_s/b = 4GM/(bc^2)$

P973 Thus, in the Newtonian regime, the propagation-speed gradient generated by the same N(R) distribution reproduces the leading-order light-deflection angle of general relativity. The ray equation for an inhomogeneous medium is a geometrical-optics approximation; a more complete wave description requires the propagation dynamics of the FCC lattice.

37.5 Comparison with Newtonian gravitation acting on a hypothetical photon mass

P974 For comparison, if light is treated solely as a particle moving at speed c under a transverse Newtonian acceleration, without including the change in propagation speed associated with the energy metric, then

[723] $a_\gamma \approx -GMb/(x^2 + b^2)^{3/2}$

[724] $\alpha_n \approx -(1/c^2) \int_{-\infty}^{+\infty} a_\gamma\, dx$

[725] $\alpha_n \approx 2GM/(bc^2) = R_s/b$

P975 When the N-dependent propagation-speed gradient is included, however, the preceding result gives

[726] $\alpha/\alpha_n \approx 2$

P976 Consequently, to first order, the deflection arising from the ramion energy metric distribution is **twice** the deflection in the Newtonian model of gravitation acting on a hypothetical photon mass. The factor of two follows from the fundamental N^{-2} dependence of propagation speed, and hence from the refractive index N^2; it does not follow from assigning rest mass to the photon or introducing an arbitrary refractive index.

Table 28

Model	Weak-field deflection	Relative factor
Newtonian hypothetical photon mass	$2GM/(bc^2)$	1
Ramionics N-gradient propagation	$4GM/(bc^2)$	2
General relativity, leading order	$4GM/(bc^2)$	2

37.6 Scope of the result

P977 This derivation applies to a weak spherical field, an approximately straight trajectory and geometrical-optics propagation. For gravitational lensing on galactic and cluster scales, the full Ramionics field function must replace the approximation $f(R) \approx R_s/R$ in N(R) and in the refractive-index gradient, after which the ray trajectory must be calculated. Reproducing the deflection coefficient in the Newtonian limit demonstrates the computational consistency of the model, but does not, by itself, provide empirical validation of all Ramionics assumptions.

[727] Final kissing numbers: $k_1 = 2\ k_2 = 6\ k_3 = 12\ k_4 = 24\ k_5 = 40\ k_6 = 72\ k_7 = 126$
$k_8 = 240\ k_9 = 360\ k_{10} = 540\ k_{11} = 792\ k_{12} = 1080\ k_{13} = 1456\ k_{14} = 2016\ k_{15} = 2700$
$k_{16} = 4320\ k_{17} = 6120\ k_{18} = 10368\ k_{19} = 17024\ k_{20} = 30800\ k_{21} = 51744\ k_{22} = 81312$
$k_{23} = 129536\ k_{24} = 196560\ k_{25} = 283500\ k_{26} = 397488\ k_{27} = 534600\ k_{28} = 709632$
$k_{29} = 918720\ k_{30} = 1188000\ k_{31} = 1562400\ k_{32} = 2132480\ k_{33} = 3057912$

38 Experimental values for the muon and tau

[728] $g_{mx} = 2.00233184123 \pm 82 \times 10^{-11}$
$E_{mx} = 105.6583755 \pm 23 \times 10^{-7}\ \text{MeV}$
$E_{m2x} = 1273 \pm 4\ \text{MeV}$
$E_{m1x} = 93.4 \pm 86 \times 10^{-1}\ \text{MeV}$
$g_{tx} = 2.00235442 \pm 1 \times 10^{-7}$
$E_{tx} = 1776.86 \pm 12 \times 10^{-2}\ \text{MeV}$
$E_{t2x} = 172690 \pm 300\ \text{MeV}$
$E_{t1x} = 4183 \pm 7\ \text{MeV}$

39 Historical reference data

P978 The comparison metric uses the change in central value divided by the previous displayed edition's quoted 1σ uncertainty. It is not a combined significance of two independent measurements.

39.1 Inverse Fine-Structure Constant CODATA Recommended Values

Table 29

Year	Central Value α^{-1}	Standard Uncertainty (1σ)	Change From Previous	Change / Previous σ	Source Page
2002	137.03599911	0.00000046	—	—	S1
2006	137.035999679	0.000000094	+0.000000569	+1.24σ	S2
2010	137.035999074	0.000000044	−0.000000605	−6.44σ	S3
2014	137.035999139	0.000000031	+0.000000065	+1.48σ	S4
2018	137.035999084	0.000000021	−0.000000055	−1.77σ	S5
2022	137.035999177	0.000000021	+0.000000093	+4.43σ	S6

S1 https://physics.nist.gov/cuu/pdf/all_2002.pdf

S2 https://physics.nist.gov/cuu/pdf/all_2006.pdf

S3 https://physics.nist.gov/cuu/pdf/all_2010.pdf

S4 https://physics.nist.gov/cuu/pdf/all_2014.pdf

S5 https://physics.nist.gov/cuu/pdf/all_2018.pdf

S6 https://physics.nist.gov/cuu/pdf/all.pdf

P979 CODATA recommended values; uncertainty is the quoted standard uncertainty.

39.2 Electron Mass Energy Equivalent CODATA Recommended Values

Table 30

Year	Central Value (MeV)	Standard Uncertainty (1σ, MeV)	Change From Previous (MeV)	Change / Previous σ	Source Page
2002	0.510998918	0.000000044	—	—	S1
2006	0.510998910	0.000000013	−0.000000008	−0.18σ	S2
2010	0.510998928	0.000000011	+0.000000018	+1.38σ	S3
2014	0.5109989461	0.0000000031	+0.0000000181	+1.65σ	S4
2018	0.51099895000	0.00000000015	+0.00000000390	+1.26σ	S5
2022	0.51099895069	0.00000000016	+0.00000000069	+4.60σ	S6

S1 https://physics.nist.gov/cuu/pdf/all_2002.pdf

S2 https://physics.nist.gov/cuu/pdf/all_2006.pdf

S3 https://physics.nist.gov/cuu/pdf/all_2010.pdf

S4 https://physics.nist.gov/cuu/pdf/all_2014.pdf

S5 https://physics.nist.gov/cuu/pdf/all_2018.pdf

S6 https://physics.nist.gov/cuu/pdf/all.pdf

P980 CODATA electron mass-energy equivalent in MeV.

39.3 Up-Quark Mass PDG Evaluations at 2 GeV

Table 31

Year	Central Value (MeV)	Quoted Uncertainty (MeV)	Change From Previous (MeV)	Change / Previous σ	Source Page
2010	2.49	+0.81/−0.79	—	—	S1
2014	2.30	+0.70/−0.50	−0.19	−0.24σ	S2
2018	2.20	+0.50/−0.40	−0.10	−0.20σ	S3
2022	2.16	+0.49/−0.26	−0.04	−0.10σ	S4

S1 https://pdg.lbl.gov/2010/listings/rpp2010-list-light-quarks.pdf

S2 https://pdg.lbl.gov/2014/listings/rpp2014-list-light-quarks.pdf

S3 https://pdg.lbl.gov/2018/listings/rpp2018-list-light-quarks.pdf

S4 https://pdg.lbl.gov/2022/listings/rpp2022-list-light-quarks.pdf

P981 $M\bar{S}$ mass at the 2 GeV scale. For asymmetric uncertainty, the previous uncertainty in the direction of the central-value change is used.

39.4 Down-Quark Mass PDG Evaluations at 2 GeV

Table 32

Year	Central Value (MeV)	Quoted Uncertainty (MeV)	Change From Previous (MeV)	Change / Previous σ	Source Page
2010	5.05	+0.75/−0.95	—	—	S1
2014	4.80	+0.50/−0.30	−0.25	−0.26σ	S2
2018	4.70	+0.50/−0.30	−0.10	−0.33σ	S3
2022	4.67	+0.48/−0.17	−0.03	−0.10σ	S4

S1 https://pdg.lbl.gov/2010/listings/rpp2010-list-light-quarks.pdf

S2 https://pdg.lbl.gov/2014/listings/rpp2014-list-light-quarks.pdf

S3 https://pdg.lbl.gov/2018/listings/rpp2018-list-light-quarks.pdf

S4 https://pdg.lbl.gov/2022/listings/rpp2022-list-light-quarks.pdf

P982 $M\bar{S}$ mass at the 2 GeV scale. For asymmetric uncertainty, the previous uncertainty in the direction of the central-value change is used.

39.5 Proton Mass Energy Equivalent CODATA Recommended Values

Table 33

Year	Central Value (MeV)	Standard Uncertainty (1σ, MeV)	Change From Previous (MeV)	Change / Previous σ	Source Page
2002	938.272029	0.000080	—	—	S1
2006	938.272013	0.000023	−0.000016	−0.20σ	S2
2010	938.272046	0.000021	+0.000033	+1.43σ	S3
2014	938.2720813	0.0000058	+0.0000353	+1.68σ	S4
2018	938.27208816	0.00000029	+0.00000686	+1.18σ	S5
2022	938.27208943	0.00000029	+0.00000127	+4.38σ	S6

S1 https://physics.nist.gov/cuu/pdf/all_2002.pdf

S2 https://physics.nist.gov/cuu/pdf/all_2006.pdf

S3 https://physics.nist.gov/cuu/pdf/all_2010.pdf

S4 https://physics.nist.gov/cuu/pdf/all_2014.pdf

S5 https://physics.nist.gov/cuu/pdf/all_2018.pdf

S6 https://physics.nist.gov/cuu/pdf/all.pdf

P983 CODATA proton mass-energy equivalent in MeV.

39.6 Neutron Mass Energy Equivalent CODATA Recommended Values

Table 34

Year	Central Value (MeV)	Standard Uncertainty (1σ, MeV)	Change From Previous (MeV)	Change / Previous σ	Source Page
2002	939.565360	0.000081	—	—	S1

Year	Central Value (MeV)	Standard Uncertainty (1σ, MeV)	Change From Previous (MeV)	Change / Previous σ	Source Page
2006	939.565346	0.000023	−0.000014	−0.17σ	S2
2010	939.565379	0.000021	+0.000033	+1.43σ	S3
2014	939.5654133	0.0000058	+0.0000343	+1.63σ	S4
2018	939.56542052	0.00000054	+0.00000722	+1.24σ	S5
2022	939.56542194	0.00000048	+0.00000142	+2.63σ	S6

S1 https://physics.nist.gov/cuu/pdf/all_2002.pdf

S2 https://physics.nist.gov/cuu/pdf/all_2006.pdf

S3 https://physics.nist.gov/cuu/pdf/all_2010.pdf

S4 https://physics.nist.gov/cuu/pdf/all_2014.pdf

S5 https://physics.nist.gov/cuu/pdf/all_2018.pdf

S6 https://physics.nist.gov/cuu/pdf/all.pdf

P984 CODATA neutron mass-energy equivalent in MeV.

39.7 Muon Mass Energy Equivalent CODATA Recommended Values

Table 35

Year	Central Value (MeV)	Standard Uncertainty (1σ, MeV)	Change From Previous (MeV)	Change / Previous σ	Source Page
2002	105.6583692	0.0000094	—	—	S1
2006	105.6583668	0.0000038	−0.0000024	−0.26σ	S2
2010	105.6583715	0.0000035	+0.0000047	+1.24σ	S3
2014	105.6583745	0.0000024	+0.0000030	+0.86σ	S4
2018	105.6583755	0.0000023	+0.0000010	+0.42σ	S5

S1 https://physics.nist.gov/cuu/pdf/all_2002.pdf

S2 https://physics.nist.gov/cuu/pdf/all_2006.pdf

S3 https://physics.nist.gov/cuu/pdf/all_2010.pdf

S4 https://physics.nist.gov/cuu/pdf/all_2014.pdf

S5 https://physics.nist.gov/cuu/pdf/all_2018.pdf

P985 Editions with unchanged central value and unchanged uncertainty are omitted.

39.8 Tau Mass Energy Equivalent CODATA Recommended Values

Table 36

Year	Central Value (MeV)	Standard Uncertainty (1σ, MeV)	Change From Previous (MeV)	Change / Previous σ	Source Page
2002	1776.99	0.29	—	—	S1
2010	1776.82	0.16	−0.17	−0.59σ	S2
2018	1776.86	0.12	+0.04	+0.25σ	S3

S1 https://physics.nist.gov/cuu/pdf/all_2002.pdf

S2 https://physics.nist.gov/cuu/pdf/all_2010.pdf

S3 https://physics.nist.gov/cuu/pdf/all_2018.pdf

P986 Editions with unchanged central value and unchanged uncertainty are omitted.

39.9 Absolute Electron g-Factor CODATA Recommended Values

Table 37

Year	Central Value	Standard Uncertainty (1σ)	Change From Previous	Change / Previous σ	Source Page
2002	2.0023193043718	0.0000000000075	—	—	S1
2006	2.0023193043622	0.0000000000015	−0.0000000000096	−1.28σ	S2
2010	2.00231930436153	0.00000000000053	−0.00000000000067	−0.45σ	S3
2014	2.00231930436182	0.00000000000052	+0.00000000000029	+0.55σ	S4
2018	2.00231930436256	0.00000000000035	+0.00000000000074	+1.42σ	S5
2022	2.00231930436092	0.00000000000036	−0.00000000000164	−4.69σ	S6

S1 https://physics.nist.gov/cuu/pdf/all_2002.pdf

S2 https://physics.nist.gov/cuu/pdf/all_2006.pdf

S3 https://physics.nist.gov/cuu/pdf/all_2010.pdf

S4 https://physics.nist.gov/cuu/pdf/all_2014.pdf

S5 https://physics.nist.gov/cuu/pdf/all_2018.pdf

S6 https://physics.nist.gov/cuu/pdf/all.pdf

P987 Absolute magnitude is shown; the CODATA signed electron g-factor is negative.

39.10 Absolute Muon g-Factor CODATA Recommended Values

Table 38

Year	Central Value	Standard Uncertainty (1σ)	Change From Previous	Change / Previous σ	Source Page
2002	2.0023318396	0.0000000012	—	—	S1
2006	2.0023318414	0.0000000012	+0.0000000018	+1.50σ	S2
2010	2.0023318418	0.0000000013	+0.0000000004	+0.33σ	S3
2022	2.00233184123	0.00000000082	−0.00000000057	−0.44σ	S4

S1 https://physics.nist.gov/cuu/pdf/all_2002.pdf

S2 https://physics.nist.gov/cuu/pdf/all_2006.pdf

S3 https://physics.nist.gov/cuu/pdf/all_2010.pdf

S4 https://physics.nist.gov/cuu/pdf/all.pdf

P988 Absolute magnitude is shown; unchanged editions are omitted.

39.11 Proton g-Factor CODATA Recommended Values

Table 39

Year	Central Value	Standard Uncertainty (1σ)	Change From Previous	Change / Previous σ	Source Page

Year	Central Value	Standard Uncertainty (1σ)	Change From Previous	Change / Previous σ	Source Page
2002	5.585694701	0.000000056	—	—	S1
2006	5.585694713	0.000000046	+0.000000012	+0.21σ	S2
2014	5.585694702	0.000000017	−0.000000011	−0.24σ	S3
2018	5.5856946893	0.0000000016	−0.0000000127	−0.75σ	S4

S1 https://physics.nist.gov/cuu/pdf/all_2002.pdf

S2 https://physics.nist.gov/cuu/pdf/all_2006.pdf

S3 https://physics.nist.gov/cuu/pdf/all_2014.pdf

S4 https://physics.nist.gov/cuu/pdf/all_2018.pdf

P989 Editions with unchanged central value and unchanged uncertainty are omitted.

39.12 Absolute Neutron g-Factor CODATA Recommended Values

Table 40

Year	Central Value	Standard Uncertainty (1σ)	Change From Previous	Change / Previous σ	Source Page
2002	3.82608546	0.00000090	—	—	S1
2006	3.82608545	0.00000090	−0.00000001	−0.01σ	S2
2022	3.82608552	0.00000090	+0.00000007	+0.08σ	S3

S1 https://physics.nist.gov/cuu/pdf/all_2002.pdf

S2 https://physics.nist.gov/cuu/pdf/all_2006.pdf

S3 https://physics.nist.gov/cuu/pdf/all.pdf

P990 Absolute magnitude is shown; unchanged editions are omitted.

39.13 Historical Shift Summary

Table 41

Quantity	Largest Historical Shift / Previous σ	Year of Largest Shift	Latest Shift / Previous σ	Latest Displayed Year
α^{-1}	−6.44σ	2010	+4.43σ	2022
Electron Mass	+4.60σ	2022	+4.60σ	2022
Up-Quark Mass	−0.24σ	2014	−0.10σ	2022
Down-Quark Mass	−0.33σ	2018	−0.10σ	2022
Proton Mass	+4.38σ	2022	+4.38σ	2022
Neutron Mass	+2.63σ	2022	+2.63σ	2022
Muon Mass	+1.24σ	2010	+0.42σ	2018
Tau Mass	−0.59σ	2010	+0.25σ	2018

Quantity	Largest Historical Shift / Previous σ	Year of Largest Shift	Latest Shift / Previous σ	Latest Displayed Year
Absolute g_e	−4.69σ	2022	−4.69σ	2022
Absolute g_m	+1.50σ	2006	−0.44σ	2022
g_p	−0.75σ	2018	−0.75σ	2018
Absolute g_n	+0.08σ	2022	+0.08σ	2022

P991 The shift metric uses the previous displayed edition’s quoted uncertainty and is not a combined two-measurement significance.

P992 Tau g-factor note: the experimental Standard-Model value is not included as a CODATA-style precision historical measurement series.